A time viscosity-splitting method for incompressible flows with temperature-dependent viscosity and thermal conductivity

Mofdi El-Amrani[a], Anouar Obbadi[a], Mohammed Seaid[b,*], Driss Yakoubi[c]

[a] *Laboratory of Mathematics and Applications, FSTT, Abdelmalek Essaadi University, Tangier, Morocco*
[b] *Department of Engineering, University of Durham, South Road, DH1 3LE, United Kingdom*
[c] *Léonard de Vinci Pôle Universitaire, Research Center, 92 916 Paris La Défense, France*

Abstract

A fractional-step method is proposed and analyzed for solving the incompressible thermal Navier-Stokes equations coupled to the convection-conduction equation for heat transfer with a generalized source term for which the viscosity and thermal conductivity are temperature-dependent under the Boussinesq assumption. The proposed method consists of four steps all based on a viscosity-splitting algorithm where the convection and diffusion terms of both velocity and temperature solutions are separated while a viscosity term is kept in the correction step at all times. This procedure preserves the original boundary conditions on the corrected velocity and it removes any pressure inconsistencies. As a main feature, our method allows the temperature to be transported by a non-divergence-free velocity, in which case we show how to handle the subtle temperature convection term in the error analysis and establish full first-order error estimates for the velocity and the temperature solutions and 1/2-order estimates for the pressure solution in their appropriate norms. The theoretical results are examined by an accuracy test example with known analytical solution and using a benchmark problem of Rayleigh-Benard convection with temperature-dependent viscosity and thermal conductivity. We also apply the method for solving a problem of unsteady flow over a heated airfoil. The obtained results demonstrate the convergence, accuracy and applicability of the proposed time viscosity-splitting method.

Keywords: Navier-Stokes equations, Natural convection, Fractional time-stepping, Viscosity-splitting method, Error analysis.

---

1. Introduction

Natural convection is one of the most abundant heat transfer phenomena in many thermal applications in engineering and industry. It is basically a fluid dynamics process in which the motion of the fluid, unlike the forced convection, is not driven by an external force such as a heat pump or fan, but by the buoyancy effects that result from density variations the fluid undergoes due to temperature differences (temperature gradients). This process receives a great deal of attention as it is involved in a myriad of physical and industrial problems of interest such as greenhouse drying [1], electronic devices cooling [2], solar air heaters [3], chemical and food industries in addition to meteorology, geophysics and astrophysics research projects among others. In general, the motion of a fluid subject to natural convection effects is modeled by the incompressible Navier-Stokes equations for the flow augmented by the buoyancy force coupled with a convection-diffusion equation for the temperature. The momentum equation is derived under the Boussinesq approximation which simply implies that the density variations due to the temperature are ignored except in the gravitational force (the buoyancy force) which becomes proportional to the temperature difference,

*Corresponding author
Email addresses: `moelamrani@uae.ac.ma` (Mofdi El-Amrani), `anouar.obbadi@etu.uae.ac.ma` (Anouar Obbadi), `m.seaid@durham.ac.uk` (Mohammed Seaid), `driss.yakoubi@devinci.fr` (Driss Yakoubi)

see for instance [4, 5] for more details. The resulting equations are also known by the Boussinesq equations in computational fluid dynamics. Often, the fluid viscosity and thermal conductivity coefficients appearing in the resulting system are set to be constants. However, in order to cover more complex fluid flows and extend the scope of the current work, these coefficients are allowed to be dependent on the temperature in a nonlinear form. In addition, general source terms that depend on the temperature solution are also accounted for in the analysis under some theoretical assumptions. Under these conditions, the mathematical analysis of the continuous problem is not a trivial task, mainly due to the strong coupling between the incompressible Navier-Stokes equations and temperature, along with the presence of temperature-dependent viscosity and thermal conductivity coefficients. For instance, authors in [6] analyzed the asymptotical stability of the time-dependent problem and derived a uniqueness result for the steady convective flows in bounded regions under some relation between the Rayleigh and the Reynolds numbers. Authors in [7] studied the linearized system of the stationary case and analyzed its bifurcation and stability. In [8], authors studied the bifurcation and stability of several mathematical problems, in a generalized framework, including the time-dependent Benard problem using group-theoretic methods. Authors in [9] generalized the results reported in [10] for a two-dimensional rectangular domain under constraints on the physical parameters and they proved the existence and uniqueness of a local solution for the steady-state problem in two- and three-dimensional bounded domains. In [11], the existence and uniqueness are studied for the steady problem with temperature dependent parameters and no-slip boundary conditions, whereas in [12] the well-posedness has been established in the case of infinite Prandtl number with free-slip boundary conditions. The numerical solution of natural convection problem, which is the focus of this work, faces major difficulties related to the nonlinearity and the saddle point structure introduced by the momentum and continuity equations in the Navier-Stokes system, in addition to the strong coupling between the velocity and temperature which is known to be a source of destabilization. In three-dimensional problems, any special discretization, following a monolithic approach, where all the three primal unknowns are calculated simultaneously, would give rise to very large systems with a prohibitive computational cost, thus requiring sophisticated and problem-tailored solvers, see for example [13, 14]. Therefore, it would be more efficient to separate the original problem into subsequent easier-to-solve sub-problems. This is the key idea behind the projection of fractional-step methods that were originally designed for solving the incompressible Navier-Stokes equations but still efficient here for the same reasons. This class of methods, initiated by the early works of Chorin [15] and Temam [16], consists of separating the diffusion term and the incompressibility constraint into two (or more) steps in the time integration process. However, the original projection method suffered from inconsistent pressure boundary conditions degrading its accuracy and convergence order, and therefore several techniques of its variants were developed and analyzed in the subsequent years to overcome this drawback, see for example [17, 18, 19, 20, 21, 22, 23] and for detailed review we refer to [24].

As far as natural convection problems are concerned, fractional-step methods were applied in various studies in the literature in conjunction with the finite element method [25, 26, 27, 28, 29] and with the finite volume method [30, 31, 32, 33] among others. However, the literature devoted to error analysis of time fractional-step methods in the framework of natural convection problems is rather scarce. Authors in [34] developed a class of three-step pressure-correction methods and provided first-order error estimates, then in [35] the same authors modified their scheme and proved higher-order error estimates for the temperature and velocity solutions. However, in their approach the temperature is advected by an old velocity and it does not take advantage of the new information of the updated velocity. In [36], first-order and second-order pressure-correction methods have been proposed for the problem with temperature-independent parameters using a mixed finite element discretization and proved first-order error estimates for the three primal variables in the L^2 and H^1 norms. It should be noted that this approach can be viewed as the basic projection method introduced in [37] but with inactive fixed-point iteration for which the temperature is transported by the corrected divergence-free velocity. In a related but different approach, authors in [37] considered the fully implicit problem and derived a coupled prediction scheme relying on the idea that the predicted velocity (although not divergence-free) is rich enough to be injected in the temperature equation. They provided existence and convergence results in [37] has also shown that the proposed method is at least of first-order and at best of second-order in the H^1 norm. Unfortunately, all the previous attempts that are based on standard projection methods (with or without pressure-correction procedures) are inevitably prone to nonphysical pressure boundary conditions. Recently, authors in [38] studied a three-step viscosity-splitting method for the natural convection equations with temperature-independent parameters and homogeneous Dirichlet boundary conditions, and established first-order error estimates in both time and space discretizations. In this method, the velocity is predicted then corrected in the first two steps using an old temperature solution, whereas the updated temperature is computed until the last step in order to be advected by the corrected divergence-free velocity. In the framework of discontinuous Galerkin methods, authors in [39] have also proposed a viscosity-splitting-based scheme and studied its error estimates for the temperature-dependent problem with homogeneous Dirichlet boundary conditions. In this approach, the temperature is computed in the second step but using an old velocity that is divergence-free. Moreover, the computed temperature is not exploited to correct the velocity in the last step and an old temperature is used instead, thus throwing away valuable up-to-date information. It is stressed that most of the numerical methods analyzed in the literature do not consider non-divergence-free velocity in the convection term for the temperature.

In the present study, we are interested in the viscosity-splitting approach which differs from the fractional-step projection methods by the fact that a viscous term is still existing in the incompressibility step allowing to impose the full original boundary conditions on the end-of-step velocity, thus removing any unwanted pressure boundary conditions. The idea was originally proposed in [40] (see also [41, 42] for other earlier viscosity-splitting approaches) and it is analyzed in [43, 44] for the incompressible Navier-Stokes equations with constant viscosity, in [45] using a pressure-correction strategy, and in [46] for non-Newtonian fluids with shear-rate dependent viscosity. Here, we extend this approach to account for natural convection systems with temperature-dependent viscosity and thermal conductivity along with generalized source terms. We also establish full first-order error estimates for both the velocity and temperature solutions, and study the pressure error estimates as well. The designed four-step method has the following distinguishing features:

(i) The convection term is separated from the diffusion term for both velocity and temperature during the time integration process. This is particularly useful in the case of large three-dimensional problems where iterative solvers are required. In this type of problems, solving the separate sub-problems is much less demanding than solving the whole convection-diffusion problem.

(ii) The mixed boundary conditions are allowed on the temperature, which occur in many realistic thermal applications and make more physical sense than the homogeneous Dirichlet boundary conditions. The considered boundary conditions also include non-homogeneous Dirichlet boundary conditions on a part of the boundary and non-homogeneous Neumann boundary conditions on the other part of the computational domain.

(iii) Following [37], the temperature is transported by the predicted velocity, which is not divergence-free, while maintaining the rate of convergence as shown by the established error estimates. To the best of our knowledge, this feature differs our method from the vast majority of fractional-step methods including the very recent ones proposed in [38, 39] for solving natural convection problems, in which the temperature is often transported by a divergence-free velocity. It is worth noting here that establishing error estimates in our situation is not straightforward due to the fact that specific temperature convection terms require careful treatment as it will be clear later.

The remainder of the article is organized as follows: In section 2 the governing equations for incompressible flows with temperature-dependent viscosity and thermal conductivity along with some notations and preliminaries are introduced. The proposed viscosity-splitting method is formulated in section 3 for the variational form along with some regularity assumptions on the continuous solution. In section 4 the error estimates are carried out for all the variables in their relevant norms. Three numerical examples including the problem of Rayleigh-Benard convection and the problem of unsteady flow over a heated airfoil are presented in section 5 to verify the theoretical results and validate the method. Finally, section 6 contains concluding remarks.

2. Governing equations and preliminaries

Let Ω be a bounded domain in $\mathbb{R}^d$ (with $d = 2$ or 3) which is either a convex polygon or a connected of class $C^{1,1}$ with the boundary $\partial\Omega = \Gamma_D \cup \Gamma_N$, and let Ω_t the open set $\Omega \times (0, T_f)$, where $T_f > 0$ is the final time. In the present study, we are interested in the numerical solution of the incompressible Navier-Stokes equations for a Newtonian fluid coupled with a convection-diffusion equation for the temperature subject to the well-established Boussinesq approximation as

$$\left\{\begin{array}{rcll} \dfrac{\partial \boldsymbol{u}}{\partial t} + (\boldsymbol{u}\cdot\nabla)\,\boldsymbol{u} - \nabla\cdot(\nu(T)\nabla\boldsymbol{u}) + \nabla\, p &=& \boldsymbol{F}(T), & \text{in } \Omega_t,\\ \nabla\cdot\boldsymbol{u} &=& 0, & \text{in } \Omega_t,\\ \dfrac{\partial T}{\partial t} + (\boldsymbol{u}\cdot\nabla)\,T - \nabla\cdot(\lambda(T)\nabla T) &=& G, & \text{in } \Omega_t, \end{array}\right. \tag{1}$$

where the unknowns $\boldsymbol{u}$, p and T are the velocity, pressure and temperature variables, respectively. The function $\boldsymbol{F}$ depends on the temperature T and represents an external volumic force such as gravity while the function G represents an external heat source which depends only on the position $\boldsymbol{x}$. Here, the viscosity ν and the thermal conductivity λ are assumed to be dependent on the temperature T. Moreover, the function $\boldsymbol{F}$ is no longer restricted to be proportional to the temperature variation ($\boldsymbol{F}\propto(T-T_0)$) but only dependent on T with a more general assumption. For the function $\boldsymbol{F}:\mathbb{R}\to\mathbb{R}^d$ is a $C^1(\mathbb{R})$, there exists a real T_0 such that $\boldsymbol{F}(T_0)=0$ and a non-negative real $\alpha>0$ such that

$$\left\|\boldsymbol{F}'\right\|_\infty \leq \alpha. \tag{2}$$

In what follows, we introduce the temperature $\widehat{\theta}=T-T_0$ and set the function $\boldsymbol{f}(\widehat{\theta})=\dfrac{1}{\alpha}\boldsymbol{F}(T)$. Then, from the assumption (2), we assume

$$\boldsymbol{f}(0)=\boldsymbol{0} \qquad \text{and} \qquad \forall \ell\in\mathbb{R} \quad |\boldsymbol{f}'(\ell)|\leq 1 \implies |\boldsymbol{f}(\ell)|\leq|\ell|. \tag{3}$$

Hence, the system (1) can be rewritten in terms of $\widehat{\theta}$ and $\boldsymbol{f}$ as

$$\left\{\begin{array}{rcll} \dfrac{\partial \boldsymbol{u}}{\partial t} + (\boldsymbol{u}\cdot\nabla)\,\boldsymbol{u} - \nabla\cdot(\nu(\widehat{\theta})\nabla\boldsymbol{u}) + \nabla\, p &=& \alpha\,\boldsymbol{f}(\theta), & \text{in } \Omega_t,\\ \nabla\cdot\boldsymbol{u} &=& 0, & \text{in } \Omega_t,\\ \dfrac{\partial \widehat{\theta}}{\partial t} + (\boldsymbol{u}\cdot\nabla)\,\widehat{\theta} + \dfrac{1}{2}\widehat{\theta}\nabla\cdot\boldsymbol{u} - \nabla\cdot(\lambda(\widehat{\theta})\nabla\widehat{\theta}) &=& g, & \text{in } \Omega_t. \end{array}\right. \tag{4}$$

We also complete the system (4) with the following initial conditions

$$\boldsymbol{u}(\boldsymbol{x},0)=\boldsymbol{u}^0(\boldsymbol{x})\in\boldsymbol{L}^2(\Omega), \;\text{ with }\; \nabla\cdot\boldsymbol{u}^0=0 \;\text{ and }\; \theta(\boldsymbol{x},0)=\theta^0(\boldsymbol{x})\in L^2(\Omega), \tag{5}$$

and the following boundary conditions

$$\boldsymbol{u}=0 \;\text{ on }\; \partial\Omega, \quad \widehat{\theta}=\theta_D \;\text{ on }\; \Gamma_D, \quad \text{and} \quad \lambda(\widehat{\theta})\frac{\partial\widehat{\theta}}{\partial\boldsymbol{n}}=\theta_N \;\text{ on }\Gamma_N, \qquad \text{a.e} \quad t\in(0,T_f). \tag{6}$$

For the sake of simplicity in the presentation, we consider homogeneous Dirichlet boundary conditions for $\boldsymbol{u}$ and we assume that the intersection $\overline{\Gamma}_D\cap\overline{\Gamma}_N$ is a Lipschitz-continuous submanifold of $\partial\Omega$. Note that we have slightly modified the temperature equation in system (1) by adding the term $\frac{1}{2}\widehat{\theta}\nabla\cdot\boldsymbol{u}$, which is obviously vanishing since the velocity is divergence-free. In fact, the additional term allows to restore the skew-symmetry structure which is essential in the error analysis, see for instance [47, 48] for more details on this artifice. We also assume that the coefficients ν and λ are bounded functions in $W^{1,\infty}(\Omega)$, with

$$\left\{\begin{array}{l} 0<\nu_0\leq\nu(r)\leq\nu_1, \quad \|\nu'\|_\infty=\nu_2,\\ 0<\lambda_0\leq\lambda(r)\leq\lambda_1, \quad \|\lambda'\|_\infty=\lambda_2, \end{array}\right. \qquad \forall r\in\mathbb{R}. \tag{7}$$

In what follows, $L^p(\Omega)$ represents the usual set of pth power measurable functions, and $\boldsymbol{L}^p(\Omega)=(L^p(\Omega))^3$. The scalar product defined on $L^2(\Omega)$ or $\mathbf{L}^2(\Omega)$ is denoted (without distinction) by $(\cdot,\cdot)$ and its norm by $\|\cdot\|$. The Sobolev spaces denoted by $W^{m,p}(\Omega)$ and $\boldsymbol{W}^{m,p}(\Omega)$, with $p\in[1,+\infty)$, p integer are defined as

$$W^{m,p}(\Omega)=\Big\{u\in L^p(\Omega):\quad D^{\boldsymbol{k}}u\in L^p(\Omega),\quad \forall|\boldsymbol{k}|\leq m\Big\}, \qquad \boldsymbol{W}^{m,p}(\Omega)=(W^{m,p}(\Omega))^3,$$

where $\boldsymbol{k}$ is a multi-index in $\mathbb{N}^3$. These spaces are equipped with the norm $\|\cdot\|_{m,p}$ and semi-norm $|\cdot|_{m,p}$. The spaces $W^{s,2}(\Omega)$ and $\boldsymbol{W}^{s,2}(\Omega)$, with $s \in \mathbb{R}$, are denoted respectively, by $H^s(\Omega)$ and $\boldsymbol{H}^s(\Omega)$ with the associated norm denoted by $\|\cdot\|_s$ and semi-norm by $|\cdot|_s$. Without distinction for the dimension, we denote the duality pairing between $H_0^1(\Omega)$ and its dual $H^{-1}(\Omega)$ (or between $\boldsymbol{H}_0^1(\Omega)$ and $\boldsymbol{H}^{-1}(\Omega)$) by $\langle\cdot,\cdot\rangle$. More generally, for a space V and its dual V', we denote the duality pairing by $\langle\cdot,\cdot\rangle_{V',V}$. For a fixed positive real variable T_f and a separable Banach space E equipped with the norm $\|\cdot\|_E$, we denote by $\mathcal{C}^0(0,T_f;E)$ the space of continuous functions from $[0,T_f]$ with values in E. For a positive integer p, we introduce the following Bochner spaces

$$L^p(0,T_f;E) = \left\{ u : (0,T_f) \mapsto E : \qquad \left(\int_0^{T_f} \|u(\tau)\|_E^p \, d\tau \right)^{1/p} < \infty \right\},$$

and for m a non-negative integer, the space $H^m(0,T_f;E)$ is defined as

$$H^m(0,T_f;E) = \Big\{ u \in L^2(0,T_f;E) : \qquad \partial_t^l u \in L^2(0,T_f;E), \quad 0 \le l \le m \Big\}.$$

For details on these spaces, we refer for example to [49] and [50, Chapter 2]. In order to derive the variational formulation of the problem (4), (5) and (6), we start by introducing the following spaces

$$\begin{aligned} \boldsymbol{H} &= \Big\{ \boldsymbol{v} \in \boldsymbol{L}^2(\Omega) : \quad \nabla\cdot\boldsymbol{v} = 0, \quad \boldsymbol{v}\cdot\boldsymbol{n}\Big|_{\partial\Omega} = 0 \Big\}, \\ \boldsymbol{V} &= \Big\{ \boldsymbol{v} \in \boldsymbol{H}_0^1(\Omega) : \qquad \nabla\cdot\boldsymbol{v} = 0 \Big\}. \end{aligned}$$

Notice that the set $\boldsymbol{H}$ is the closure of $\boldsymbol{V}$ in $\boldsymbol{L}^2$ with

$$\boldsymbol{V} \subset \boldsymbol{H} \subset \boldsymbol{V}'.$$

We also define the temperature space as follows

$$H^1_{\Gamma_D}(\Omega) = \Big\{ \varphi \in H^1(\Omega) : \qquad \varphi = 0, \quad \text{on} \quad \Gamma_D \Big\}.$$

The space $H^1_{\Gamma_D}(\Omega)$ can be provided with the $H^1_0(\Omega)$-norm, and based on the Poincaré-Friedrichs inequality $|\varphi|_{1,\Omega} = \|\nabla\varphi\|$. The dual of $H^1_{\Gamma_D}(\Omega)$ is denoted by $H^{-1}_{\Gamma_D}$ and its norm is also denoted by $\|\cdot\|_{-1}$ when there is no confusion and the context is clear. The traces of functions in $H^1_{\Gamma_D}(\Omega)$ on Γ_N belong to a special space $H_{00}^{\frac{1}{2}}(\Gamma_N)$, see [51, Chap.1] for the definition of this space. We also introduce its dual space $H_{00}^{\frac{1}{2}}(\Gamma_N)'$ and denote by $\langle\cdot,\cdot\rangle_{\Gamma_N}$ the duality pairing between $H_{00}^{\frac{1}{2}}(\Gamma_N)$ and $H_{00}^{\frac{1}{2}}(\Gamma_N)'$. Thus, we assume that the partition of $\partial\Omega$ into Γ_N and Γ_D is sufficiently smooth for $\mathcal{D}(\Omega\cup\Gamma_N)$ to be dense in $H^1_{\Gamma_D}(\Omega)$ (sufficient conditions for this are given in [52] among others). Next, let us recall some useful properties that can be found for example in [53]: For all $\boldsymbol{u} \in \boldsymbol{V}$, $\boldsymbol{v}, \boldsymbol{w} \in \boldsymbol{H}^1(\Omega)$ and $\varphi, \psi \in H^1(\Omega)$,

$$\begin{aligned} &\textstyle\int_\Omega (\boldsymbol{u}\cdot\nabla)\boldsymbol{v}\cdot\boldsymbol{v}\,d\boldsymbol{x} = 0, \qquad \textstyle\int_\Omega (\boldsymbol{u}\cdot\nabla)\boldsymbol{v}\cdot\boldsymbol{w}\,d\boldsymbol{x} = -\textstyle\int_\Omega (\boldsymbol{u}\cdot\nabla)\boldsymbol{w}\cdot\boldsymbol{v}\,d\boldsymbol{x}, \\ &\textstyle\int_\Omega (\boldsymbol{u}\cdot\nabla)\varphi\cdot\varphi\,d\boldsymbol{x} = 0, \qquad \textstyle\int_\Omega (\boldsymbol{u}\cdot\nabla)\varphi\cdot\psi\,d\boldsymbol{x} = -\textstyle\int_\Omega (\boldsymbol{u}\cdot\nabla)\psi\cdot\varphi\,d\boldsymbol{x}, \end{aligned} \tag{8}$$

and

$$\int_\Omega (\boldsymbol{u}\cdot\nabla)\boldsymbol{v}\cdot\boldsymbol{w}\,d\boldsymbol{x} \le \begin{cases} C|\boldsymbol{u}|_1|\boldsymbol{v}|_1|\boldsymbol{w}|_1, & \text{for all } \boldsymbol{u},\boldsymbol{v},\boldsymbol{w} \in \boldsymbol{H}_0^1(\Omega), \\ C\|\boldsymbol{u}\|\,\|\boldsymbol{v}\|_2\,|\boldsymbol{w}|_1, & \text{for all } \boldsymbol{v} \in \boldsymbol{H}^2(\Omega)\cap\boldsymbol{H}_0^1(\Omega),\ \boldsymbol{u},\boldsymbol{w} \in \boldsymbol{H}_0^1(\Omega), \\ C\|\boldsymbol{u}\|\,|\boldsymbol{v}|_1\,\|\boldsymbol{w}\|_2, & \text{for all } \boldsymbol{w} \in \boldsymbol{H}^2(\Omega)\cap\boldsymbol{H}_0^1(\Omega),\ \boldsymbol{u},\boldsymbol{v} \in \boldsymbol{H}_0^1(\Omega), \\ C\|\boldsymbol{u}\|_2\,|\boldsymbol{v}|_1\,\|\boldsymbol{w}\|, & \text{for all } \boldsymbol{u} \in \boldsymbol{H}^2(\Omega)\cap\boldsymbol{H}_0^1(\Omega),\ \boldsymbol{v},\boldsymbol{w} \in \boldsymbol{H}_0^1(\Omega), \\ C|\boldsymbol{u}|_1\,|\boldsymbol{v}|_1\,\|\boldsymbol{w}\|^{1/2}\,|\boldsymbol{w}|_1^{1/2}, & \text{for all } \boldsymbol{u},\boldsymbol{v},\boldsymbol{w} \in \boldsymbol{H}_0^1(\Omega), \\ C\|\boldsymbol{u}\|^{1/2}\,|\boldsymbol{u}|_1^{1/2}\,|\boldsymbol{v}|_1\,|\boldsymbol{w}|_1, & \text{for all } \boldsymbol{u},\boldsymbol{v},\boldsymbol{w} \in \boldsymbol{H}_0^1(\Omega), \end{cases} \tag{9}$$

where C is a generic constant independent from the time step that may have different expressions at each occurrence.

For the time integration of equations (4)-(6), we divide the time interval $[0, T_f]$ into $N+1$ sub-intervals $[t_n, t_{n+1}]$ with length $\Delta t = t_{n+1} - t_n$, $0 = t_0 < t_1 < \cdots < t_{N+1} = T_f$, and we use the notation $\boldsymbol{w}^n = \boldsymbol{w}(t_n, \boldsymbol{x})$ as the value of a generic function w at time t_n. We also announce the following discrete Gronwall lemma [54] that will be used several times in what follows:

Lemma 1. *For $n \in \mathbb{N}$, let κ, a_n, b_n, c_n and d_n be nonnegative numbers such that*

$$a_N + \Delta t \sum_{n=0}^{N} b_n \leq \kappa + \Delta t \sum_{n=0}^{N-1} a_n\, d_n + \Delta t \sum_{n=0}^{N-1} c_n, \qquad \forall\, N \geq 1.$$

Then, for all $N \geq 1$, the following inequality

$$a_N + \Delta t \sum_{n=0}^{N} b_n \leq \left(\kappa + \Delta t \sum_{n=0}^{N-1} c_n \right) \exp \left(\Delta t \sum_{n=0}^{N-1} d_n \right),$$

holds.

■

3. Time viscosity-splitting method for incompressible flows

In this section we formulate the proposed time viscosity-splitting method for solving the incompressible flows with temperature-dependent viscosity and thermal conductivity governed by the coupled system (4)-(6). To this end we assume that

$$\begin{array}{ll} g \in L^2\left(0, T_f; L^2(\Omega)\right), & \theta_N \in L^2\left(0, T_f; H^{\frac{1}{2}}_{00}(\Gamma_N)'\right), \\ \theta_D \in L^2\left(0, T_f; H^{\frac{1}{2}}(\Gamma_D)\right), & \partial_t \theta_D \in L^2\left(0, T_f; L^2(\Gamma_D)\right). \end{array} \tag{10}$$

Thanks to Lemma 2.8 in [9], for all $\varepsilon > 0$, there exists a lifting $\mathcal{R}_\theta \in H^1(\Omega)$ of the value of θ_D on Γ_D and satisfying for $a.e\ \ t \in (0, T_f)$

$$\|\mathcal{R}_\theta\|_{L^4(\Omega)} \leq \varepsilon \|\theta_D\|_{H^{\frac{1}{2}}(\Gamma_D)} \qquad \text{and} \qquad \|\mathcal{R}_\theta\|_{H^1(\Omega)} \leq c_{\mathcal{R}} \|\theta_D\|_{H^{\frac{1}{2}}(\Gamma_D)}, \tag{11}$$

where the constant $c_{\mathcal{R}}$ depends only on Ω. Since θ_D belongs to $L^2\left(0, T_f; H^{\frac{1}{2}}(\Gamma_D)\right)$, $\mathcal{R}_\theta$ belongs to $L^2\left(0, T_f; H^1(\Omega)\right)$ and

$$\begin{aligned} \|\mathcal{R}_\theta\|_{L^2(0,T_f;H^1(\Omega))} &\leq c_{\mathcal{R}} \|\theta_D\|_{L^2\left(0,T_f;H^{\frac{1}{2}}(\Gamma_D)\right)}, \\ \|\mathcal{R}_\theta\|_{L^2(0,T_f;L^4(\Omega))} &\leq \varepsilon \|\theta_D\|_{L^2\left(0,T_f;H^{\frac{1}{2}}(\Gamma_D)\right)}. \end{aligned} \tag{12}$$

Furthermore, from (10), $\partial_t \theta_D \in L^2\left(0, T_f; L^2(\Gamma_D)\right)$, we have also $\partial_t \mathcal{R}_\theta \in L^2\left(0, T_f; L^2(\Omega)\right)$. Let us introduce the following notation

$$\widehat{\theta} := \theta + \mathcal{R}_\theta.$$

Finally, the weak formulation of (4)-(6) can be written as follows: Find $\boldsymbol{u} \in L^2\left(0, T_f; \boldsymbol{H}^1_0(\Omega)\right) \cap H^1\left(0, T_f; \boldsymbol{L}^2(\Omega)\right)$, $p \in L^2\left(0, T_f; L^2_0(\Omega)\right)$ and $\theta \in L^2\left(0, T_f; H^1_{\Gamma_D}(\Omega)\right) \cap H^1\left(0, T_f; L^2(\Omega)\right)$ such that for all $(\boldsymbol{v}, q, \varphi)$ in $\boldsymbol{H}^1_0(\Omega) \times L^2_0(\Omega) \times H^1_{\Gamma_D}(\Omega)$

$$\begin{aligned} \int_\Omega (\partial_t \boldsymbol{u} + (\boldsymbol{u} \cdot \nabla)\boldsymbol{u}) \cdot \boldsymbol{v}\, d\boldsymbol{x} + \int_\Omega \nu(\theta_{\mathcal{R}})\, \nabla \boldsymbol{u} : \nabla \boldsymbol{v}\, d\boldsymbol{x} - \int_\Omega \nabla \cdot \boldsymbol{v}\, p\, d\boldsymbol{x} &= \alpha \int_\Omega \boldsymbol{f}(\theta_{\mathcal{R}}) \cdot \boldsymbol{v}\, d\boldsymbol{x}, \\ \int_\Omega \nabla \cdot \boldsymbol{u}\, q\, d\boldsymbol{x} &= 0, \end{aligned} \tag{13}$$

$$
\int_\Omega (\partial_t\theta + \boldsymbol{u}\cdot\nabla\theta)\,\varphi\, d\boldsymbol{x} + \int_\Omega \lambda(\theta_{\mathcal{R}})\,\nabla\theta\cdot\nabla\varphi\, d\boldsymbol{x} = \int_\Omega (-\partial_t\mathcal{R}_\theta - \boldsymbol{u}\cdot\nabla\,\mathcal{R}_\theta)\,\varphi\, d\boldsymbol{x} - \int_\Omega \lambda(\theta_{\mathcal{R}})\nabla\mathcal{R}_\theta\cdot\nabla\varphi\, d\boldsymbol{x} + \int_\Omega g\,\varphi + \langle\theta_N,\varphi\rangle_{\Gamma_N}. \tag{14}
$$

Using a first-order implicit scheme for the time integration of (13)-(14) results in a system of the form

$$
\begin{aligned}
\int_\Omega \frac{\boldsymbol{u}^{n+1}-\boldsymbol{u}^n}{\Delta t}\cdot\boldsymbol{v}\, d\boldsymbol{x} + \int_\Omega \left(\boldsymbol{u}^{n+1}\cdot\nabla\right)\boldsymbol{u}^{n+1}\cdot\boldsymbol{v}\, d\boldsymbol{x} + \int_\Omega \nu(\theta^{n+1}+\mathcal{R}_\theta^{n+1})\nabla\boldsymbol{u}^{n+1} : \nabla\boldsymbol{v}\, d\boldsymbol{x}& \\
-\int_\Omega (\nabla\cdot\boldsymbol{v})\,p^{n+1}\, d\boldsymbol{x} = \int_\Omega \alpha\boldsymbol{f}(\theta^{n+1}+\mathcal{R}_\theta^{n+1})\cdot\boldsymbol{v}\, d\boldsymbol{x},& \quad (15)\\
\int_\Omega (\nabla\cdot\boldsymbol{u}^{n+1})\,q\, d\boldsymbol{x} = 0,&
\end{aligned}
$$

$$
\int_\Omega \frac{\theta^{n+1}-\theta^n}{\Delta t}\varphi\, d\boldsymbol{x} + \int_\Omega \left(\boldsymbol{u}^{n+1}\cdot\nabla\right)\theta^{n+1}\varphi\, d\boldsymbol{x} + \int_\Omega (\lambda(\theta^{n+1}+\mathcal{R}_\theta^{n+1})\nabla\theta^{n+1})\cdot\nabla\varphi\, d\boldsymbol{x} = -\int_\Omega \partial_t\mathcal{R}_\theta^{n+1}\varphi\, d\boldsymbol{x}
- \int_\Omega \left(\boldsymbol{u}^{n+1}\cdot\nabla\right)\mathcal{R}_\theta^{n+1}\varphi\, d\boldsymbol{x} - \int_\Omega \lambda(\theta^{n+1}+\mathcal{R}_\theta^{n+1})\nabla\mathcal{R}_\theta^{n+1}\cdot\nabla\varphi\, d\boldsymbol{x} + \int_\Omega g^{n+1}\varphi\, d\boldsymbol{x} + \langle\theta_N^{n+1},\varphi\rangle_{\Gamma_N}. \tag{16}
$$

It should be stressed that to study the stability of the semi-discrete solution $(\boldsymbol{u}^{n+1},\theta^{n+1})$, we take $\boldsymbol{v}=\boldsymbol{u}^{n+1}$ and $\varphi=\theta^{n+1}$ and deduce the following result:

Lemma 2. *For large enough ν_0, the semi-discrete solution $(\boldsymbol{u}^{n+1},\theta^{n+1})$ given by the scheme* (15)-(16), *satisfies*

$$
\begin{aligned}
\|\boldsymbol{u}^{N+1}\|^2 + \|\theta^{N+1}\|^2 + \sum_{n=0}^{N}\left(\|\boldsymbol{u}^{n+1}-\boldsymbol{u}^n\|^2 + \|\theta^{n+1}-\theta^n\|^2\right) + \frac{\nu_0\Delta t}{2}\sum_{n=0}^{N}\|\nabla\boldsymbol{u}^{n+1}\|^2 + \frac{\lambda_0\Delta t}{4}\sum_{n=0}^{N}\|\nabla\theta^{n+1}\|^2& \\
\le \|\boldsymbol{u}_0\|^2 + \|\theta_0\|^2 + \frac{\nu_0\Delta t}{2}\|\nabla\boldsymbol{u}_0\|^2 + \frac{\lambda_0\Delta t}{4}\|\nabla\theta_0\|^2 + C\|\theta_D\|^2_{l^2(0,T_f;H^{\frac{1}{2}}(\Gamma_D))}& \\
+ C\left(\|\partial_t\theta_D\|^2_{l^2(0,T_f;L^2(\Gamma_D))} + \|g\|^2_{l^2(0,T_f;L^2(\Omega))} + \|\theta_N\|^2_{l^2(0,T_f;H_{00}^{\frac{1}{2}}(\Gamma_N)')}\right).& \quad (17)
\end{aligned}
$$

■

The resulting viscosity-splitting method considered in this study to solve the equations (15)-(16) is carried out using the following two steps:

Step 1: For all $\boldsymbol{v}\in\boldsymbol{H}_0^1(\Omega)$, compute $\bar{\boldsymbol{u}}^{n+1}\in\boldsymbol{H}_0^1(\Omega)$ solution of

$$
\int_\Omega \frac{\bar{\boldsymbol{u}}^{n+1}-\boldsymbol{u}^n}{\Delta t}\cdot\boldsymbol{v}\, d\boldsymbol{x} + \int_\Omega (\boldsymbol{u}^n\cdot\nabla)\,\bar{\boldsymbol{u}}^{n+1}\cdot\boldsymbol{v}\, d\boldsymbol{x} + \int_\Omega \nu\left(\theta^n+\mathcal{R}_\theta^{n+1}\right)\nabla\bar{\boldsymbol{u}}^{n+1} : \nabla\boldsymbol{v}\, d\boldsymbol{x} = \alpha\int_\Omega \boldsymbol{f}\left(\theta^n+\mathcal{R}_\theta^{n+1}\right)\cdot\boldsymbol{v}\, d\boldsymbol{x}. \tag{18}
$$

Step 2: For all $\varphi\in H^1_{\Gamma_D}(\Omega)$, compute $\bar{\theta}^{n+1}\in H^1_{\Gamma_D}(\Omega)$ solution of

$$
\begin{aligned}
\int_\Omega \frac{\bar{\theta}^{n+1}-\theta^n}{\Delta t}\varphi\, d\boldsymbol{x} + \int_\Omega \bar{\boldsymbol{u}}^{n+1}\cdot\nabla\bar{\theta}^{n+1}\varphi\, d\boldsymbol{x} + \int_\Omega \frac{1}{2}\bar{\theta}^{n+1}\,\nabla\cdot\bar{\boldsymbol{u}}^{n+1}\varphi\, d\boldsymbol{x} +& \\
\int_\Omega \lambda(\theta^n+\mathcal{R}_\theta^{n+1})\,\nabla\bar{\theta}^{n+1}\cdot\nabla\varphi\, d\boldsymbol{x} = -\int_\Omega \lambda(\theta^n+\mathcal{R}_\theta^{n+1})\nabla\mathcal{R}_\theta^{n+1}\cdot\nabla\varphi\, d\boldsymbol{x} - \int_\Omega \bar{\boldsymbol{u}}^{n+1}\cdot\nabla\,\mathcal{R}_\theta^{n+1}\varphi\, d\boldsymbol{x}& \\
-\int_\Omega \frac{1}{2}\mathcal{R}_\theta^{n+1}\,\nabla\cdot\bar{\boldsymbol{u}}^{n+1}\varphi\, d\boldsymbol{x} + \int_\Omega g^{n+1}\,\varphi\, d\boldsymbol{x} + \langle\theta_N^{n+1},\,\varphi\rangle - \int_\Omega \partial_t\mathcal{R}_\theta^{n+1}\varphi\, d\boldsymbol{x}.& \quad (19)
\end{aligned}
$$

Step 3: For all $(\boldsymbol{v}, q) \in \boldsymbol{V} \times L_0^2(\Omega)$, compute $\left(\boldsymbol{u}^{n+1}, p^{n+1}\right) \in \boldsymbol{V} \times L_0^2(\Omega)$ solution of the following Stokes problem

$$\int_\Omega \frac{\boldsymbol{u}^{n+1} - \bar{\boldsymbol{u}}^{n+1}}{\Delta t} \cdot \boldsymbol{v}\, d\boldsymbol{x} + \int_\Omega \nu(\bar{\theta}^{n+1} + \mathcal{R}_\theta^{n+1}) \nabla \boldsymbol{u}^{n+1} : \nabla \boldsymbol{v}\, d\boldsymbol{x} - \int_\Omega p^{n+1}\, \nabla \cdot \boldsymbol{v}\, d\boldsymbol{x} = \int_\Omega \nu(\theta^n + \mathcal{R}_\theta^{n+1}) \nabla \bar{\boldsymbol{u}}^{n+1} : \nabla \boldsymbol{v}\, d\boldsymbol{x}, \quad (20)$$

$$- \int_\Omega q\, \nabla \cdot \boldsymbol{u}^{n+1}\, d\boldsymbol{x} = 0.$$

Step 4: For all $\varphi \in H^1_{\Gamma_D}(\Omega)$, compute $\theta^{n+1} \in H^1_{\Gamma_D}(\Omega)$ solution of

$$\int_\Omega \frac{\theta^{n+1} - \bar{\theta}^{n+1}}{\Delta t} \varphi\, d\boldsymbol{x} + int_\Omega \lambda(\bar{\theta}^{n+1} + \mathcal{R}_\theta^{n+1})\, \nabla \theta^{n+1} \cdot \nabla \varphi\, d\boldsymbol{x} = \int_\Omega \lambda(\theta^n + \mathcal{R}_\theta^{n+1})\, \nabla \bar{\theta}^{n+1} \cdot \nabla \varphi\, d\boldsymbol{x}. \quad (21)$$

Notice that in this work, we opt to not include any pressure-correction strategy for the sake of clarity since we are mainly interested in the error analysis of the considered viscosity-splitting method. It should be noted though used in our case, a pressure-correction procedure would have no advantage on the error estimates, see for example [45]. Some remarks are in order:

i. In (19), the Neuman boundary condition on the intermediate temperature is set as

$$\lambda(\theta^n + \mathcal{R}_\theta^{n+1}) \frac{\partial \bar{\theta}^{n+1}}{\partial n} = \theta_N^{n+1},$$

while in (21), the Neuman boundary condition on the end-of-step temperature is taken to be

$$\lambda(\bar{\theta}^{n+1} + \mathcal{R}_\theta^{n+1}) \frac{\partial \theta^{n+1}}{\partial n} = \theta_N^{n+1}.$$

ii. Treating the nonlinear term in the momentum equation semi-implicitly removes the nonlinearity, thus there is no need for a fixed-point iteration. In addition, the temperature-dependent parameters are treated explicitly which removes the coupling between the velocity and temperature solutions.

iii. Note that in (19), the temperature is advected by the intermediate velocity which is not necessarily divergence-free. As stated earlier in the introduction, This particular term requires subtle treatment in order to derive the full order for the error estimates.

4. Error estimates for the viscosity-splitting method

We first provide the error estimates in $l^\infty(0, T; \boldsymbol{L}^2(\Omega))$ and $l^2(0, T; \boldsymbol{H}^1(\Omega))$ norms for the approximation of $\boldsymbol{u}$ by the semi-discrete velocities $\bar{\boldsymbol{u}}^{n+1}$ and $\boldsymbol{u}^{n+1}$ using (18) in **Step 2** and (20) in **Step 4**, which give a bound where some terms still appear in the temperature solution. Then, this bound is injected into the temperature error bound, which will be established later using (19) in **Step 1** and (21) in **Step 3**, to have 1/2-order estimates for the approximation of θ by the semi-discrete temperature solutions $\bar{\theta}^{n+1}$ and θ^{n+1} in $l^\infty(0, T, L^2(\Omega))$ and $l^2(0, T; H^1(\Omega))$ norms. Thereafter, injecting these last temperature estimates back into the velocity error bound will ensures 1/2-order estimates as well for the semi-discrete velocity solutions. Finally, these bounds will be improved to reach full first-order estimates for both the velocity and the temperature solutions. We will also give error estimates for the pressure approximation using the considered viscosity-splitting method. To this end, let set the following assumptions which will be repeatedly used in proofs of the error estimates established in this section

$$\begin{cases} \underset{t\in(0,T_f)}{sup} \left\{\|\theta(t)\|_2^2 + \|\partial_{tt}\theta\|_{-1}^2 + \|\partial_t\theta\|^2\right\} \leq C. & (22)\\ \underset{t\in(0,T_f)}{sup} \left\{\|\boldsymbol{u}\|_2^2 + \|\partial_{tt}\boldsymbol{u}\|_{-1}^2 + \|\partial_t\boldsymbol{u}\|^2 + \|p(t)\|_1^2\right\} \leq C. & (23)\\ \boldsymbol{u} \in L^\infty\left(0,T_f;\boldsymbol{W}^{2,3+s}(\Omega)\right),\ s>0, \quad \text{which implies} \quad \sup_{t\in(0,T_f)} \|\nabla\boldsymbol{u}(t)\|^2_{\mathbf{R}^{d\times d}} \leq C. & (24)\\ \theta \in L^\infty\left(0,T_f;W^{2,3+s}(\Omega)\right),\ s>0, \quad \text{which implies} \quad \sup_{t\in(0,T_f)} \|\nabla\theta(t)\|^2_{\mathbf{R}^{d}} \leq C. & (25) \end{cases}$$

It should be stressed that all the above assumptions are achievable. For instance:

i. If the initial data satisfy $(\boldsymbol{u}_0,\theta_0) \in \left(\boldsymbol{H}^2(\Omega)\cap\boldsymbol{V}\right)\times H^2(\Omega)$ and $(g,\partial_t g) \in L^\infty(0,T_f;L^2(\Omega))\times L^2(0,T_f;L^2(\Omega))$, then (see for example [50])

$$(\boldsymbol{u},\theta) \in L^\infty(0,T_f;\boldsymbol{H}^2(\Omega))\times L^\infty(0,T_f;H^2(\Omega)) \quad \text{and} \quad \nabla p \in L^\infty(0,T_f;\boldsymbol{L}^2(\Omega)).$$

ii. Additionally, following for instance [55, 56], if the domain Ω is of class C^2 or it is a convex polygon, then

$$\sqrt{t}\,(\partial_{tt}\boldsymbol{u},\partial_{tt}\theta) \in L^2(0,T_f;\boldsymbol{L}^2(\Omega))\times L^2(0,T_f;L^2(\Omega)).$$

iii. Furthermore, as demonstrated in [57, 58], when certain nonlocal compatibility conditions at $t=0$ are introduced,

$$(\partial_{tt}\boldsymbol{u},\partial_{tt}\theta) \in L^2(0,T_f;\boldsymbol{V}')\times L^2(0,T_f;H^{-1}(\Omega)).$$

iv. The last two regularity assumptions (24) and (25) are satisfied based on the general theory for elliptic systems by Agmon-Douglis-Nirenberg [59, 60]. This methodology can also be applied to prove the regularity results for the Navier-Stokes equations, see for example [50]. However, we must assume initial conditions $(\boldsymbol{u}_0,\theta_0)$ in $\left(\boldsymbol{W}^{2,3+s}(\Omega)\cap\boldsymbol{V}\right)\times W^{2,3+s}(\Omega)$, the boundary condition $\theta_D \in W^{2-\frac{1}{3+s},3+s}(\Gamma_D)$ and the source term $(g,\partial_t g)$ belongs to $L^\infty(0,T_f;W^{-1,3+s}(\Omega))\times L^2(0,T_f;W^{-1,3+s}(\Omega))$.

v. Finally, it is well-known that if $C\dfrac{\alpha}{\nu_0^2} < 1$ (where $C>0$ depends only on Ω) then, the Navier-Stokes system is well-posed, see for instance [50, 61, 62, 47]. Indeed, while $C\dfrac{\alpha}{\nu_0^2} < 1$ is not a necessary condition for the uniqueness, it is known that for sufficiently large data (*i.e.*, ν_0 small enough), the uniqueness breaks down [61], and the Navier-Stokes equations would admit multiple solutions. This means that the value of the viscosity ν_0 should not be too small and, for similar reasons, the value of λ_0 must not be very small. For brevity, one can demonstrate this by considering the simple equation

$$-\nabla\cdot(\lambda(\theta)\nabla\theta) = g. \tag{26}$$

Therefore, the uniqueness of the solution for this equations is obtained by taking the difference between two solutions θ_1 and θ_2 and writing

$$\lambda_0\|\nabla(\theta_1-\theta_2)\|^2 \leq \int_\Omega |\lambda(\theta_1)-\lambda(\theta_2)|\,|\nabla\theta_1|\,\nabla(\theta_1-\theta_2)\,d\boldsymbol{x} \ \leq C\lambda_2\,\|\nabla\theta_1\|_{L^\infty}\,\|\nabla(\theta_1-\theta_2)\|^2,$$

where $\lambda_2 = \|\lambda'\|_\infty$, and using the regularity condition (25) to control the integral in the right-hand side. Hence, it is clear that one must assume $C\dfrac{\lambda_2}{\lambda_0}\|\theta_1\|_{W^{1,3+s}} < 1$ to get $\theta_1=\theta_2$ except for the situation with a constant diffusion coefficient (in this case $\lambda_2=0$). Note that the regularity condition (24) would appear if one adds the transport term $\boldsymbol{u}\cdot\nabla\theta$ to the equation (26).

Additionally, let $\bar{e}_\theta^{n+1}$, e_θ^{n+1}, $\bar{\boldsymbol{e}}_u^{n+1}$ and $\boldsymbol{e}_u^{n+1}$ be respectively, the semi-discrete errors associated to $\bar{\theta}^{n+1}$, θ^{n+1}, $\bar{\boldsymbol{u}}^{n+1}$ and $\boldsymbol{u}^{n+1}$ defined as

$$\begin{aligned} \bar{e}_\theta^{n+1} &= \theta(t_{n+1}) - \bar{\theta}^{n+1}, & e_\theta^{n+1} &= \theta(t_{n+1}) - \theta^{n+1}, \\ \bar{\boldsymbol{e}}_u^{n+1} &= \boldsymbol{u}(t_{n+1}) - \bar{\boldsymbol{u}}^{n+1}, & \boldsymbol{e}_u^{n+1} &= \boldsymbol{u}(t_{n+1}) - \boldsymbol{u}^{n+1}. \end{aligned}$$

The following lemma delivers a first bound for the velocity errors $\bar{\boldsymbol{e}}_u^{n+1}$ and $\boldsymbol{e}_u^{n+1}$ in $\mathrm{L}^\infty(0,T;\boldsymbol{L}^2(\Omega))$ and $L^2(0,T;\boldsymbol{H}^1(\Omega))$ norms

Lemma 3. *Assuming* (7), (3), (22), (23) *and* (24) *in addition to* $\nu_1 < 2\nu_0$, *then*

$$\|\boldsymbol{e}_u^{N+1}\|^2 + \sum_{n=0}^{N}\left(\|\bar{\boldsymbol{e}}_u^{n+1} - \boldsymbol{e}_u^n\|^2 + \frac{1}{2}\|\boldsymbol{e}_u^{n+1} - \bar{\boldsymbol{e}}_u^{n+1}\|^2\right) + \frac{\nu_0\Delta t}{2}\sum_{n=0}^{N}|\bar{\boldsymbol{e}}_u^{n+1}|_1^2 +$$
$$\Delta t\sum_{n=0}^{N}\left((2\nu_0 - \nu_1)|\boldsymbol{e}_u^{n+1}|_1^2 + \frac{\nu_0}{2}|\boldsymbol{e}_u^{n+1} - \bar{\boldsymbol{e}}_u^{n+1}|_1^2\right) \le C\Delta t + C\Delta t\sum_{n=0}^{N}\left(\|e_\theta^n\|^2 + \|\bar{e}_\theta^{n+1} - e_\theta^n\|^2\right). \quad \square$$

Proof. Reformulating the momentum equation (4) at $t = t_{n+1}$, including the lifting $\mathcal{R}_\theta$ of the temperature, and applying the Taylor's expansion with an integral reminder and taking the inner product with $\boldsymbol{v} \in \boldsymbol{H}_0^1(\Omega)$, we obtain

$$\int_\Omega \left(\frac{\boldsymbol{u}(t_{n+1}) - \boldsymbol{u}(t_n)}{\Delta t} + (\boldsymbol{u}(t_{n+1})\cdot\nabla)\boldsymbol{u}(t_{n+1})\right)\cdot\boldsymbol{v}\,d\boldsymbol{x} + \int_\Omega \nu(\theta_{\mathcal{R}}(t_{n+1}))\,\nabla\boldsymbol{u}(t_{n+1}) : \nabla\boldsymbol{v}\,d\boldsymbol{x}$$
$$- \int_\Omega p(t_{n+1})\,\nabla\cdot\boldsymbol{v}\,d\boldsymbol{x} = \alpha\int_\Omega \boldsymbol{f}(\theta_{\mathcal{R}}(t_{n+1}))\cdot\boldsymbol{v}\,d\boldsymbol{x} + \langle\boldsymbol{I}_u^n, \boldsymbol{v}\rangle, \quad (27)$$

where $\boldsymbol{I}_u^n$ is the truncation error associated with the velocity $\boldsymbol{u}$ and defined as

$$\boldsymbol{I}_u^n = \frac{1}{\Delta t}\int_{t_n}^{t_{n+1}}(t - t_n)\partial_{tt}\boldsymbol{u}(t)dt.$$

By subtracting (18) from (27), fixing $\boldsymbol{v} = 2\Delta t\bar{\boldsymbol{e}}_u^{n+1}$ and using the standard identity

$$2(a-b)a = a^2 - b^2 + (a-b)^2, \quad (28)$$

we obtain

$$\|\bar{\boldsymbol{e}}_u^{n+1}\|^2 - \|\boldsymbol{e}_u^n\|^2 + \|\bar{\boldsymbol{e}}_u^{n+1} - \boldsymbol{e}_u^n\|^2 + 2\Delta t\int_\omega \nu(\theta^n + \mathcal{R}_\theta^{n+1})\nabla\bar{\boldsymbol{e}}_u^{n+1} : \nabla\bar{\boldsymbol{e}}_u^{n+1}\,d\boldsymbol{x}$$
$$= 2\alpha\Delta t\int_\Omega \left(\boldsymbol{f}(\theta_{\mathcal{R}}(t_{n+1})) - \boldsymbol{f}(\theta^n + \mathcal{R}_\theta^{n+1})\right)\cdot\bar{\boldsymbol{e}}_u^{n+1}\,d\boldsymbol{x} - 2\Delta t\int_\Omega \nabla p(t_{n+1})\cdot\bar{\boldsymbol{e}}_u^{n+1}\,d\boldsymbol{x}$$
$$- 2\Delta t\int_\Omega (\boldsymbol{u}(t_{n+1})\cdot\nabla)\boldsymbol{u}(t_{n+1})\cdot\bar{\boldsymbol{e}}_u^{n+1}\,d\boldsymbol{x} + 2\Delta t\int_\Omega (\boldsymbol{u}^n\cdot\nabla)\bar{\boldsymbol{u}}_u^{n+1}\cdot\bar{\boldsymbol{e}}_u^{n+1}\,d\boldsymbol{x}$$
$$- 2\Delta t\int_\Omega \left(\nu(\theta_{\mathcal{R}}(t_{n+1})) - \nu(\theta^n + \mathcal{R}_\theta^{n+1})\right)\nabla\boldsymbol{u}(t_{n+1}) : \nabla\bar{\boldsymbol{e}}_u^{n+1}\,d\boldsymbol{x} + 2\Delta t\langle\boldsymbol{I}_u^n, \bar{\boldsymbol{e}}_u^{n+1}\rangle. \quad (29)$$

Taking $\boldsymbol{v} = 2\Delta t\boldsymbol{e}_u^{n+1}$ in (20),

$$\|\boldsymbol{e}_u^{n+1}\|^2 - \|\bar{\boldsymbol{e}}_u^{n+1}\|^2 + \|\boldsymbol{e}_u^{n+1} - \bar{\boldsymbol{e}}_u^{n+1}\|^2 + \Delta t\int_\Omega \left(2\nu(\bar{\theta}_{\mathcal{R}}^{n+1}) - \nu(\theta^n + \mathcal{R}_\theta^{n+1})\right)\nabla\boldsymbol{e}_u^{n+1} : \nabla\boldsymbol{e}_u^{n+1}\,d\boldsymbol{x}$$
$$- \Delta t\int_\Omega \nu(\theta^n + \mathcal{R}_\theta^{n+1})\nabla\bar{\boldsymbol{e}}_u^{n+1} : \nabla\bar{\boldsymbol{e}}_u^{n+1}\,d\boldsymbol{x} + \Delta t\int_\Omega \nu(\theta^n + \mathcal{R}_\theta^{n+1})\nabla(\boldsymbol{e}_u^{n+1} - \bar{\boldsymbol{e}}_u^{n+1}) : \nabla(\boldsymbol{e}_u^{n+1} - \bar{\boldsymbol{e}}_u^{n+1})\,d\boldsymbol{x}$$
$$= 2\Delta t\int_\Omega \left(\nu(\bar{\theta}_{\mathcal{R}}^{n+1}) - \nu(\theta^n + \mathcal{R}_\theta^{n+1})\right)\nabla\boldsymbol{u}(t_{n+1}) : \nabla\boldsymbol{e}_u^{n+1}\,d\boldsymbol{x}. \quad (30)$$

Adding (30) to (29) and using the assumptions on ν in (7), we obtain

$$\|\boldsymbol{e}_u^{n+1}\|^2-\|\boldsymbol{e}_u^n\|^2+\|\bar{\boldsymbol{e}}_u^{n+1}-\boldsymbol{e}_u^n\|^2+\|\boldsymbol{e}_u^{n+1}-\bar{\boldsymbol{e}}_u^{n+1}\|^2+\Delta t\left(\nu_0|\bar{\boldsymbol{e}}_u^{n+1}|_1^2+(2\nu_0-\nu_1)|\boldsymbol{e}_u^{n+1}|_1^2+\nu_0|\boldsymbol{e}_u^{n+1}-\bar{\boldsymbol{e}}_u^{n+1}|_1^2\right)$$
$$\le \underbrace{2\alpha\Delta t\int_\Omega \left(\boldsymbol{f}(\theta_{\mathcal{R}}(t_{n+1}))-\boldsymbol{f}(\theta^n+\mathcal{R}_\theta^{n+1})\right)\cdot\bar{\boldsymbol{e}}_u^{n+1}\,d\boldsymbol{x}}_{=B_1}\underbrace{-2\Delta t\int_\Omega \nabla p(t_{n+1})\cdot\bar{\boldsymbol{e}}_u^{n+1}\,d\boldsymbol{x}}_{=B_2}$$
$$\underbrace{-2\Delta t\left(\int_\Omega(\boldsymbol{u}(t_{n+1})\cdot\nabla)\boldsymbol{u}(t_{n+1})\cdot\bar{\boldsymbol{e}}_u^{n+1}\,d\boldsymbol{x}-\int_\Omega(\boldsymbol{u}^n\cdot\nabla)\bar{\boldsymbol{u}}^{n+1}\cdot\bar{\boldsymbol{e}}_u^{n+1}\,d\boldsymbol{x}\right)}_{=B_3}$$
$$\underbrace{-2\Delta t\int_\Omega\left(\nu(\theta_{\mathcal{R}}(t_{n+1}))-\nu(\theta^n+\mathcal{R}_\theta^{n+1})\right)\nabla\boldsymbol{u}(t_{n+1})\colon\nabla\bar{\boldsymbol{e}}_u^{n+1}\,d\boldsymbol{x}}_{=B_4}$$
$$\underbrace{+2\Delta t\int_\Omega\left(\nu(\bar{\theta}_{\mathcal{R}}^{n+1})-\nu(\theta^n+\mathcal{R}_\theta^{n+1})\right)\nabla\boldsymbol{u}(t_{n+1})\colon\nabla\boldsymbol{e}_u^{n+1}\,d\boldsymbol{x}}_{=B_5}+2\Delta t\langle\boldsymbol{I}_u^n,\bar{\boldsymbol{e}}_u^{n+1}\rangle$$

Next, we bound each term on the right-hand side separately.

- The integral residual term is bounded as

$$\begin{aligned}
2\Delta t\langle\boldsymbol{I}_u^n,\bar{\boldsymbol{e}}_u^{n+1}\rangle &\le C\Delta t\,\|\boldsymbol{I}_u^n\|_{-1}^2+\frac{\nu_0\Delta t}{10}\left|\bar{\boldsymbol{e}}_u^{n+1}\right|_1^2,\\
&\le \frac{C}{\Delta t}\left\|\int_{t_n}^{t_{n+1}}(t-t_n)\partial_{tt}\boldsymbol{u}(t)dt\right\|_{-1}^2+\frac{\nu_0\Delta t}{10}\left|\bar{\boldsymbol{e}}_u^{n+1}\right|_1^2,\\
&\le \frac{C}{\Delta t}\int_{t_n}^{t_{n+1}}(t-t_n)^2dt\int_{t_n}^{t_{n+1}}\|\partial_{tt}\boldsymbol{u}\|_{-1}^2\,dt+\frac{\nu_0\Delta t}{10}\left|\bar{\boldsymbol{e}}_u^{n+1}\right|_1^2,\\
&\le C(\Delta t)^2\int_{t_n}^{t_{n+1}}\|\partial_{tt}\boldsymbol{u}\|_{-1}^2dt+\frac{\nu_0\Delta t}{10}\left|\bar{\boldsymbol{e}}_u^{n+1}\right|_1^2.
\end{aligned}$$

- Using the second property in (3) on the function $\boldsymbol{f}$ and the Poincaré inequality on $\bar{e}_u^{n+1}$, we have

$$\begin{aligned}
B_1 &= 2\alpha\Delta t\int_\Omega\left(\boldsymbol{f}(\theta_{\mathcal{R}}(t_{n+1}))-\boldsymbol{f}(\theta^n+\mathcal{R}_\theta^{n+1})\right)\cdot\bar{\boldsymbol{e}}_u^{n+1}\,d\boldsymbol{x},\\
&\le 2\alpha\Delta t\|\theta(t_{n+1})-\theta(t_n)+e_\theta^n\|\|\bar{\boldsymbol{e}}_u^{n+1}\|,\\
&\le C(\Delta t)^2\int_{t_n}^{t_{n+1}}\|\partial_t\theta\|^2dt+C\Delta t\|e_\theta^n\|^2+\frac{\nu_0\Delta t}{10}|\bar{\boldsymbol{e}}_u^{n+1}|_1^2.
\end{aligned}$$

- Since $\boldsymbol{e}_u^{n+1}$ is divergence-free, the pressure term B_2 can be treated by

$$\begin{aligned}
B_2 &= -2\Delta t\int_\Omega\nabla p(t_{n+1})\cdot\bar{\boldsymbol{e}}_u^{n+1}\,d\boldsymbol{x}=2\Delta t\int_\Omega\nabla p(t_{n+1})\cdot\left(\boldsymbol{e}_u^{n+1}-\bar{\boldsymbol{e}}_u^{n+1}\right)\,d\boldsymbol{x}\\
&\le 2\Delta t|p(t_{n+1})|_1\left\|\boldsymbol{e}_u^{n+1}-\bar{\boldsymbol{e}}_u^{n+1}\right\|\le C(\Delta t)^2|p(t_{n+1})|_1^2+\frac{1}{2}\left\|\boldsymbol{e}_u^{n+1}-\bar{\boldsymbol{e}}_u^{n+1}\right\|^2.
\end{aligned}$$

- Thanks to the properties (8), the term B_3 can be rewritten as

$$\begin{aligned}
B_3 &= -2\Delta t\left(\int_\Omega(\boldsymbol{u}(t_{n+1})\cdot\nabla)\boldsymbol{u}(t_{n+1})\cdot\bar{\boldsymbol{e}}_u^{n+1}\,d\boldsymbol{x}-\int_\Omega(\boldsymbol{u}^n\cdot\nabla)\bar{\boldsymbol{u}}^{n+1}\cdot\bar{\boldsymbol{e}}_u^{n+1}\,d\boldsymbol{x}\right),\\
&= -2\Delta t\left(\int_\Omega(\boldsymbol{u}(t_{n+1})\cdot\nabla)\boldsymbol{u}(t_{n+1})\cdot\bar{\boldsymbol{e}}_u^{n+1}\,d\boldsymbol{x}-\int_\Omega(\boldsymbol{u}^n\cdot\nabla)\boldsymbol{u}(t_{n+1})\cdot\bar{\boldsymbol{e}}_u^{n+1}\,d\boldsymbol{x}\right),\\
&= -2\Delta t\int_\Omega\left((\boldsymbol{u}(t_{n+1})-\boldsymbol{u}(t_n))\cdot\nabla\right)\boldsymbol{u}(t_{n+1})\cdot\bar{\boldsymbol{e}}_u^{n+1}\,d\boldsymbol{x}-2\Delta t\int_\Omega(\boldsymbol{e}_u^n\cdot\nabla)\boldsymbol{u}(t_{n+1})\cdot\bar{\boldsymbol{e}}_u^{n+1}\,d\boldsymbol{x}.
\end{aligned}$$

Using (9) and taking into account the assumptions (23), this can be bounded as

$$\begin{aligned} B_3 &\leq 2\Delta t\,\|\boldsymbol{u}(t_{n+1})-\boldsymbol{u}(t_n)\|\,\|\boldsymbol{u}(t_{n+1})\|_2\,\left|\bar{\boldsymbol{e}}_u^{n+1}\right|_1 + 2\Delta t\,\|\boldsymbol{e}_u^n\|\,\|\boldsymbol{u}(t_{n+1})\|_2\,\left|\bar{\boldsymbol{e}}_u^{n+1}\right|_1, \\ &\leq C(\Delta t)^2\int_{t_n}^{t_{n+1}}\|\partial_t\boldsymbol{u}\|^2\,dt + C\Delta t\,\|\boldsymbol{e}_u^n\|^2 + \frac{\nu_0\Delta t}{10}\left|\bar{\boldsymbol{e}}_u^{n+1}\right|_1^2. \end{aligned}$$

- By assumptions (7) on the function ν

$$\begin{aligned} B_4 &= -2\Delta t\int_\Omega \left(\nu(\theta_{\mathcal{R}}(t_{n+1})) - \nu(\theta^n+\mathcal{R}_\theta^{n+1})\right)\nabla\boldsymbol{u}(t_{n+1})\colon\nabla\bar{\boldsymbol{e}}_u^{n+1}\,d\boldsymbol{x}, \\ &\leq 2\nu_2\Delta t\int_\Omega |\theta(t_{n+1})-\theta^n|\,|\nabla\boldsymbol{u}(t_{n+1})\colon\nabla\bar{\boldsymbol{e}}_u^{n+1}|\,d\boldsymbol{x}. \end{aligned}$$

Using the assumption (24), the above inequality is developed as follows

$$\begin{aligned} B_4 &\leq C\Delta t\|\theta(t_{n+1})-\theta^n\|\,|\bar{\boldsymbol{e}}_u^{n+1}|_1 \leq C\Delta t\|\theta(t_{n+1})-\theta(t_n)\|^2 + C\Delta t\|e_\theta^n\|^2 + \frac{\nu_0\Delta t}{10}|\bar{\boldsymbol{e}}_u^{n+1}|_1^2 \\ &\leq C(\Delta t)^2\int_{t_n}^{t_{n+1}}\|\partial_t\theta\|^2dt + C\Delta t\|e_\theta^n\|^2 + \frac{\nu_0\Delta t}{10}|\bar{\boldsymbol{e}}_u^{n+1}|_1^2. \end{aligned}$$

- Again, thanks to the properties (7) of the function ν and the assumption (24) on the exact velocity u, we have

$$\begin{aligned} B_5 &= 2\Delta t\int_\Omega \left(\nu(\bar{\theta}_{\mathcal{R}}^{n+1}) - \nu(\theta^n+\mathcal{R}_\theta^{n+1})\right)\nabla\boldsymbol{u}(t_{n+1})\colon\nabla\boldsymbol{e}_u^{n+1}\,d\boldsymbol{x} \leq C\Delta t\|\bar{\theta}^{n+1}-\theta^n\|\,|\boldsymbol{e}_u^{n+1}|_1, \\ &\leq C(\Delta t)^2\int_{t_n}^{t_{n+1}}\|\partial_t\theta\|^2dt + C\Delta t\|\bar{e}_\theta^{n+1}-e_\theta^n\|^2 + \frac{\nu_0\Delta t}{2}|\boldsymbol{e}_u^{n+1}-\bar{\boldsymbol{e}}_u^{n+1}|_1^2 + \frac{\nu_0\Delta t}{10}|\bar{\boldsymbol{e}}_u^{n+1}|_1^2. \end{aligned}$$

Gathering the above inequalities and taking the sum over $n = 0, 1, \ldots, N$, we obtain

$$\begin{aligned} &\|\boldsymbol{e}_u^{N+1}\|^2 + \sum_{n=0}^N\left(\|\bar{\boldsymbol{e}}_u^{n+1}-\boldsymbol{e}_u^n\|^2 + \frac{1}{2}\|\boldsymbol{e}_u^{n+1}-\bar{\boldsymbol{e}}_u^{n+1}\|^2\right) + \\ &\qquad \Delta t\sum_{n=0}^N\left(\frac{\nu_0}{2}|\bar{\boldsymbol{e}}_u^{n+1}|_1^2 + (2\nu_0-\nu_1)|\boldsymbol{e}_u^{n+1}|_1^2 + \frac{\nu_0}{2}|\boldsymbol{e}_u^{n+1}-\bar{\boldsymbol{e}}_u^{n+1}|_1^2\right), \\ &\qquad \leq C\Delta t\sum_{n=0}^N\left(\|e_\theta^n\|^2 + \|\bar{e}_\theta^{n+1}-e_\theta^n\|^2\right) + C\Delta t\sum_{n=0}^N\|\boldsymbol{e}_u^n\|^2 + \\ &\qquad\qquad C(\Delta t)^2\sum_{n=0}^N|p(t_{n+1})|_1^2 + C(\Delta t)^2\int_0^{T_f}\left(\|\partial_{tt}\boldsymbol{u}\|_{-1}^2 + \|\partial_t\boldsymbol{u}\|^2 + \|\partial_t\theta\|^2\right)dt. \end{aligned}$$

Using the assumptions (23) and (22), the above inequality becomes

$$\begin{aligned} &\|\boldsymbol{e}_u^{N+1}\|^2 + \sum_{n=0}^N\left(\|\bar{\boldsymbol{e}}_u^{n+1}-\boldsymbol{e}_u^n\|^2 + \frac{1}{2}\|\boldsymbol{e}_u^{n+1}-\bar{\boldsymbol{e}}_u^{n+1}\|^2\right) + \\ &\qquad \Delta t\sum_{n=0}^N\left(\frac{\nu_0}{2}|\bar{\boldsymbol{e}}_u^{n+1}|_1^2 + (2\nu_0-\nu_1)|\boldsymbol{e}_u^{n+1}|_1^2 + \frac{\nu_0}{2}|\boldsymbol{e}_u^{n+1}-\bar{\boldsymbol{e}}_u^{n+1}|_1^2\right), \\ &\qquad\qquad \leq C\Delta t + C\Delta t\sum_{n=0}^N\|\boldsymbol{e}_u^n\|^2 + C\Delta t\sum_{n=0}^N\left(\|e_\theta^n\|^2 + \|\bar{e}_\theta^{n+1}-e_\theta^n\|^2\right). \end{aligned}$$

Applying the discrete Gronwall Lemma 1, we get

$$\|\boldsymbol{e}_u^{N+1}\|^2 + \sum_{n=0}^{N}\left(\|\bar{\boldsymbol{e}}_u^{n+1} - \boldsymbol{e}_u^n\|^2 + \frac{1}{2}\|\boldsymbol{e}_u^{n+1} - \bar{\boldsymbol{e}}_u^{n+1}\|^2\right) +$$
$$\Delta t \sum_{n=0}^{N}\left(\frac{\nu_0}{2}|\bar{\boldsymbol{e}}_u^{n+1}|_1^2 + (2\nu_0 - \nu_1)|\boldsymbol{e}_u^{n+1}|_1^2 + \frac{\nu_0}{2}|\boldsymbol{e}_u^{n+1} - \bar{\boldsymbol{e}}_u^{n+1}|_1^2\right),$$
$$\leq C\Delta t + C\Delta t \sum_{n=0}^{N}\left(\|e_\theta^n\|^2 + \|\bar{e}_\theta^{n+1} - e_\theta^n\|^2\right). \quad \blacksquare$$

The next lemma establishes a 1/2-error estimates for the temperature solution in $l^\infty\left(0, T_f; L^2(\Omega)\right)$ and $l^2\left(0, T_f; H^1(\Omega)\right)$ norms. Before announcing the result, let first add this assumption

$$\theta_D \in L^\infty\left(0, T_f; W^{\frac{2+s}{3+s}, 3+s}(\Gamma_D)\right), \qquad s > 0, \tag{31}$$

which will be required to prove the temperature error estimates in three space dimensions. It is worth noting that this additional assumption is due only to the non-homogeneous Dirichlet boundary conditions on the temperature. Thanks to (31), the lifting $\mathcal{R}_\theta$ belong to $L^\infty\left(0, T_f; W^{2,3+s}(\Omega)\right)$ which implies that

$$\sup_{t\in(0,T_f)} \|\nabla \mathcal{R}_\theta(t)\|^2_{\mathbf{R}^d} \leq C.$$

Lemma 4. *Under the assumptions in (7), (22), (25), (31), $\lambda_1 < 2\lambda_0$ and for small enough Δt, we have*

$$\|e_\theta^{N+1}\|^2 + \frac{1}{2}\sum_{n=0}^{N}\|\bar{e}_\theta^{n+1} - e_\theta^n\|^2 + \sum_{n=0}^{N}\|e_\theta^{n+1} - \bar{e}_\theta^{n+1}\|^2 +$$
$$\Delta t \sum_{n=0}^{N}\left(\frac{\lambda_0}{2}|\bar{e}_\theta^{n+1}|_1^2 + \frac{\lambda_0}{2}|e_\theta^{n+1} - \bar{e}_\theta^{n+1}|_1^2 + (2\lambda_0 - \lambda_1)|e_\theta^{n+1}|_1^2\right) \leq C\Delta t. \quad \square \tag{32}$$

Proof. Writing the temperature equation in (4) at $t = t_{n+1}$ after including the lifting $\mathcal{R}_\theta$ of the temperature, using the Taylor's expansion with an integral reminder, and taking the inner product with $\varphi \in H^1_{\Gamma_D}(\Omega)$, we get

$$\int_\Omega \left(\frac{\theta(t_{n+1}) - \theta(t_n)}{\Delta t} + \boldsymbol{u}(t_{n+1}) \cdot \nabla\, \theta(t_{n+1})\right) \varphi\, d\boldsymbol{x} + \int_\Omega \lambda(\theta_{\mathcal{R}}(t_{n+1}))\, \nabla\theta(t_{n+1}) \cdot \nabla\varphi\, d\boldsymbol{x}$$
$$= \int_\Omega \left(g(t_{n+1}) - \partial_t \mathcal{R}_\theta(t_{n+1}) - \boldsymbol{u}(t_{n+1}) \cdot \nabla\, \mathcal{R}_\theta(t_{n+1})\right) \varphi\, d\boldsymbol{x}$$
$$- \int_\Omega \lambda(\theta_{\mathcal{R}}(t_{n+1}))\nabla\mathcal{R}_\theta(t_{n+1}) \cdot \nabla\varphi\, d\boldsymbol{x} + \langle \theta_N(t_{n+1}), \varphi\rangle_{\Gamma_N} + \langle I_\theta^n, \varphi\rangle, \tag{33}$$

where I_θ^n is the truncation error associated to θ and it is defined by

$$I_\theta^n = \frac{1}{\Delta t}\int_{t_n}^{t_{n+1}} (t - t_n)\partial_{tt}\theta(t) dt.$$

By subtracting (19) from (33), taking $\varphi = 2\Delta t\, \bar{e}_\theta^{n+1}$ and using the identity (28), we obtain

$$
\begin{aligned}
&\|\bar{e}_\theta^{n+1}\|^2 - \|e_\theta^n\|^2 + \|\bar{e}_\theta^{n+1} - e_\theta^n\|^2 + 2\Delta t \int_\Omega \lambda(\theta^n + \mathcal{R}_\theta^{n+1}) \nabla \bar{e}_\theta^{n+1} \cdot \nabla \bar{e}_\theta^{n+1}\, d\boldsymbol{x} \\
&\qquad = -2\Delta t \int_\Omega \left(\lambda(\theta_{\mathcal{R}}(t_{n+1})) - \lambda(\theta^n + \mathcal{R}_\theta^{n+1})\right) \nabla\theta(t_{n+1}) \cdot \nabla \bar{e}_\theta^{n+1}\, d\boldsymbol{x} \\
&- 2\Delta t \left(\int_\Omega (\boldsymbol{u}(t_{n+1}) \cdot \nabla)\theta(t_{n+1}) \bar{e}_\theta^{n+1}\, d\boldsymbol{x} - \int_\Omega (\bar{\boldsymbol{u}}^{n+1} \cdot \nabla)\bar{\theta}^{n+1}\, \bar{e}_\theta^{n+1}\, d\boldsymbol{x} - \int_\Omega \frac{1}{2} \bar{\theta}^{n+1}\, \nabla \cdot \bar{\boldsymbol{u}}^{n+1}\, \bar{e}_\theta^{n+1}\, d\boldsymbol{x} \right) \\
&\qquad - 2\Delta t \int_\Omega [\lambda(\theta_{\mathcal{R}}(t_{n+1})) - \lambda(\theta^n + \mathcal{R}_\theta^{n+1})] \nabla \mathcal{R}_\theta(t_{n+1}) \cdot \nabla \bar{e}_\theta^{n+1}\, d\boldsymbol{x} \\
&- 2\Delta t \left(\int_\Omega \boldsymbol{u}(t_{n+1}) \cdot \nabla\, \mathcal{R}_\theta(t_{n+1})\, \bar{e}_\theta^{n+1} - \int_\Omega \quad \bar{\boldsymbol{u}}^{n+1} \quad \cdot \nabla\, \mathcal{R}_\theta^{n+1} \quad \bar{e}_\theta^{n+1}\, d\boldsymbol{x} - \int_\Omega \frac{1}{2} \mathcal{R}_\theta^{n+1}\, \nabla \cdot \bar{\boldsymbol{u}}^{n+1}\, \bar{e}_\theta^{n+1}\, d\boldsymbol{x} \right) \\
&\qquad + 2\Delta t \langle I_\theta^n, \bar{e}_\theta^{n+1} \rangle. \qquad (34)
\end{aligned}
$$

By taking $\varphi = 2\Delta t\, e_\theta^{n+1}$ in (21), we get

$$
\begin{aligned}
&\|e_\theta^{n+1}\|^2 - \|\bar{e}_\theta^{n+1}\|^2 + \|e_\theta^{n+1} - \bar{e}_\theta^{n+1}\|^2 + \Delta t \int_\Omega \lambda(\theta^n + \mathcal{R}_\theta^{n+1}) \nabla e_\theta^{n+1} \cdot \nabla e_\theta^{n+1}\, d\boldsymbol{x} - \\
&\Delta t \int_\Omega \lambda(\theta^n + \mathcal{R}_\theta^{n+1}) \nabla \bar{e}_\theta^{n+1} \cdot \nabla \bar{e}_\theta^{n+1}\, d\boldsymbol{x} + \Delta t \int_\Omega \lambda(\theta^n + \mathcal{R}_\theta^{n+1}) \nabla (e_\theta^{n+1} - \bar{e}_\theta^{n+1}) \cdot \nabla (e_\theta^{n+1} - \bar{e}_\theta^{n+1})\, d\boldsymbol{x} \\
&\qquad + 2\Delta t \int_\Omega \left(\lambda(\bar{\theta}_{\mathcal{R}}^{n+1}) - \lambda(\theta^n + \mathcal{R}_\theta^{n+1})\right) \nabla e_\theta^{n+1} \cdot \nabla e_\theta^{n+1}\, d\boldsymbol{x} \\
&\qquad 2\Delta t \int_\Omega \left(\lambda(\bar{\theta}_{\mathcal{R}}^{n+1}) - \lambda(\theta^n + \mathcal{R}_\theta^{n+1})\right) \nabla\theta(t_{n+1}) \cdot \nabla e_\theta^{n+1}\, d\boldsymbol{x}. \qquad (35)
\end{aligned}
$$

By adding (34) to (35) and considering the assumptions (7), we have

$$
\begin{aligned}
&\|e_\theta^{n+1}\|^2 - \|e_\theta^n\|^2 + \|\bar{e}_\theta^{n+1} - e_\theta^n\|^2 + \|e_\theta^{n+1} - \bar{e}_\theta^{n+1}\|^2 + \lambda_0 \Delta t |\bar{e}_\theta^{n+1}|_1^2 + \lambda_0 \Delta t |e_\theta^{n+1} - \bar{e}_\theta^{n+1}|_1^2 + (2\lambda_0 - \lambda_1)\Delta t |e_\theta^{n+1}|_1^2 \\
&\leq \underbrace{-2\Delta t \int_\Omega \left(\lambda(\theta_{\mathcal{R}}(t_{n+1})) - \lambda(\theta^n + \mathcal{R}_\theta^{n+1})\right) \nabla\theta(t_{n+1}) \cdot \nabla \bar{e}_\theta^{n+1}\, d\boldsymbol{x}}_{=A_1} \\
&\underbrace{-2\Delta t \left(\int_\Omega (\boldsymbol{u}(t_{n+1}) \cdot \nabla)\theta(t_{n+1}) \bar{e}_\theta^{n+1} - \int_\Omega (\bar{\boldsymbol{u}}^{n+1} \cdot \nabla)\bar{\theta}^{n+1}\, \bar{e}_\theta^{n+1} - \int_\Omega \frac{1}{2} \bar{\theta}^{n+1}\, \nabla \cdot \bar{\boldsymbol{u}}^{n+1}\, \bar{e}_\theta^{n+1} \right) d\boldsymbol{x}}_{=A_2} \\
&\underbrace{-2\Delta t \int_\Omega \left(\lambda(\theta_{\mathcal{R}}(t_{n+1})) - \lambda(\theta^n + \mathcal{R}_\theta^{n+1})\right) \nabla \mathcal{R}_\theta(t_{n+1}) \cdot \nabla \bar{e}_\theta^{n+1}\, d\boldsymbol{x}}_{=A_3} \\
&\underbrace{-2\Delta t \left(\int_\Omega \boldsymbol{u}(t_{n+1}) \cdot \nabla\, \mathcal{R}_\theta(t_{n+1})\, \bar{e}_\theta^{n+1} - \int_\Omega \quad \bar{\boldsymbol{u}}^{n+1} \quad \cdot \nabla\, \mathcal{R}_\theta^{n+1} \quad \bar{e}_\theta^{n+1} - \int_\Omega \frac{1}{2} \mathcal{R}_\theta^{n+1}\, \nabla \cdot \bar{\boldsymbol{u}}^{n+1}\, \bar{e}_\theta^{n+1} \right) d\boldsymbol{x}}_{=A_4} \\
&\underbrace{+2\Delta t \int_\Omega \left(\lambda(\bar{\theta}_{\mathcal{R}}^{n+1}) - \lambda(\theta^n + \mathcal{R}_\theta^{n+1})\right) \nabla\theta(t_{n+1}) \cdot \nabla e_\theta^{n+1}\, d\boldsymbol{x}}_{=A_5} + 2\Delta t \langle I_\theta^n, \bar{e}_\theta^{n+1} \rangle. \qquad (36)
\end{aligned}
$$

Next, we bound the terms in the right-hand side one by one:

- For the integral residual term associated to the temperature θ

$$\begin{aligned}2\Delta t\langle I_\theta^n, \bar{e}_\theta^{n+1}\rangle &\leq C\Delta t\, \|I_\theta^n\|_{-1}^2 + \frac{\lambda_0 \Delta t}{12}\left|\bar{e}_\theta^{n+1}\right|_1^2 = \frac{C}{\Delta t}\|\int_{t_n}^{t_{n+1}}(t-t_n)\partial_{tt}\theta(t)dt\|_{-1}^2 + \frac{\lambda_0 \Delta t}{12}\left|\bar{e}_\theta^{n+1}\right|_1^2, \\ &\leq C(\Delta t)^2 \int_{t_n}^{t_{n+1}} \|\partial_{tt}\theta\|_{-1}^2\, dt + \frac{\lambda_0 \Delta t}{12}\left|\bar{e}_\theta^{n+1}\right|_1^2 \end{aligned} \tag{37}$$

- Considering the assumptions 7 on λ, the assumption (25) on the exact temperature θ, and the embedding of $H^1(\Omega)$ onto $L^4(\Omega)$, the term A_1 is treated as

$$\begin{aligned} A_1 &= -2\Delta t \int_\Omega \left(\lambda(\theta_{\mathcal{R}}(t_{n+1})) - \lambda(\theta^n + \mathcal{R}_\theta^{n+1})\right)\nabla\theta(t_{n+1})\cdot\nabla\bar{e}_\theta^{n+1}\, d\boldsymbol{x}, \\ &\leq 2\lambda_2\Delta t \int_\Omega |\theta(t_{n+1}) - \theta^n|\,|\nabla\theta(t_{n+1})\cdot\nabla\bar{e}_\theta^{n+1}|\, d\boldsymbol{x}, \\ &\leq C\Delta t\|\theta(t_{n+1}) - \theta^n\|\,|\bar{e}_\theta^{n+1}|_1, \\ &\leq C\Delta t\|\theta(t_{n+1}) - \theta(t_n)\|^2 + C\Delta t\|e_\theta^n\|^2 + \frac{\lambda_0\Delta t}{12}|\bar{e}_\theta^{n+1}|_1^2, \\ &\leq C(\Delta t)^2\int_{t_n}^{t_{n+1}}\|\partial_t\theta\|^2 dt + C\Delta t\|e_\theta^n\|^2 + \frac{\lambda_0\Delta t}{12}|\bar{e}_\theta^{n+1}|_1^2. \end{aligned}$$

- In order to upper-bound the term A_2, we first observe that

$$\int_\Omega (\bar{\boldsymbol{u}}^{n+1}\cdot\nabla)\bar{\theta}^{n+1}\,\bar{e}_\theta^{n+1}\, d\boldsymbol{x} + \int_\Omega \bar{\theta}^{n+1}\,\nabla\cdot\bar{\boldsymbol{u}}^{n+1}\,\bar{e}_\theta^{n+1}\, d\boldsymbol{x} = -\int_\Omega (\bar{\boldsymbol{u}}^{n+1}\cdot\nabla)\bar{e}_\theta^{n+1}\bar{\theta}^{n+1}\, d\boldsymbol{x}.$$

Hence, by using the properties (8), we get

$$\begin{aligned} A_2 &= -2\Delta t\Bigg(\int_\Omega(\boldsymbol{u}(t_{n+1})\cdot\nabla)\theta(t_{n+1})\bar{e}_\theta^{n+1}\, d\boldsymbol{x} - \int_\Omega (\bar{\boldsymbol{u}}^{n+1}\cdot\nabla)\bar{\theta}^{n+1}\,\bar{e}_\theta^{n+1}\, d\boldsymbol{x} \\ &\quad - \int_\Omega \frac{1}{2}\bar{\theta}^{n+1}\,\nabla\cdot\bar{\boldsymbol{u}}^{n+1}\,\bar{e}_\theta^{n+1}\, d\boldsymbol{x}\Bigg), \\ &= -\Delta t\left(\int_\Omega(\boldsymbol{u}(t_{n+1})\cdot\nabla)\theta(t_{n+1})\bar{e}_\theta^{n+1}\, d\boldsymbol{x} - \int_\Omega(\bar{\boldsymbol{u}}^{n+1}\cdot\nabla)\bar{\theta}^{n+1}\,\bar{e}_\theta^{n+1}\, d\boldsymbol{x}\right) \\ &\quad + \Delta t\left(\int_\Omega(\boldsymbol{u}(t_{n+1})\cdot\nabla)\bar{e}_\theta^{n+1}\theta(t_{n+1})\, d\boldsymbol{x} - \int_\Omega(\bar{\boldsymbol{u}}^{n+1}\cdot\nabla)\bar{e}_\theta^{n+1}\bar{\theta}^{n+1}\, d\boldsymbol{x}\right), \\ &= -\Delta t\int_\Omega(\bar{\boldsymbol{e}}_u^{n+1}\cdot\nabla)\theta(t_{n+1})\bar{e}_\theta^{n+1}\, d\boldsymbol{x} + \Delta t\int_\Omega(\bar{\boldsymbol{e}}_u^{n+1}\cdot\nabla)\bar{e}_\theta^{n+1}\theta(t_{n+1})\, d\boldsymbol{x}, \end{aligned}$$

which can be upper-bounded, using the embedding of $H^1(\Omega)$ onto $L^4(\Omega)$ and the assumptions (22) on the exact temperature θ, as

$$\begin{aligned} A_2 &\leq C\Delta t|\bar{\boldsymbol{e}}_u^{n+1}|_1\,|\theta(t_{n+1})|_1\,|\bar{e}_\theta^{n+1}|_1 + C\Delta t|\bar{\boldsymbol{e}}_u^{n+1}|_1\,|\theta(t_{n+1})|_1\,|\bar{e}_\theta^{n+1}|_1, \\ &\leq C\Delta t|\bar{\boldsymbol{e}}_u^{n+1}|_1^2 + \frac{\lambda_0\Delta t}{12}|\bar{e}_\theta^{n+1}|_1^2. \end{aligned} \tag{38}$$

- Similarly to A_1, the term A_3 is bounded as

$$
\begin{aligned}
A_3 &= -2\Delta t \int_\Omega \left(\lambda(\theta_{\mathcal{R}}(t_{n+1})) - \lambda(\theta^n + \mathcal{R}_\theta^{n+1})\right) \nabla \mathcal{R}_\theta(t_{n+1}) \cdot \nabla \bar{e}_\theta^{n+1} \, d\boldsymbol{x}, \\
&\overset{\text{By (7)}}{\leq} 2\lambda_2 \Delta t \int_\Omega |\theta_{\mathcal{R}}(t_{n+1}) - \theta^n - \mathcal{R}_\theta^{n+1}| \, |\nabla \mathcal{R}_\theta(t_{n+1}) \cdot \nabla \bar{e}_\theta^{n+1}| \, d\boldsymbol{x}, \\
&\overset{\text{Using (31)}}{\leq} C\|\theta(t_{n+1}) - \theta^n\| \, |\bar{e}_\theta^{n+1}|_1, \\
&\leq C(\Delta t)^2 \int_{t_n}^{t_{n+1}} \|\partial_t \theta\|^2 dt + C\Delta t \|e_\theta^n\|^2 + \frac{\lambda_0 \Delta t}{12} |\bar{e}_\theta^{n+1}|_1^2.
\end{aligned}
$$

- As for the term A_2, the term A_2 satifies

$$
\int_\Omega (\bar{\boldsymbol{u}}^{n+1} \cdot \nabla) \mathcal{R}_\theta^{n+1} \, \bar{e}_\theta^{n+1} \, d\boldsymbol{x} + \int_\Omega \mathcal{R}_\theta^{n+1} \, \nabla \cdot \bar{\boldsymbol{u}}^{n+1} \, \bar{e}_\theta^{n+1} \, d\boldsymbol{x} = -\int_\Omega (\bar{\boldsymbol{u}}^{n+1} \cdot \nabla) \bar{e}_\theta^{n+1} \mathcal{R}_\theta^{n+1} \, d\boldsymbol{x},
$$

and by using the properties (8) we obtain

$$
\begin{aligned}
A_4 &= -2\Delta t \Bigg(\int_\Omega \boldsymbol{u}(t_{n+1}) \cdot \nabla \mathcal{R}_\theta(t_{n+1}) \, \bar{e}_\theta^{n+1} \, d\boldsymbol{x} - \int_\Omega \bar{\boldsymbol{u}}^{n+1} \cdot \nabla \mathcal{R}_\theta^{n+1} \, \bar{e}_\theta^{n+1} \, d\boldsymbol{x} \\
&\quad - \int_\Omega \frac{1}{2} \mathcal{R}_\theta^{n+1} \, \nabla \cdot \bar{\boldsymbol{u}}^{n+1} \, \bar{e}_\theta^{n+1} \, d\boldsymbol{x} \Bigg) \\
&= -\Delta t \int_\Omega (\bar{\boldsymbol{e}}_u^{n+1} \cdot \nabla) \mathcal{R}_\theta(t_{n+1}) \bar{e}_\theta^{n+1} \, d\boldsymbol{x} + \Delta t \int_\Omega (\bar{\boldsymbol{e}}_u^{n+1} \cdot \nabla) \bar{e}_\theta^{n+1} \mathcal{R}_\theta(t_{n+1}) \, d\boldsymbol{x}.
\end{aligned}
$$

Using the embedding of $H^1(\Omega)$ onto $L^4(\Omega)$ and the assumptions (22) on the lifting $\mathcal{R}_\theta$,

$$
\begin{aligned}
A_4 &\leq C\Delta t |\bar{\boldsymbol{e}}_u^{n+1}|_1 \, |\mathcal{R}_\theta(t_{n+1})|_1 \, |\bar{e}_\theta^{n+1}|_1 + C\Delta t |\bar{\boldsymbol{e}}_u^{n+1}|_1 \, |\mathcal{R}_\theta(t_{n+1})|_1 \, |\bar{e}_\theta^{n+1}|_1, \\
&\leq C\Delta t |\bar{\boldsymbol{e}}_u^{n+1}|_1^2 + \frac{\lambda_0 \Delta t}{12} |\bar{e}_\theta^{n+1}|_1^2.
\end{aligned} \tag{39}
$$

- Using the assumptions (7) on λ, and the assumption (25) on the exact temperature θ,

$$
\begin{aligned}
A_5 &= 2\Delta t \int_\Omega \left(\lambda(\bar{\theta}_{\mathcal{R}}^{n+1}) - \lambda(\theta^n + \mathcal{R}_\theta^{n+1})\right) \nabla \theta(t_{n+1}) \cdot \nabla e_\theta^{n+1} \, d\boldsymbol{x}, \\
&\leq C\lambda_2 \Delta t \|\bar{\theta}^{n+1} - \theta^n\| \, |e_\theta^{n+1}|_1, \\
&\leq C\lambda_2 \Delta t \left(\|\bar{e}_\theta^{n+1} - e_\theta^n\| + \|\theta(t_{n+1}) - \theta(t_n)\|\right) \left(|e_\theta^{n+1} - \bar{e}_\theta^{n+1}|_1 + |\bar{e}_\theta^{n+1}|_1\right), \\
&\leq C\Delta t \|\bar{e}_\theta^{n+1} - e_\theta^n\|^2 + C(\Delta t)^2 \int_{t_n}^{t_{n+1}} \|\partial_t \theta\|^2 dt + \frac{\lambda_0 \Delta t}{2} |e_\theta^{n+1} - \bar{e}_\theta^{n+1}|_1^2 + \frac{\lambda_0 \Delta t}{12} |\bar{e}_\theta^{n+1}|_1^2.
\end{aligned}
$$

Combining all the above inequalities and taking the sum over $n = 0, 1, \ldots, N$, we get

$$
\begin{aligned}
&\|e_\theta^{N+1}\|^2 + \sum_{n=0}^N \left(\|\bar{e}_\theta^{n+1} - e_\theta^n\|^2 + \|e_\theta^{n+1} - \bar{e}_\theta^{n+1}\|^2\right) + \\
&\qquad \Delta t \sum_{n=0}^N \left(\frac{\lambda_0}{2} |\bar{e}_\theta^{n+1}|_1^2 + \frac{\lambda_0}{2} |e_\theta^{n+1} - \bar{e}_\theta^{n+1}|_1^2 + (2\lambda_0 - \lambda_1) |e_\theta^{n+1}|_1^2\right) \\
&\qquad \leq C\Delta t \sum_{n=0}^N \|e_\theta^n\|^2 + C\Delta t \sum_{n=0}^N |\bar{\boldsymbol{e}}_u^{n+1}|_1^2 + C\Delta t \sum_{n=0}^N \|\bar{e}_\theta^{n+1} - e_\theta^n\|^2 + \\
&\qquad\qquad C(\Delta t)^2 \int_0^{T_f} \left(\|\partial_t \theta\|^2 + \|\partial_{tt} \theta\|_{-1}^2\right) dt.
\end{aligned} \tag{40}
$$

From Lemma 3, the second term in the right-hand side of the above inequality is bounded by

$$\Delta t\sum_{n=0}^{N}|\bar{\boldsymbol{e}}_u^{n+1}|_1^2\le C\Delta t+C\Delta t\sum_{n=0}^{N}\left(\|e_\theta^n\|^2+\|\bar{e}_\theta^{n+1}-e_\theta^n\|^2\right).$$

For small enough Δt, we can write

$$C\Delta t\sum_{n=0}^{N}\|\bar{e}_\theta^{n+1}-e_\theta^n\|^2\le\frac{1}{2}\sum_{n=0}^{N}\|\bar{e}_\theta^{n+1}-e_\theta^n\|^2.$$

Hence, using the assumptions (22), the inequality (40) is developed into

$$\|e_\theta^{N+1}\|^2+\sum_{n=0}^{N}\left(\frac{1}{2}\|\bar{e}_\theta^{n+1}-e_\theta^n\|^2+\|e_\theta^{n+1}-\bar{e}_\theta^{n+1}\|^2\right)+$$
$$\Delta t\sum_{n=0}^{N}\left(\frac{\lambda_0}{2}|\bar{e}_\theta^{n+1}|_1^2+\frac{\lambda_0}{2}|e_\theta^{n+1}-\bar{e}_\theta^{n+1}|_1^2+(2\lambda_0-\lambda_1)|e_\theta^{n+1}|_1^2\right)\le C\Delta t+\ C\Delta t\sum_{n=0}^{N}\|e_\theta^n\|^2.$$

Finally, applying the discrete Gronwall lemma 1 ends the proof. ■

It should be stressed that from Lemma 4, we deduce that

$$\|e_\theta^{n+1}\|^2\le C\Delta t,\quad\text{for all } n=0,1,\ldots,N,$$

and therefore,

$$\Delta t\sum_{n=0}^{N}\|e_\theta^{n+1}\|^2\le C\Delta t. \tag{41}$$

Now, the error terms associated with the temperature that appear in the right-hand side of the velocity error estimates (3), can be bounded thanks to Lemma 4 and the above inequality. The new velocity estimates are announced in the following corollary:

Corollary 1. *Under the assumptions of Lemma 3 and Lemma 4, we have*

$$\|\boldsymbol{e}_u^{N+1}\|^2+\sum_{n=0}^{N}\left(\|\bar{\boldsymbol{e}}_u^{n+1}-\boldsymbol{e}_u^n\|^2+\frac{1}{2}\|\boldsymbol{e}_u^{n+1}-\bar{\boldsymbol{e}}_u^{n+1}\|^2\right)+\frac{\nu_0\Delta t}{2}\sum_{n=0}^{N}|\bar{\boldsymbol{e}}_u^{n+1}|_1^2+$$
$$\Delta t\sum_{n=0}^{N}\left((2\nu_0-\nu_1)|\boldsymbol{e}_u^{n+1}|_1^2+\frac{\nu_0}{2}|\boldsymbol{e}_u^{n+1}-\bar{\boldsymbol{e}}_u^{n+1}|_1^2\right)\le C\Delta t. \tag{42}$$ ■

As noted before, the established Lemma 4 and Corollary 1 so far, provide only 1/2-order estimates for both velocity and temperature solutions. These estimates can further be improved to obtain a full first-order as will be shown below. It should be also noted that, a simple inspection of the proof of temperature estimates, it can be seen that the term $\Delta t\sum_{n=0}^{N}|\bar{\boldsymbol{e}}_u^{n+1}|_1^2$ is the only one preventing from having the full-first order estimates, and it is originated from the treatment of the terms A_2 in (38) and A_4 in (39). It could be possible to make the term $\Delta t\sum_{n=0}^{N}\|\bar{\boldsymbol{e}}_u^{n+1}\|^2$ appears instead of $\Delta t\sum_{n=0}^{N}|\bar{\boldsymbol{e}}_u^{n+1}|_1^2$, but it would not be helpful at that stage. However, the $1/2-$order estimates being now established, we can get an improved estimate for the term $\Delta t\sum_{n=0}^{N}\|\bar{\boldsymbol{e}}_u^{n+1}\|^2$ (see Theorem 1) which will be useful to reach the full first-order estimates for the temperature (see Theorem 2). The latter will guarantee full-first order estimates for the velocity as well.

Theorem 1. *Under the assumptions of Lemma 4 and Corollary 1, we have*

$$\|\boldsymbol{e}_u^{N+1}\|_{\boldsymbol{V}'}^2 + \sum_{n=0}^{N} \|\boldsymbol{e}_u^{n+1} - \boldsymbol{e}_u^{n}\|_{\boldsymbol{V}'}^2 + \Delta t \sum_{n=0}^{N} \left(\|\boldsymbol{e}_u^{n+1}\|^2 + \|\bar{\boldsymbol{e}}_u^{n+1}\|^2\right) \leq C(\Delta t)^2 + C\Delta t \sum_{n=0}^{N} \|e_\theta^n\|^2. \quad \square$$

PROOF. Let first define the Stokes operator $A\boldsymbol{w} = -P_H\left(\nabla\cdot(\nu(\bar{\theta}^{n+1})\nabla\boldsymbol{w})\right)$, where P_H is the orthogonal projection onto $\boldsymbol{H}$. Here, the operator A acts on $D(A) = \boldsymbol{V}\cap\boldsymbol{H}^2(\Omega)$ and its inverse, denoted A^{-1}, is compact on $\boldsymbol{H}$ and defined as follows: For a given $\boldsymbol{\varphi}\in\boldsymbol{H}$, $\boldsymbol{v} = A^{-1}\boldsymbol{\varphi}$ is the solution of the Stokes problem

$$\begin{aligned} -\nabla\cdot\left(\nu(\bar{\theta}_{\mathcal{R}}^{n+1})\nabla\boldsymbol{v}\right) + \nabla q &= \boldsymbol{\varphi}, && \text{in } \Omega,\\ \nabla\cdot\boldsymbol{v} &= 0, && \text{in } \Omega,\\ \boldsymbol{v} &= 0, && \text{on } \partial\Omega \end{aligned} \tag{43}$$

Thanks to the regularity of Stokes problem (see [63]), there exists a constant $C_1 > 0$, independent of n, such that

$$\text{for all } \boldsymbol{\varphi}\in\boldsymbol{H}, \qquad \|A^{-1}\boldsymbol{\varphi}\|_s = \|\boldsymbol{v}\|_s \leq C_1\|\boldsymbol{\varphi}\|_{s-2}, \qquad \text{for } s = 1, 2. \tag{44}$$

Furthermore, using the notation $(\cdot,\cdot)$ for the inner product in $L^2(\Omega)$ and the bounds (7) of ν, we have from (43)

$$(A^{-1}\boldsymbol{\varphi},\boldsymbol{\varphi}) = (\boldsymbol{v},\boldsymbol{\varphi}) = -(\nabla\cdot(\nu(\bar{\theta}_{\mathcal{R}}^{n+1})\nabla\boldsymbol{v}),\boldsymbol{v}) + (\nabla q,\boldsymbol{v}) = (\nu(\bar{\theta}_{\mathcal{R}}^{n+1})\nabla\boldsymbol{v},\nabla\boldsymbol{v}) \leq \nu_1|\boldsymbol{v}|_1^2,$$

and

$$(A^{-1}\boldsymbol{\varphi},\boldsymbol{\varphi}) = (\nu(\bar{\theta}_{\mathcal{R}}^{n+1})\nabla\boldsymbol{v},\nabla\boldsymbol{v}) \geq \nu_0|\boldsymbol{v}|_1^2.$$

On the other hand,

$$\|\boldsymbol{\varphi}\|_{\boldsymbol{V}'} = \sup_{\boldsymbol{w}\in\boldsymbol{V}} \frac{\langle\boldsymbol{\varphi},\boldsymbol{w}\rangle_{\boldsymbol{V}',\boldsymbol{V}}}{|\boldsymbol{w}|_1} \leq C|\boldsymbol{v}|_1.$$

Hence, there exists constants $C_2, C_3 > 0$ such that

$$C_3(A^{-1}\boldsymbol{\varphi},\boldsymbol{\varphi}) \leq \|\boldsymbol{\varphi}\|_{\boldsymbol{V}'}^2 \leq C_2(A^{-1}\boldsymbol{\varphi},\boldsymbol{\varphi}), \qquad \forall\,\boldsymbol{\varphi}\in\boldsymbol{H}. \tag{45}$$

Next, adding (18) to (20) and substracting the sum from (27)and taking $\boldsymbol{v} = 2\Delta t\,A^{-1}\boldsymbol{e}_u^{n+1}$, we get

$$\begin{aligned} &\int_\Omega \boldsymbol{e}_u^{n+1}\cdot A^{-1}\boldsymbol{e}_u^{n+1}\,d\boldsymbol{x} - \int_\Omega \boldsymbol{e}_u^{n}\cdot A^{-1}\boldsymbol{e}_u^{n}\,d\boldsymbol{x} + \int_\Omega (\boldsymbol{e}_u^{n+1}-\boldsymbol{e}_u^{n})\cdot A^{-1}(\boldsymbol{e}_u^{n+1}-\boldsymbol{e}_u^{n})\,d\boldsymbol{x} +\\ &\quad 2\Delta t\int_\Omega \nu(\bar{\theta}_{\mathcal{R}}^{n+1})\nabla\boldsymbol{e}_u^{n+1} \colon \nabla A^{-1}\boldsymbol{e}_u^{n+1}\,d\boldsymbol{x} = \underbrace{2\alpha\Delta t\int_\Omega (\boldsymbol{f}(\theta_{\mathcal{R}}(t_{n+1})) - \boldsymbol{f}(\theta_{\mathcal{R}}^n))\cdot A^{-1}\boldsymbol{e}_u^{n+1}\,d\boldsymbol{x}}_{=D_1}\\ &\quad \underbrace{-2\Delta t\int_\Omega \left(\nu(\theta_{\mathcal{R}}(t_{n+1})) - \nu(\bar{\theta}_{\mathcal{R}}^{n+1})\right)\nabla\boldsymbol{u}(t_{n+1}) \colon \nabla(A^{-1}\boldsymbol{e}_u^{n+1})\,d\boldsymbol{x}}_{=D_2}\\ &\quad \underbrace{-2\Delta t\left(\int_\Omega (\boldsymbol{u}(t_{n+1})\cdot\nabla)\boldsymbol{u}(t_{n+1})\cdot A^{-1}\boldsymbol{e}_u^{n+1}\,d\boldsymbol{x} - \int_\Omega (\boldsymbol{u}^n\cdot\nabla)\bar{\boldsymbol{u}}^{n+1}\cdot A^{-1}\boldsymbol{e}_u^{n+1}\,d\boldsymbol{x}\right)}_{=D_3}\\ &\quad + 2\Delta t\langle \boldsymbol{I}_u^n, A^{-1}\boldsymbol{e}_u^{n+1}\rangle. \end{aligned} \tag{46}$$

The viscosity term in the left-hand side is treated by setting $\boldsymbol{u} = \boldsymbol{e}_u^{n+1}$ in (43) to get

$$\begin{aligned} 2\Delta t\int_\Omega \nu(\bar{\theta}_{\mathcal{R}}^{n+1})\nabla\boldsymbol{e}_u^{n+1} \colon \nabla A^{-1}\boldsymbol{e}_u^{n+1}\,d\boldsymbol{x} &= 2\Delta t\int_\Omega \boldsymbol{e}_u^{n+1}\cdot\left(-\nabla\cdot(\nu(\bar{\theta}_{\mathcal{R}}^{n+1})\nabla(A^{-1}\boldsymbol{e}_u^{n+1}))\right)d\boldsymbol{x},\\ &= 2\Delta t\int_\Omega \boldsymbol{e}_u^{n+1}\cdot\left(\boldsymbol{e}_u^{n+1} - \nabla q\right)\,d\boldsymbol{x},\\ &= 2\Delta t\|\boldsymbol{e}_u^{n+1}\|^2. \end{aligned} \tag{47}$$

For bounding the right-hand side terms, we proceed as follows:

- Using the properties (3) of $\boldsymbol{f}$ the source term D_1 is bounded by

$$\begin{aligned} D_1 &= 2\alpha\Delta t\int_\Omega (\boldsymbol{f}(\theta_{\mathcal{R}}(t_{n+1}))-\boldsymbol{f}(\theta_{\mathcal{R}}^n))\cdot A^{-1}\boldsymbol{e}_u^{n+1}\,d\boldsymbol{x},\\ &\le C\Delta t\|\theta(t_{n+1})-\theta^n\|\,|A^{-1}\boldsymbol{e}_u^{n+1}|_1,\\ &\le C(\Delta t)^2\int_{t_n}^{t_{n+1}}\|\partial_t\theta(t)\|^2dt + C\Delta t\|e_\theta^n\|^2+\Delta t\|\boldsymbol{e}_u^{n+1}\|_{\boldsymbol{V}'}^2. \end{aligned}$$

- By the embedding of $\boldsymbol{H}^1(\Omega)$ onto $\boldsymbol{L}^4(\Omega)$ in addition to the assumptions (24) on the exact velocity, and the properties (7) of ν, we have for the term D_2

$$\begin{aligned} D_2 &= -2\Delta t\int_\Omega\left(\nu(\theta_{\mathcal{R}}(t_{n+1}))-\nu(\bar{\theta}_{\mathcal{R}}^{n+1})\right)\nabla\boldsymbol{u}(t_{n+1})\colon\nabla(A^{-1}\boldsymbol{e}_u^{n+1})\,d\boldsymbol{x},\\ &\overset{By (7)\ and\ (24)}{\le} C\Delta t\|\bar{e}_\theta^{n+1}\|\,|A^{-1}\boldsymbol{e}_u^{n+1}|_1\\ &\le C\Delta t(\|\bar{e}_\theta^{n+1}-e_\theta^n\|+\|e_\theta^n\|)\|\boldsymbol{e}_u^{n+1}\|_{\boldsymbol{V}'},\\ &\le C\Delta t\|\bar{e}_\theta^{n+1}-e_\theta^n\|^2+C\Delta t\|e_\theta^n\|^2+\Delta t\|\boldsymbol{e}_u^{n+1}\|_{\boldsymbol{V}'}^2. \end{aligned}$$

- The nonlinear term D_3 is first split as

$$\begin{aligned} D_3 &= -2\Delta t\left(\int_\Omega(\boldsymbol{u}(t_{n+1})\cdot\nabla)\boldsymbol{u}(t_{n+1})\cdot A^{-1}\boldsymbol{e}_u^{n+1}\,d\boldsymbol{x}+\int_\Omega(\boldsymbol{u}^n\cdot\nabla)\bar{\boldsymbol{u}}^{n+1}\cdot A^{-1}\boldsymbol{e}_u^{n+1}\,d\boldsymbol{x}\right),\\ &= \underbrace{-2\Delta t\int_\Omega(\boldsymbol{u}(t_{n+1})-\boldsymbol{u}(t_n))\cdot\nabla\boldsymbol{u}(t_{n+1})\cdot A^{-1}\boldsymbol{e}_u^{n+1}\,d\boldsymbol{x}}_{=D_{3,1}}\underbrace{-2\Delta t\int_\Omega\boldsymbol{e}_u^n\cdot\nabla\boldsymbol{u}(t_{n+1})\cdot A^{-1}\boldsymbol{e}_u^{n+1}\,d\boldsymbol{x}}_{=D_{3,2}}\\ &\quad\underbrace{+2\Delta t\int_\Omega\boldsymbol{e}_u^n\cdot\nabla\bar{\boldsymbol{e}}_u^{n+1}\cdot A^{-1}\boldsymbol{e}_u^{n+1}\,d\boldsymbol{x}}_{=D_{3,3}}\underbrace{-2\Delta t\int_\Omega\boldsymbol{u}(t_n)\cdot\nabla\bar{\boldsymbol{e}}_u^{n+1}\cdot A^{-1}\boldsymbol{e}_u^{n+1}\,d\boldsymbol{x}}_{=D_{3,4}}, \end{aligned}$$

then, each term in the right-hand side is bounded using the inequalities (9), as follows:

$$\begin{aligned} D_{3,1} &\le C\Delta t\|\boldsymbol{u}(t_{n+1})-\boldsymbol{u}(t_n)\|\,|\boldsymbol{u}(t_{n+1})|_1\|A^{-1}\boldsymbol{e}_u^{n+1}\|_2,\\ &\overset{\text{By (23)}}{\le} C\Delta t\|\int_{t_n}^{t_{n+1}}\partial_t\boldsymbol{u}dt\|\,\|\boldsymbol{e}_u^{n+1}\|,\\ &\le C(\Delta t)^2\int_{t_n}^{t_{n+1}}\|\partial_t\boldsymbol{u}\|^2dt+\frac{\Delta t}{4}\|\boldsymbol{e}_u^{n+1}\|^2. \end{aligned}$$

$$\begin{aligned} D_{3,2} &\le C\Delta t\|\boldsymbol{e}_u^n\|\,\|\boldsymbol{u}(t_{n+1})\|_2\,|A^{-1}\boldsymbol{e}_u^{n+1}|_1,\\ &\overset{\text{By (23)}}{\le} C\Delta t\|\boldsymbol{e}_u^n\|\,\|\boldsymbol{e}_u^{n+1}\|_{\boldsymbol{V}'},\\ &\le C\Delta t\left(\|\bar{\boldsymbol{e}}_u^{n+1}-\boldsymbol{e}_u^n\|+\|\boldsymbol{e}_u^{n+1}-\bar{\boldsymbol{e}}_u^{n+1}\|+\|\boldsymbol{e}_u^{n+1}\|\right)\|\boldsymbol{e}_u^{n+1}\|_{\boldsymbol{V}'},\\ &\le \frac{\Delta t}{4}\|\boldsymbol{e}_u^{n+1}\|^2+C\Delta t\|\boldsymbol{e}_u^{n+1}\|_{\boldsymbol{V}'}^2+C\Delta t\left(\|\bar{\boldsymbol{e}}_u^{n+1}-\boldsymbol{e}_u^n\|^2+\|\boldsymbol{e}_u^{n+1}-\bar{\boldsymbol{e}}_u^{n+1}\|^2\right). \end{aligned}$$

$$\begin{aligned} D_{3,3} &\le C\Delta t\|\boldsymbol{e}_u^n\|\,\|A^{-1}\boldsymbol{e}_u^{n+1}\|_2|\bar{\boldsymbol{e}}_u^{n+1}|_1,\\ &\overset{\text{By (44)}}{\le} C\Delta t\|\boldsymbol{e}_u^n\|\,\|\boldsymbol{e}_u^{n+1}\||\bar{\boldsymbol{e}}_u^{n+1}|_1,\\ &\overset{\text{By Corollary 1}}{\le} (\Delta t)^{\frac{3}{2}}\|\boldsymbol{e}_u^{n+1}\|\,|\bar{\boldsymbol{e}}_u^{n+1}|_1\le C(\Delta t)^2|\bar{\boldsymbol{e}}_u^{n+1}|_1^2+\frac{\Delta t}{4}\|\boldsymbol{e}_u^{n+1}\|^2. \end{aligned}$$

$$
\begin{aligned}
D_{3,4} &\leq C\Delta t\|\boldsymbol{u}(t_n)\|_2\,|A^{-1}\boldsymbol{e}_u^{n+1}|_1\,\|\bar{\boldsymbol{e}}_u^{n+1}\|,\\
&\leq C\Delta t\|\boldsymbol{e}_u^{n+1}\|_{\boldsymbol{V}'}^2+\frac{\Delta t}{4}\|\bar{\boldsymbol{e}}_u^{n+1}\|^2.
\end{aligned}\tag{48}
$$

From (30), using (24), we have

$$
\begin{aligned}
\|\bar{\boldsymbol{e}}_u^{n+1}\|^2 &\leq \|\boldsymbol{e}_u^{n+1}\|^2+\|\boldsymbol{e}_u^{n+1}-\bar{\boldsymbol{e}}_u^{n+1}\|^2+3\nu_1\Delta t|\boldsymbol{e}_u^{n+1}|_1^2+\nu_1\Delta t|\boldsymbol{e}_u^{n+1}-\bar{\boldsymbol{e}}_u^{n+1}|_1^2+\nu_1\Delta t|\bar{\boldsymbol{e}}_u^{n+1}|_1^2\\
&\quad +2\nu_2 C\Delta t\|\bar{\theta}^{n+1}-\theta^n\|,\\
&\leq \|\boldsymbol{e}_u^{n+1}\|^2+\|\boldsymbol{e}_u^{n+1}-\bar{\boldsymbol{e}}_u^{n+1}\|^2+3\nu_1\Delta t|\boldsymbol{e}_u^{n+1}|_1^2+\nu_1\Delta t|\boldsymbol{e}_u^{n+1}-\bar{\boldsymbol{e}}_u^{n+1}|_1^2+\nu_1\Delta t|\bar{\boldsymbol{e}}_u^{n+1}|_1^2\\
&\quad +C\Delta t\|\bar{e}_\theta^{n+1}-e_\theta^n\|^2+C(\Delta t)^2\int_{t_n}^{t_{n+1}}\|\partial_t\theta\|^2dt+\Delta t|\boldsymbol{e}_u^{n+1}|_1^2.
\end{aligned}
$$

Hence, the inequality (48) becomes

$$
\begin{aligned}
D_{3,4} &\leq C\Delta t\|\boldsymbol{e}_u^{n+1}\|_{\boldsymbol{V}'}^2+\frac{\Delta t}{4}\|\boldsymbol{e}_u^{n+1}\|^2+C\Delta t\|\boldsymbol{e}_u^{n+1}-\bar{\boldsymbol{e}}_u^{n+1}\|^2+C(\Delta t)^2|\boldsymbol{e}_u^{n+1}|_1^2\\
&\quad +C(\Delta t)^2|\boldsymbol{e}_u^{n+1}-\bar{\boldsymbol{e}}_u^{n+1}|_1^2+C(\Delta t)^2|\bar{\boldsymbol{e}}_u^{n+1}|_1^2+C(\Delta t)^3\int_{t_n}^{t_{n+1}}\|\partial_t\theta\|^2dt+C(\Delta t)^2\|\bar{e}_\theta^{n+1}-e_\theta^n\|^2.
\end{aligned}
$$

- The integral residual term

$$
\begin{aligned}
2\Delta t\langle\boldsymbol{I}_u^n,A^{-1}\boldsymbol{e}_u^{n+1}\rangle &\leq C\Delta t\|\boldsymbol{I}_u^n\|_{-1}\,|A^{-1}\boldsymbol{e}_u^{n+1}|_1,\\
&\leq C\Delta t\|\boldsymbol{I}_u^n\|_{-1}\,\|\boldsymbol{e}_u^{n+1}\|_{\boldsymbol{V}'},\\
&\leq C\Delta t\|\boldsymbol{I}_u^n\|_{-1}^2+\Delta t\|\boldsymbol{e}_u^{n+1}\|_{\boldsymbol{V}'}^2\\
&\leq C(\Delta t)^2\int_{t_n}^{t_{n+1}}\|\partial_{tt}\boldsymbol{u}\|_{-1}^2dt+\Delta t\|\boldsymbol{e}_u^{n+1}\|_{\boldsymbol{V}'}^2.
\end{aligned}
$$

Taking the sum of (46) over $n=0,1,\dots,N$, using (45) and (47), and combining all the previous inequalities, we obtain

$$
\begin{aligned}
&\|\boldsymbol{e}_u^{N+1}\|_{\boldsymbol{V}'}^2+\sum_{n=0}^N\|\boldsymbol{e}_u^{n+1}-\boldsymbol{e}_u^n\|_{\boldsymbol{V}'}^2+\Delta t\sum_{n=0}^N\|\boldsymbol{e}_u^{n+1}\|^2\leq C\Delta t\sum_{n=0}^N\|\boldsymbol{e}_u^{n+1}\|_{\boldsymbol{V}'}^2+\\
&\quad C\Delta t\sum_{n=0}^N\left(\|e_\theta^n\|^2+\|\bar{e}_\theta^{n+1}-e_\theta^n\|^2\right)+C\Delta t\sum_{n=0}^N\left(\|\bar{\boldsymbol{e}}_u^{n+1}-\boldsymbol{e}_u^n\|^2+\|\boldsymbol{e}_u^{n+1}-\bar{\boldsymbol{e}}_u^{n+1}\|^2\right)+\\
&\quad C(\Delta t)^2\sum_{n=0}^N(|\bar{\boldsymbol{e}}_u^{n+1}|_1^2+|\boldsymbol{e}_u^{n+1}|_1^2+|\boldsymbol{e}_u^{n+1}-\bar{\boldsymbol{e}}_u^{n+1}|_1^2)+\\
&\quad C(\Delta t)^2\sum_{n=0}^N\|\bar{e}_\theta^{n+1}-e_\theta^n\|^2+C(\Delta t)^2\int_0^{T_f}\|\partial_t\theta\|^2dt+\\
&\quad C(\Delta t)^2\int_0^{T_f}\|\partial_t\boldsymbol{u}\|^2dt+C(\Delta t)^3\int_0^{T_f}\|\partial_t\theta\|^2dt+C(\Delta t)^2\int_0^{T_f}\|\partial_{tt}\boldsymbol{u}\|_{-1}^2dt.
\end{aligned}
$$

Using the estimates in Corollary 1 and Lemma 4 along with the assumptions (23) and (22) on the continuous velocity and temperature solutions, we arrive at

$$
\|\boldsymbol{e}_u^{N+1}\|_{\boldsymbol{V}'}^2+\sum_{n=0}^N\|\boldsymbol{e}_u^{n+1}-\boldsymbol{e}_u^n\|_{\boldsymbol{V}'}^2+\Delta t\sum_{n=0}^N\|\boldsymbol{e}_u^{n+1}\|^2\leq C(\Delta t)^2+C\Delta t\sum_{n=0}^N\|e_\theta^n\|^2+C\Delta t\sum_{n=0}^N\|\boldsymbol{e}_u^{n+1}\|_{\boldsymbol{V}'}^2.
$$

Applying the discrete Gronwall lemma 1, we get

$$\|\boldsymbol{e}_u^{N+1}\|_{\boldsymbol{V}'}^2 + \sum_{n=0}^{N} \|\boldsymbol{e}_u^{n+1} - \boldsymbol{e}_u^n\|_{\boldsymbol{V}'}^2 + \Delta t \sum_{n=0}^{N} \|\boldsymbol{e}_u^{n+1}\|^2 \le C(\Delta t)^2 + C\Delta t \sum_{n=0}^{N} \|e_\theta^n\|^2.$$

Finally, from the last inequality along with Corollary 1, we also deduce

$$\Delta t \sum_{n=0}^{N} \|\bar{\boldsymbol{e}}_u^{n+1}\|^2 \le 2\Delta t \sum_{n=0}^{N} (\|\boldsymbol{e}_u^{n+1} - \bar{\boldsymbol{e}}_u^{n+1}\|^2 + \|\boldsymbol{e}_u^{n+1}\|^2) \le C(\Delta t)^2 + C\Delta t \sum_{n=0}^{N} \|e_\theta^n\|^2,$$

which completes the proof.

■

Next, with the estimates of Theorem 1 at hand, it is possible to obtain full first-order estimates for the temperature errors as presented in this theorem:

Theorem 2. *Under the assumptions of Theorem 1, we have*

$$\|e_\theta^{N+1}\|^2 + \sum_{n=0}^{N} \left(\|\bar{e}_\theta^{n+1} - e_\theta^n\|^2 + \|e_\theta^{n+1} - \bar{e}_\theta^{n+1}\|^2\right) + \Delta t \sum_{n=0}^{N} \left(\frac{\lambda_0}{2} |\bar{e}_\theta^{n+1}|_1^2 + \frac{\lambda_0}{2} |e_\theta^{n+1} - \bar{e}_\theta^{n+1}|_1^2 + (2\lambda_0 - \lambda_1)|e_\theta^{n+1}|_1^2\right) \le C(\Delta t)^2. \quad \square \tag{49}$$

Proof. As noted before, the problematic term that was compromising the order in Lemma 4 of the error estimates for the temperature, was introduced by the terms A_2(38) and A_4 (39). Hence, the proof here will literally shadows the proof of Lemma 4 except for the treatment of those problematic terms that will be handled properly in order to benefit from the improved estimates of Theorem 1. In fact, the terms of interest, A_2 in (38) and A_4 in (39) could have been developed as

$$\begin{aligned} A_2 &= -\Delta t \int_\Omega (\bar{\boldsymbol{e}}_u^{n+1} \cdot \nabla)\theta(t_{n+1})\bar{e}_\theta^{n+1} \, d\boldsymbol{x} + \Delta t \int_\Omega (\bar{\boldsymbol{e}}_u^{n+1} \cdot \nabla)\bar{e}_\theta^{n+1}\theta(t_{n+1}) \, d\boldsymbol{x}, \\ &\overset{\text{By (9)}}{\le} C\Delta t \|\bar{\boldsymbol{e}}_u^{n+1}\| \, \|\theta(t_{n+1})\|_2 \, |\bar{e}_\theta^{n+1}|_1 + C\Delta t \|\bar{\boldsymbol{e}}_u^{n+1}\| \, |\bar{e}_\theta^{n+1}|_1 \, \|\theta(t_{n+1})\|_2, \\ &\overset{\text{By (22)}}{\le} C\Delta t \|\bar{\boldsymbol{e}}_u^{n+1}\|^2 + \frac{\lambda_0 \Delta t}{12} |\bar{e}_\theta^{n+1}|_1^2, \end{aligned}$$

and

$$\begin{aligned} A_4 &= -\Delta t \int_\Omega (\bar{\boldsymbol{e}}_u^{n+1} \cdot \nabla)\mathcal{R}_\theta(t_{n+1})\bar{e}_\theta^{n+1} \, d\boldsymbol{x} + \Delta t \int_\Omega (\bar{\boldsymbol{e}}_u^{n+1} \cdot \nabla)\bar{e}_\theta^{n+1}\mathcal{R}_\theta(t_{n+1}) \, d\boldsymbol{x}, \\ &\overset{\text{By (9)}}{\le} C\Delta t \|\bar{\boldsymbol{e}}_u^{n+1}\| \, \|\mathcal{R}_\theta(t_{n+1})\|_2 |\bar{e}_\theta^{n+1}|_1 + C\Delta t \|\bar{\boldsymbol{e}}_u^{n+1}\| \, |\bar{e}_\theta^{n+1}|_1 \, \|\mathcal{R}_\theta(t_{n+1})\|_2, \\ &\overset{\text{By (31)}}{\le} C\Delta t \|\bar{\boldsymbol{e}}_u^{n+1}\|^2 + \frac{\lambda_0 \Delta t}{12} |\bar{e}_\theta^{n+1}|_1^2, \end{aligned}$$

to finally get the inequality

$$\begin{aligned} &\|e_\theta^{N+1}\|^2 + \sum_{n=0}^{N} \left(\|\bar{e}_\theta^{n+1} - e_\theta^n\|^2 + \|e_\theta^{n+1} - \bar{e}_\theta^{n+1}\|^2\right) + \\ &\quad \Delta t \sum_{n=0}^{N} \left(\frac{\lambda_0}{2} |\bar{e}_\theta^{n+1}|_1^2 + \frac{\lambda_0}{2} |e_\theta^{n+1} - \bar{e}_\theta^{n+1}|_1^2 + (2\lambda_0 - \lambda_1)|e_\theta^{n+1}|_1^2\right) \le C\Delta t \sum_{n=0}^{N} \|e_\theta^n\|^2 \\ &\quad + C\Delta t \sum_{n=0}^{N} \|\bar{\boldsymbol{e}}_u^{n+1}\|^2 + C\Delta t \sum_{n=0}^{N} \|\bar{e}_\theta^{n+1} - e_\theta^n\|^2 + C(\Delta t)^2 \int_0^{T_f} \left(\|\partial_t \theta\|^2 + \|\partial_{tt}\theta\|_{-1}^2\right) dt. \end{aligned} \tag{50}$$

Thanks to Theorem 1, we have

$$\Delta t \sum_{n=0}^{N} \|\bar{\boldsymbol{e}}_u^{n+1}\|^2 \le C(\Delta t)^2 + C\Delta t \sum_{n=0}^{N} \|e_\theta^n\|^2,$$

and by Lemma 4 along with the assumptions (22), we obtain

$$\begin{aligned}\|e_\theta^{N+1}\|^2 &+ \sum_{n=0}^{N} \left(\|\bar{e}_\theta^{n+1} - e_\theta^n\|^2 + \|e_\theta^{n+1} - \bar{e}_\theta^{n+1}\|^2\right) + \\ &\Delta t \sum_{n=0}^{N} \left(\frac{\lambda_0}{2}|\bar{e}_\theta^{n+1}|_1^2 + \frac{\lambda_0}{2}|e_\theta^{n+1} - \bar{e}_\theta^{n+1}|_1^2 + (2\lambda_0 - \lambda_1)|e_\theta^{n+1}|_1^2\right) \le\ C(\Delta t)^2 + C\Delta t \sum_{n=0}^{N} \|e_\theta^n\|^2. \quad (51)\end{aligned}$$

Applying the discrete Gronwall lemma 1, ends the proof.

■

It should be noted that thanks to Theorem 2, we have from Theorem 1,

$$\|\boldsymbol{e}_u^{N+1}\|_{\boldsymbol{V}'}^2 + \sum_{n=0}^{N} \|\boldsymbol{e}_u^{n+1} - \boldsymbol{e}_u^n\|_{\boldsymbol{V}'}^2 + \Delta t \sum_{n=0}^{N} \left(\|\boldsymbol{e}_u^{n+1}\|^2 + \|\bar{\boldsymbol{e}}_u^{n+1}\|^2\right) \le C(\Delta t)^2. \quad (52)$$

At this stage, we are able (thanks to Theorem 2) to obtain the following first-order error estimates for the end-of-step velocity:

Theorem 3. *Under the assumptions of Theorem 1, we have*

$$\|\boldsymbol{e}_u^{N+1}\|^2 + \sum_{n=0}^{N} \|\boldsymbol{e}_u^{n+1} - \boldsymbol{e}_u^n\|^2 + \frac{\nu_0 \Delta t}{2} \sum_{n=0}^{N} |\boldsymbol{e}_u^{n+1}|_1^2 \le C(\Delta t)^2. \quad \square \quad (53)$$

Proof. By adding (18) to (20) and substructing the sum from (27), we get

$$\begin{aligned}\int_\Omega \frac{\boldsymbol{e}_u^{n+1} - \boldsymbol{e}_u^n}{\Delta t} \cdot \boldsymbol{v}\, d\boldsymbol{x} &+ \int_\Omega \nu(\theta_{\mathcal{R}}(t_{n+1}))\nabla \boldsymbol{u}(t_{n+1})\colon \nabla \boldsymbol{v}\, d\boldsymbol{x} - \int_\Omega \nu(\bar{\theta}_{\mathcal{R}}^{n+1})\nabla \boldsymbol{u}^{n+1}\colon \nabla \boldsymbol{v}\, d\boldsymbol{x} = \\ &\alpha \int_\Omega (\boldsymbol{f}(\theta_{\mathcal{R}}(t_{n+1})) - \boldsymbol{f}(\theta_{\mathcal{R}}^n)) \cdot \boldsymbol{v}\, d\boldsymbol{x} + \int_\Omega p(t_{n+1})\nabla \cdot \boldsymbol{v} - \int_\Omega p^{n+1}\nabla \cdot \boldsymbol{v}\, d\boldsymbol{x} - \\ &\int_\Omega (\boldsymbol{u}(t_{n+1}) \cdot \nabla)\, \boldsymbol{u}(t_{n+1}) \cdot \boldsymbol{v}\, d\boldsymbol{x} + \int_\Omega (\boldsymbol{u}^n \cdot \nabla)\, \bar{\boldsymbol{u}}^{n+1} \cdot \boldsymbol{v}\, d\boldsymbol{x} + \langle \boldsymbol{I}_u^n, \boldsymbol{v}\rangle. \quad (54)\end{aligned}$$

Taking $\boldsymbol{v} = 2\Delta t \boldsymbol{e}_u^{n+1}$ and considering the assumptions (7) on ν result in

$$\begin{aligned}\|\boldsymbol{e}_u^{n+1}\|^2 - \|\boldsymbol{e}_u^n\|^2 + \|\boldsymbol{e}_u^{n+1} - \boldsymbol{e}_u^n\|^2 + 2\nu_0 \Delta t |\boldsymbol{e}_u^{n+1}|_1^2 &\le 2\alpha\Delta t \int_\Omega (\boldsymbol{f}(\theta_{\mathcal{R}}(t_{n+1})) - \boldsymbol{f}(\theta_{\mathcal{R}}^n)) \cdot \boldsymbol{e}_u^{n+1}\, d\boldsymbol{x} \\ &- 2\Delta t \int_\Omega \left(\nu(\theta_{\mathcal{R}}(t_{n+1})) - \nu(\bar{\theta}_{\mathcal{R}}^{n+1})\right) \nabla \boldsymbol{u}(t_{n+1})\colon \nabla \boldsymbol{e}_u^{n+1}\, d\boldsymbol{x} \\ - 2\Delta t \int_\Omega (\boldsymbol{u}(t_{n+1}) \cdot \nabla)\, \boldsymbol{u}(t_{n+1}) \cdot \boldsymbol{e}_u^{n+1}\, d\boldsymbol{x} &+ \int_\Omega (\boldsymbol{u}^n \cdot \nabla)\, \bar{\boldsymbol{u}}^{n+1} \cdot \boldsymbol{e}_u^{n+1}\, d\boldsymbol{x} + 2\Delta t \langle \boldsymbol{I}_u^n, \boldsymbol{e}_u^{n+1}\rangle.\end{aligned}$$

The right-hand side terms of the above inequality are bounded as follows:

- Thanks to the second property of (3) along with the Poincaré inequality on $\boldsymbol{e}_u^{n+1}$, the source term is upper-bounded by

$$2\alpha\Delta t \int_\Omega (\boldsymbol{f}(\theta_{\mathcal{R}}(t_{n+1})) - \boldsymbol{f}(\theta_{\mathcal{R}}^n)) \cdot \boldsymbol{e}_u^{n+1}\, d\boldsymbol{x} \quad \le \quad C(\Delta t)^2 \int_{t_n}^{t_{n+1}} \|\partial_t \theta\|^2 dt + C\Delta t \|e_\theta^n\|^2 + \frac{\nu_0 \Delta t}{12} |\boldsymbol{e}_u^{n+1}|_1^2.$$

- Using the properties 7 of ν, and the assumption (24) on the exacte velocity $\boldsymbol{u}$,

$$
\begin{aligned}
-2\Delta t\int_\Omega \left(\nu(\theta_{\mathcal{R}}(t_{n+1}))-\nu(\bar{\theta}_{\mathcal{R}}^{n+1})\right)\nabla\boldsymbol{u}(t_{n+1})\colon\nabla\boldsymbol{e}_u^{n+1}\,d\boldsymbol{x} &\leq 2\nu_2\Delta t\int_\Omega |\bar{e}_\theta^{n+1}|\,|\nabla\boldsymbol{u}(t_{n+1})\colon\nabla\boldsymbol{e}_u^{n+1}|\,d\boldsymbol{x}\\
&\leq C\Delta t\|\bar{e}_\theta^{n+1}\|\,|\boldsymbol{e}_u^{n+1}|\\
&\leq C\Delta t\|\bar{e}_\theta^{n+1}\|^2+\frac{\nu_0\Delta t}{12}|\boldsymbol{e}_u^{n+1}|_1^2.
\end{aligned}
$$

- The nonlinear term is handled as follow

$$
\begin{aligned}
&-2\Delta t\int_\Omega (\boldsymbol{u}(t_{n+1})\cdot\nabla)\,\boldsymbol{u}(t_{n+1})\cdot\boldsymbol{e}_u^{n+1}\,d\boldsymbol{x}+\int_\Omega (\boldsymbol{u}^n\cdot\nabla)\,\bar{\boldsymbol{u}}^{n+1}\cdot\boldsymbol{e}_u^{n+1}\,d\boldsymbol{x}\\
&=\underbrace{-2\Delta t\int_\Omega ((\boldsymbol{u}(t_{n+1})-\boldsymbol{u}(t_n))\cdot\nabla)\,\boldsymbol{u}(t_{n+1})\cdot\boldsymbol{e}_u^{n+1}\,d\boldsymbol{x}}_{=L_1}\underbrace{-2\Delta t\int_\Omega (\boldsymbol{e}_u^n\cdot\nabla)\boldsymbol{u}(t_{n+1})\cdot\boldsymbol{e}_u^{n+1}\,d\boldsymbol{x}}_{=L_2}\\
&\underbrace{+2\Delta t\int_\Omega (\boldsymbol{u}(t_n)\cdot\nabla)\boldsymbol{e}_u^{n+1}\cdot\bar{\boldsymbol{e}}_u^{n+1}\,d\boldsymbol{x}}_{=L_3}\underbrace{-2\Delta t\int_\Omega (\boldsymbol{e}_u^n\cdot\nabla)\boldsymbol{e}_u^{n+1}\cdot\bar{\boldsymbol{e}}_u^{n+1}\,d\boldsymbol{x}}_{=L_4},
\end{aligned}
$$

where the terms L_1, L_2, L_3 and L_3 are are bounded separately as

$$
\begin{aligned}
L_1 &= -2\Delta t\int_\Omega ((\boldsymbol{u}(t_{n+1})-\boldsymbol{u}(t_n))\cdot\nabla)\,\boldsymbol{u}(t_{n+1})\cdot\boldsymbol{e}_u^{n+1}\,d\boldsymbol{x},\\
&\leq C\Delta t\|\boldsymbol{u}(t_{n+1})-\boldsymbol{u}(t_n)\|\,\|\boldsymbol{u}(t_{n+1})\|_2\,|\boldsymbol{e}_u^{n+1}|_1,\\
&\overset{\text{(using (23))}}{\leq} C\Delta t\|\boldsymbol{u}(t_{n+1})-\boldsymbol{u}(t_n)\|\,|\boldsymbol{e}_u^{n+1}|_1,\\
&\leq C(\Delta t)^2\int_{t_n}^{t_{n+1}}\|\partial_t\boldsymbol{u}\|^2dt+\frac{\nu_0\Delta t}{12}|\boldsymbol{e}_u^{n+1}|_1^2.
\end{aligned}
$$

$$
\begin{aligned}
L_2 &= -2\Delta t\int_\Omega (\boldsymbol{e}_u^n\cdot\nabla)\boldsymbol{u}(t_{n+1})\cdot\boldsymbol{e}_u^{n+1}\,d\boldsymbol{x},\\
&\leq C\Delta t\|\boldsymbol{e}_u^n\|\,\|\boldsymbol{u}(t_{n+1})\|_2\,|\boldsymbol{e}_u^{n+1}|_1\\
&\overset{\text{(using (23))}}{\leq} C\Delta t\|\boldsymbol{e}_u^n\|\,|\boldsymbol{e}_u^{n+1}|_1,\\
&\leq C\Delta t\|\boldsymbol{e}_u^n\|^2+\frac{\nu_0\Delta t}{12}|\boldsymbol{e}_u^{n+1}|_1^2.
\end{aligned}
$$

$$
\begin{aligned}
L_3 &= 2\Delta t\int_\Omega (\boldsymbol{u}(t_n)\cdot\nabla)\boldsymbol{e}_u^{n+1}\cdot\bar{\boldsymbol{e}}_u^{n+1}\,d\boldsymbol{x},\\
&\leq C\Delta t\|\boldsymbol{u}(t_n)\|_2\,|\boldsymbol{e}_u^{n+1}|_1\,\|\bar{\boldsymbol{e}}_u^{n+1}\|,\\
&\overset{\text{using (23)}}{\leq} C\Delta t\|\bar{\boldsymbol{e}}_u^{n+1}\|^2+\frac{\nu_0\Delta t}{12}|\boldsymbol{e}_u^{n+1}|_1^2.
\end{aligned}
$$

$$
\begin{aligned}
L_4 &= -2\Delta t\int_\Omega (\boldsymbol{e}_u^n\cdot\nabla)\boldsymbol{e}_u^{n+1}\cdot\bar{\boldsymbol{e}}_u^{n+1}\,d\boldsymbol{x},\\
&\overset{\text{(using (9))}}{\leq} C\Delta t|\boldsymbol{e}_u^n|_1^{\frac{1}{2}}\,\|\boldsymbol{e}_u^n\|^{\frac{1}{2}}|\boldsymbol{e}_u^{n+1}|_1\,|\bar{\boldsymbol{e}}_u^{n+1}|_1,\\
&\leq C\Delta t|\boldsymbol{e}_u^n|_1\,\|\boldsymbol{e}_u^n\|\,|\bar{\boldsymbol{e}}_u^{n+1}|_1^2+\frac{\nu_0\Delta t}{12}|\boldsymbol{e}_u^{n+1}|_1^2,\\
&\leq C\Delta t\|\boldsymbol{e}_u^n\|^2+\frac{\nu_0\Delta t}{2}|\boldsymbol{e}_u^n|_1^2+\frac{\nu_0\Delta t}{12}|\boldsymbol{e}_u^{n+1}|_1^2,
\end{aligned}
$$

where we have used
$$|\bar{\boldsymbol{e}}_u^{n+1}|_1 \leq C,$$
that follows from Corollary 1.

- The integral residual term
$$2\Delta t\langle \boldsymbol{I}_u^n, \boldsymbol{e}_u^{n+1}\rangle \quad \leq \quad C(\Delta t)^2 \int_{t_n}^{t_{n+1}} \|\partial_{tt}\boldsymbol{u}\|_{-1}^2 dt + \frac{\nu_0 \Delta t}{12}|\boldsymbol{e}_u^{n+1}|_1^2.$$

Gathering the above inequalities, we arrive at
$$\begin{aligned}
\|\boldsymbol{e}_u^{n+1}\|^2 - \|\boldsymbol{e}_u^n\|^2 + \|\boldsymbol{e}_u^{n+1} - \boldsymbol{e}_u^n\|^2 + \nu_0\Delta t|\boldsymbol{e}_u^{n+1}|_1^2 \leq C\Delta t\|\boldsymbol{e}_u^n\|^2 + C\Delta t\|e_\theta^n\|^2 + C\Delta t\|\bar{e}_\theta^{n+1}\|^2 \\
+ C(\Delta t)^2 \int_{t_n}^{t_{n+1}} \|\partial_t \boldsymbol{u}\|^2 dt + C\Delta t\|\bar{\boldsymbol{e}}_u^{n+1}\|^2 + \frac{\nu_0\Delta t}{2}|\boldsymbol{e}_u^n|_1^2 \\
+ C(\Delta t)^2 \int_{t_n}^{t_{n+1}} \|\partial_{tt}\boldsymbol{u}\|_{-1}^2 dt + C(\Delta t)^2 \int_{t_n}^{t_{n+1}} \|\partial_t\theta\|^2 dt. \quad (55)
\end{aligned}$$
Writing
$$\|\bar{\boldsymbol{e}}_u^{n+1}\|^2 \leq 2\|\bar{\boldsymbol{e}}_u^{n+1} - \boldsymbol{e}_u^n\|^2 + 2\|\boldsymbol{e}_u^n\|^2,$$
the inequality (55) becomes
$$\begin{aligned}
\|\boldsymbol{e}_u^{n+1}\|^2 - \|\boldsymbol{e}_u^n\|^2 + \|\boldsymbol{e}_u^{n+1} - \boldsymbol{e}_u^n\|^2 + \frac{\nu_0\Delta t}{2}\left(|\boldsymbol{e}_u^{n+1}|_1^2 - |\boldsymbol{e}_u^n|_1^2\right) + \frac{\nu_0\Delta t}{2}|\boldsymbol{e}_u^{n+1}|_1^2 \leq \\
C\Delta t\|\boldsymbol{e}_u^n\|^2 + C\Delta t\|e_\theta^n\|^2 + C\Delta t\|\bar{e}_\theta^{n+1}\|^2 + C(\Delta t)^2 \int_{t_n}^{t_{n+1}} \|\partial_t\boldsymbol{u}\|^2 dt + C\Delta t\|\bar{\boldsymbol{e}}_u^{n+1} - \boldsymbol{e}_u^n\|^2 + \\
C(\Delta t)^2 \int_{t_n}^{t_{n+1}} \|\partial_{tt}\boldsymbol{u}\|_{-1}^2 dt + C(\Delta t)^2 \int_{t_n}^{t_{n+1}} \|\partial_t\theta\|^2 dt.
\end{aligned}$$
Taking the sum over $n = 0, 1, \ldots, N$, considering the bounds of Corollary 1 for the term $\|\bar{\boldsymbol{e}}_u^{n+1} - \boldsymbol{e}_u^n\|^2$, the conditions (23) and (22) along with the bounds
$$\Delta t \sum_{n=0}^{N} \|e_\theta^n\|^2 \leq C(\Delta t)^2,$$
and
$$C\Delta t \sum_{n=0}^{N} \|\bar{e}_\theta^{n+1}\|^2 \leq \ 2\Delta t \sum_{n=0}^{N} (\|\bar{e}_\theta^{n+1} - e_\theta^n\|^2 + \|e_\theta^n\|^2) \leq C(\Delta t)^2,$$
which results from Theorem 2, we get
$$\|\boldsymbol{e}_u^{N+1}\|^2 \ + \ \frac{\nu_0\Delta t}{2}|\boldsymbol{e}_u^{N+1}|_1^2 \ + \ \sum_{n=0}^{N} \|\boldsymbol{e}_u^{n+1} \ - \ \boldsymbol{e}_u^n\|^2 \ + \ \frac{\nu_0\Delta t}{2} \sum_{n=0}^{N} |\boldsymbol{e}_u^{n+1}|_1^2 \quad \leq \ C(\Delta t)^2 \ + \ C\Delta t \sum_{n=0}^{N} \|\boldsymbol{e}_u^n\|^2.$$
The discrete Gronwall Lemma 1 applied to the above inequality, ends the proof. ■

In the next lemma, we establish 1/2-order estimates for the semi-discrete pressure in the $L^2\left(0, T_f; L^2(\Omega)\right)$ norm.

Theorem 4. *Under the same assumptions as Theorem 1, we have*
$$\Delta t \sum_{n=0}^{N} \|p(t_{n+1}) - p^{n+1}\|^2 \leq C\Delta t. \quad \square \tag{56}$$

Proof. From (54), we have

$$\int_\Omega \left(p(t_{n+1}) - p^{n+1}\right) \nabla\cdot \boldsymbol{v}\, d\boldsymbol{x} = \int_\Omega \frac{\boldsymbol{e}_u^{n+1} - \boldsymbol{e}_u^n}{\Delta t}\cdot \boldsymbol{v}\, d\boldsymbol{x} + \int_\Omega \left(\nu(\theta_{\mathcal{R}}(t_{n+1})) - \nu(\bar{\theta}_{\mathcal{R}}^{n+1})\right) \nabla \boldsymbol{u}(t_{n+1}) \colon \nabla \boldsymbol{v}\, d\boldsymbol{x} + \int_\Omega \nu(\bar{\theta}_{\mathcal{R}}^{n+1}) \nabla \boldsymbol{e}_u^{n+1} \colon \nabla \boldsymbol{v}\, d\boldsymbol{x} - \alpha \int_\Omega \left(\boldsymbol{f}(\theta_{\mathcal{R}}(t_{n+1})) - \boldsymbol{f}(\theta_{\mathcal{R}}^n)\right)\cdot \boldsymbol{v}\, d\boldsymbol{x} + \int_\Omega \left(\boldsymbol{u}(t_{n+1})\cdot\nabla\right) \boldsymbol{u}(t_{n+1})\cdot \boldsymbol{v}\, d\boldsymbol{x} - \int_\Omega \left(\boldsymbol{u}^n\cdot\nabla\right) \bar{\boldsymbol{u}}^{n+1}\cdot \boldsymbol{v}\, d\boldsymbol{x} - \langle \boldsymbol{I}_u^n, \boldsymbol{v}\rangle. \quad (57)$$

The Inf-Sup condition [64] leads to

$$\|p(t_{n+1}) - p^{n+1}\| \le C \sup_{\boldsymbol{v}\in \boldsymbol{H}_0^1(\Omega} \frac{\int_\Omega \left(p(t_{n+1}) - p^{n+1}\right)\nabla\cdot \boldsymbol{v}\, d\boldsymbol{x}}{|v|_1}.$$

Furthermore, the right-hand side terms of (57) have the following bounds

$$\int_\Omega \frac{\boldsymbol{e}_u^{n+1} - \boldsymbol{e}_u^n}{\Delta t}\cdot \boldsymbol{v}\, d\boldsymbol{x} \le C \|\frac{\boldsymbol{e}_u^{n+1} - \boldsymbol{e}_u^n}{\Delta t}\|\, |\boldsymbol{v}|_1, \qquad \text{(By Cauchy-Schwarz and Poincaré inequalities)},$$

$$\int_\Omega \left(\nu(\theta_{\mathcal{R}}(t_{n+1})) - \nu(\bar{\theta}_{\mathcal{R}}^{n+1})\right) \nabla \boldsymbol{u}(t_{n+1}) \colon \nabla \boldsymbol{v}\, d\boldsymbol{x} \le \nu_2 \int_\Omega |\theta_{\mathcal{R}}(t_{n+1}) - \bar{\theta}_{\mathcal{R}}^{n+1}|\, |\nabla \boldsymbol{u}(t_{n+1}) \colon \nabla \boldsymbol{v}|\, d\boldsymbol{x} \le C \|\bar{e}_\theta^{n+1}\|\, |\boldsymbol{v}|_1,$$

and

$$\int_\Omega \nu(\bar{\theta}_{\mathcal{R}}^{n+1}) \nabla \boldsymbol{e}_u^{n+1} \colon \nabla \boldsymbol{v}\, d\boldsymbol{x} \le \nu_1 |\boldsymbol{e}_u^{n+1}|_1 |\boldsymbol{v}|_1,$$

where we have used the properties (7) of ν and the assumption (24) on the continuous velocity.

$$\begin{aligned} -\alpha \int_\Omega \left(\boldsymbol{f}(\theta_{\mathcal{R}}(t_{n+1})) - \boldsymbol{f}(\theta_{\mathcal{R}}^n)\right)\cdot \boldsymbol{v} &\le \|\theta(t_{n+1}) - \theta^n\|\, \|\boldsymbol{v}\|\, d\boldsymbol{x} \le \left(\| \int_{t_n}^{t_{n+1}} \partial_t \theta dt\| + \|e_\theta^n\| \right) |\boldsymbol{v}|_1, \\ &\le \left(\Delta t \int_{t_n}^{t_{n+1}} \|\partial_t \theta\|^2 dt\right)^{\frac{1}{2}} |\boldsymbol{v}|_1 + \|e_\theta^n\|\, |\boldsymbol{v}|_1, \end{aligned}$$

thanks to (3) and Poincaré's inequality.

$$\langle \boldsymbol{I}_u^n, \boldsymbol{v}\rangle \le \|\boldsymbol{I}_u^n\|_{-1} |\boldsymbol{v}|_1 \le \left(\Delta t \int_{t_n}^{t_{n+1}} \|\partial_{tt} \boldsymbol{u}\|_{-1}^2 dt\right)^{\frac{1}{2}} |\boldsymbol{v}|_1.$$

The nonlinear term is split into three terms and bounded as follows:

$$\int_\Omega \left(\boldsymbol{u}(t_{n+1})\cdot\nabla\right) \boldsymbol{u}(t_{n+1})\cdot \boldsymbol{v}\, d\boldsymbol{x} - \int_\Omega \left(\boldsymbol{u}^n\cdot\nabla\right) \bar{\boldsymbol{u}}^{n+1}\cdot \boldsymbol{v}\, d\boldsymbol{x} = \int_\Omega \left(\boldsymbol{u}(t_{n+1}) - \boldsymbol{u}(t_n)\cdot\nabla\right) \boldsymbol{u}(t_{n+1})\cdot \boldsymbol{v}\, d\boldsymbol{x} + \int_\Omega (\boldsymbol{e}_u^n\cdot\nabla)\boldsymbol{u}(t_{n+1})\cdot \boldsymbol{v}\, d\boldsymbol{x} + \int_\Omega \left(\boldsymbol{u}^n\cdot\nabla\right) \bar{\boldsymbol{e}}_u^{n+1}\cdot \boldsymbol{v}\, d\boldsymbol{x}.$$

$$\begin{aligned} \int_\Omega \left(\boldsymbol{u}(t_{n+1}) - \boldsymbol{u}(t_n)\cdot\nabla\right) \boldsymbol{u}(t_{n+1})\cdot \boldsymbol{v}\, d\boldsymbol{x} &\le C \|\boldsymbol{u}(t_{n+1}) - \boldsymbol{u}(t_n)\|\, \|\boldsymbol{u}(t_{n+1})\|_2 |\boldsymbol{v}|_1 \\ &\overset{\text{By (23)}}{\le} C \left(\Delta t \int_{t_n}^{t_{n+1}} \|\partial_t \boldsymbol{u}\|^2 dt\right)^{\frac{1}{2}} |\boldsymbol{v}|_1. \end{aligned}$$

$$\begin{aligned} \int_\Omega (\boldsymbol{e}_u^n\cdot\nabla)\boldsymbol{u}(t_{n+1})\cdot \boldsymbol{v}\, d\boldsymbol{x} &\le C |\boldsymbol{e}_u^n|_1 |\boldsymbol{u}(t_{n+1})|_1 |\boldsymbol{v}|_1, \\ &\overset{\text{Using (23)}}{\le} C |\boldsymbol{e}_u^n|_1 |\boldsymbol{v}|_1. \end{aligned}$$

$$\begin{aligned}\int_\Omega (\boldsymbol{u}^n\cdot\nabla)\,\bar{\boldsymbol{e}}_u^{n+1}\cdot\boldsymbol{v}\,d\boldsymbol{x} &= -\int_\Omega (\boldsymbol{e}_u^n\cdot\nabla)\bar{\boldsymbol{e}}_u^{n+1}\cdot\boldsymbol{v}\,d\boldsymbol{x} - \int_\Omega (\boldsymbol{u}(t_n)\cdot\nabla)\boldsymbol{v}\cdot\bar{\boldsymbol{e}}_u^{n+1}\,d\boldsymbol{x}\\ &\leq C|\boldsymbol{e}_u^n|_1\,|\bar{\boldsymbol{e}}_u^{n+1}|_1\,|\boldsymbol{v}|_1 + C\|\boldsymbol{u}(t_n)\|_2\,|\boldsymbol{v}|_1\,\|\bar{\boldsymbol{e}}_u^{n+1}\| \leq C|\boldsymbol{e}_u^n|_1\,|\boldsymbol{v}|_1 + C|\boldsymbol{v}|_1\,\|\bar{\boldsymbol{e}}_u^{n+1}\|,\end{aligned}$$

where we have used $\|\boldsymbol{u}(t_n)\|_2 \leq C$ and $|\bar{\boldsymbol{e}}_u^{n+1}|_1 \leq C$ that result from (23) and Corollary 1, respectively. Combining the above inequalities, we get

$$\begin{aligned}\Delta t\|p(t_{n+1}) - p^{n+1}\|^2 \leq C\frac{1}{\Delta t}\|\boldsymbol{e}_u^{n+1} - \boldsymbol{e}_u^n\|^2 + C\Delta t\left(\|\bar{e}_\theta^{n+1}\|^2 + |\boldsymbol{e}_u^{n+1}|_1^2 + |\boldsymbol{e}_u^n|_1^2 + \|\bar{\boldsymbol{e}}_u^{n+1}\|^2 + \|e_\theta^n\|^2\right) +\\ C(\Delta t)^2\int_{t_n}^{t_{n+1}}\|\partial_t\theta\|^2 dt + C(\Delta t)^2\int_{t_n}^{t_{n+1}}\|\partial_{tt}\boldsymbol{u}\|_{-1}^2 dt + C(\Delta t)^2\int_{t_n}^{t_{n+1}}\|\partial_t\boldsymbol{u}\|^2 dt.\end{aligned}$$

Hence, summing up the last inequality for $n = 0, 1, \ldots, N$, and considering the already established estimates of Corollary 1, Lemma 4, Lemma 3 along with the assumptions (22), (23) on the continuous temperature and velocity solutions, we obtain (56).

■

5. Numerical results and examples

In this section we examine the performance of the proposed viscosity-splitting method for solving two examples of incompressible flows with temperature-dependent viscosity and thermal conductivity governed by the equations (4). We first solve a three-dimensional problem with manufactured exact solutions to validate the theoretical error estimates presented in the present study regarding the semi-discrete velocity, temperature and pressure computed by the proposed method. In the second example, we consider the two-dimensional benchmark problem of Rayleigh-Bénard flows to demonstrate the ability of the proposed viscosity-splitting algorithm to resolve complex thermal and flow patterns. We also solve the problem of unsteady flow over a heated airfoil. In all these examples, the spatial discretization is performed using the standard Taylor-Hood $\mathbb{P}_2/\mathbb{P}_1$ mixed finite elements such that the quadratic $\mathbb{P}_2$ finite elements are used for the velocity $\boldsymbol{u}$ and temperature θ whereas the linear $\mathbb{P}_1$ finite elements are used for the pressure p. Note that it is well known that this class of mixed finite elements satisfies the inf-sup condition required in Step 3 of the viscosity-splitting algorithm. For completeness, the mixed finite element method for solving the semi-discrete equations (18)-(21) is formulated in Appendix A. In all the computations reported herein, the resulting linear systems of algebraic equations are solved using the Generalized Minimal Residual (GMRES) iterative solver with a tolerance of 10^{-7} to stop the iterations.

5.1. Accuracy example

To assess the accuracy of the proposed viscosity-splitting method and its theoretical error estimates, we consider a problem with known analytical solution. Here, we solve the equations (4) in the three-dimensional domain $\Omega = [0,1]^3$ subject to Dirichlet-type boundary conditions and temperature-dependent viscosity and thermal conductivity defined as

$$\nu(\theta) = \lambda(\theta) = \left(1 + \sin^2(\theta)\right) \times 10^{-4}. \tag{58}$$

The boundary functions are defined such that the analytical solution of the system (4) is given by

$$\begin{aligned}\boldsymbol{u}(t,x,y,z) &= \left(x^2 + xy - z^2 + yz, 2xy + 0.5y^2 + 2yz - 2xz, z^2 + y^2 - x^2 + 3xy\right)^\top \sin(t)\exp(-2t),\\ \theta(t,x,y,z) &= 2 + \left(x^2 + y^2 + z^2 + 1\right)\sin(t)\exp(-2t),\\ p(t,x,y,z) &= \left(x - y + 3z - \frac{3}{2}\right)\sin(t)\exp(-2t).\end{aligned} \tag{59}$$

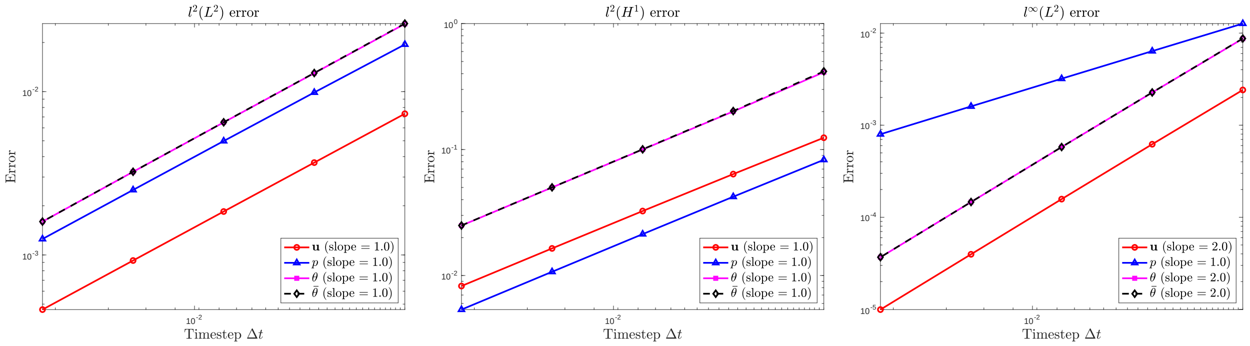

Figure 1: Convergence results for the velocity $\boldsymbol{u}$, pressure p, intermediate temperature $\bar{\theta}$ and the end-of-step temperature θ obtained for the accuracy example.

Using these exact solutions and (58), expressions of the source terms $\boldsymbol{f}$ and g in (4) are calculated as

$$\begin{aligned} \alpha\boldsymbol{f} &= \frac{\partial \boldsymbol{u}}{\partial t} + (\boldsymbol{u}\cdot\nabla)\,\boldsymbol{u} - \nabla\cdot(\nu(\theta)\nabla\boldsymbol{u}) + \nabla p - 2\,(1-\exp(-\theta))\,, \\ g &= \frac{\partial \theta}{\partial t} + (\boldsymbol{u}\cdot\nabla)\,\theta - \nabla\cdot(\lambda(\theta)\nabla\theta)\,. \end{aligned}$$

Note that the analytical solution (59) is constructed to be polynomials in space with the same degree as the finite element polynomial basis, that would drastically eliminate the spacial errors and enable a better assessment of the behavior of time errors which are the prime interest of the present work. Hence, the convergence rates are evaluated using errors between the analytical and numerical solutions calculated by the following discrete norms

$$\|\boldsymbol{e}\|_{l^2(X)} = \left(\Delta t \sum_{n=0}^{N} \|e^n\|_X\right)^{1/2}, \qquad \|\boldsymbol{e}\|_{l^\infty(X)} = \sup_{n=0,\dots,N} \|\boldsymbol{e}^n\|_X\,,$$

where X is assumed to be $\boldsymbol{L}^2(\Omega)$ or $\boldsymbol{H}^1(\Omega)$ for the velocity solution, and as $L^2(\Omega)$ or $H^1(\Omega)$ for temperature and pressure solutions. Different timesteps defined by $\Delta t = \dfrac{0.1}{2^n}$ $(n = 1,\dots,5)$ are used in our simulations and the obtained results are presented at the final time $t = 0.5$ using a structured finite element mesh with $20\times20\times20$ elements.

Figure 1 presents the time errors for the velocity $\boldsymbol{u}$, the pressure p, the intermediate temperature $\bar{\theta}$ and the end-of-step temperature θ, in the selected norms $l^2\left(0,T_f;L^2(\Omega)\right)$, $l^2\left(0,T_f;H^1(\Omega)\right)$ and $l^\infty\left(0,T_f;L^2(\Omega)\right)$. For the considered flow conditions, the convergence plots indicate that the $\boldsymbol{L}^2$-error and $\boldsymbol{H}^1$-error for the velocity solution and the L^2-error and H^1-error for the temperature solution are of full first-order as predicted by the established error estimates. However, the $l^\infty(\boldsymbol{L}^2)$-error for the velocity solution and the $l^\infty(L^2)$-error for the temperature solution are higher than the predicted first-order as they reach the second-order. It should be pointed out that the convergence rates achieved for the pressure solution in this example indicate a higher order than the theoretical 1/2-order estimated above, which stipulates that the established error estimates of the pressure are sub-optimal and they can be further improved. In addition, it is clear for this test example that the obtained error plots maintain the same trend which is also consistent with the error estimates proved in the present study for the proposed viscosity-splitting method.

5.2. Problem of Rayleigh-Bénard convection

Next, we consider the well-established flow benchmark of Rayleigh-Bénard convection widely used in the literature to assess numerical methods in computational fluid dynamics and heat transfer, see for instance

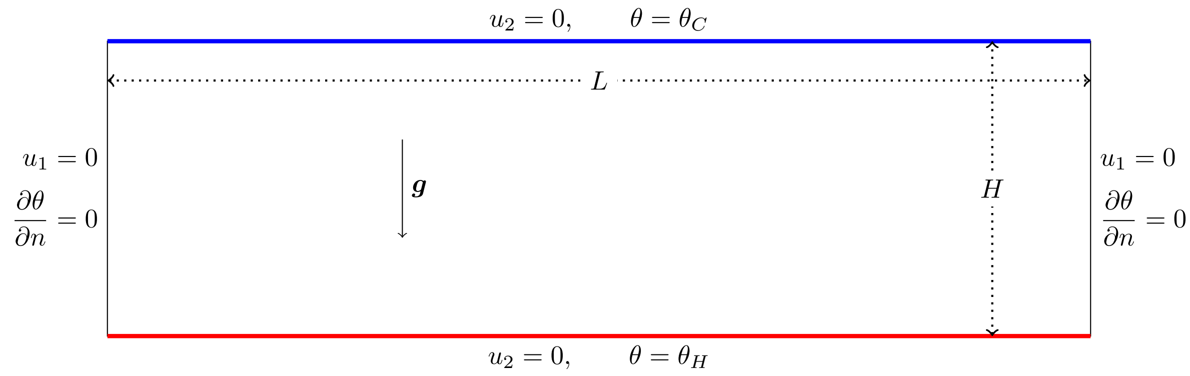

Figure 2: Configuration of the computational domain along with the boundary conditions used for the problem of Rayleigh-Bénard convection.

[65, 66]. In our computations for this example we used the same thermal flow configuration and the same boundary conditions as detailed in the previous references. Hence, we solve the equations (4) in a rectangular domain of length L and height H as shown in Figure 2. This figure also depicts the boundary conditions used for the temperature and flow velocity. Here, the fluid is confined between two horizontal heat-conducting plates fixed at hot temperature θ_H and cold temperature θ_C, and when the temperature difference between the two plates is large enough, it triggers a convection flow phenomena in which the high-temperature fluid rises up and the low-temperature fluid falls down under the effect of the buoyancy force. Thus, using the Boussinesq approximation, the source terms in (4) are given by

$$\alpha\, \boldsymbol{f}(\theta) = \beta \boldsymbol{g}\, (\theta - \theta_C)\,, \qquad g = 0,$$

where β is the coefficient of thermal expansion and $\boldsymbol{g}$ the gravitational force. In all the simulations reported in this section $\nu = 1.54{\times}10^{-5}\, m^2/s$, $\lambda = 2.2{\times}10^{-5}\, m^2/s$, $\beta = 3{\times}10^{-3}\,/K$, $\boldsymbol{g} = (0, 9.8\; m/s^2)^\top$, $\theta_C = 313\, K$ and $\theta_H = 323\, K$. Based on a mesh convergence study not reported here for brevity, an unstructured triangular mesh of 53472 mixed elements with 27287 pressure nodes and 108045 velocity and temperature nodes is used in the simulations as it offers a compromise between accuracy and efficiency in the proposed viscosity-splitting method. The timestep Δt is fixed to 0.01 s and steady-state numerical results are presented for four different aspect ratios $\frac{L}{H} = 6$, 7, 8 and 10 with $H = 1\; m$. Here, the time stepping is terminated when the relative difference in the velocity and temperature solutions in L^2-norm between two consecutive timesteps is less than a tolerance of 10^{-7}.

In Figure 3 we present the streamlines and velocity magnitudes obtained using the selected values of the aspect ratio $\frac{L}{H}$. Those results obtained for the isothermal lines and temperature distributions are illustrated in Figure 4. For the considered natural convection regimes, it can be clearly seen that the complicated flow and heat features are well captured by the proposed viscosity-splitting method. As it can be seen from the results shown in these figures, the formation of convection cells is clearly detected for all the considered domains with more flow recirculation cells in longer domains, and the flow in each of these cells is rotating in the opposite direction to its neighboring cells. This is mainly due to the important temperature difference $(\theta_H - \theta_C)$ between the two horizontal plates in the computational domain. In fact, with a small temperature gradient, the fluid viscosity overcomes the buoyancy force and the fluid remains at rest while the temperature is transported by the conduction only (no convection effects). As the temperature difference increases, the buoyancy force dominates the viscous effects and tends to push the heated fluid from the bottom up to the surface. On the other hand, the colder fluid is pushed down (which explains the wavy temperature distribution in Figure 4) where it is heated and then pushed upward by the same mechanism. Consequently, the convection motion occurs and the well-known Rayleigh-Bénard cells appear in the computational domain. These observations are in good agreement with those reported in the literature, see for example [65, 66] confirming that the proposed viscosity-splitting method accurately captures the overall thermal patterns of this class of natural convection problems.

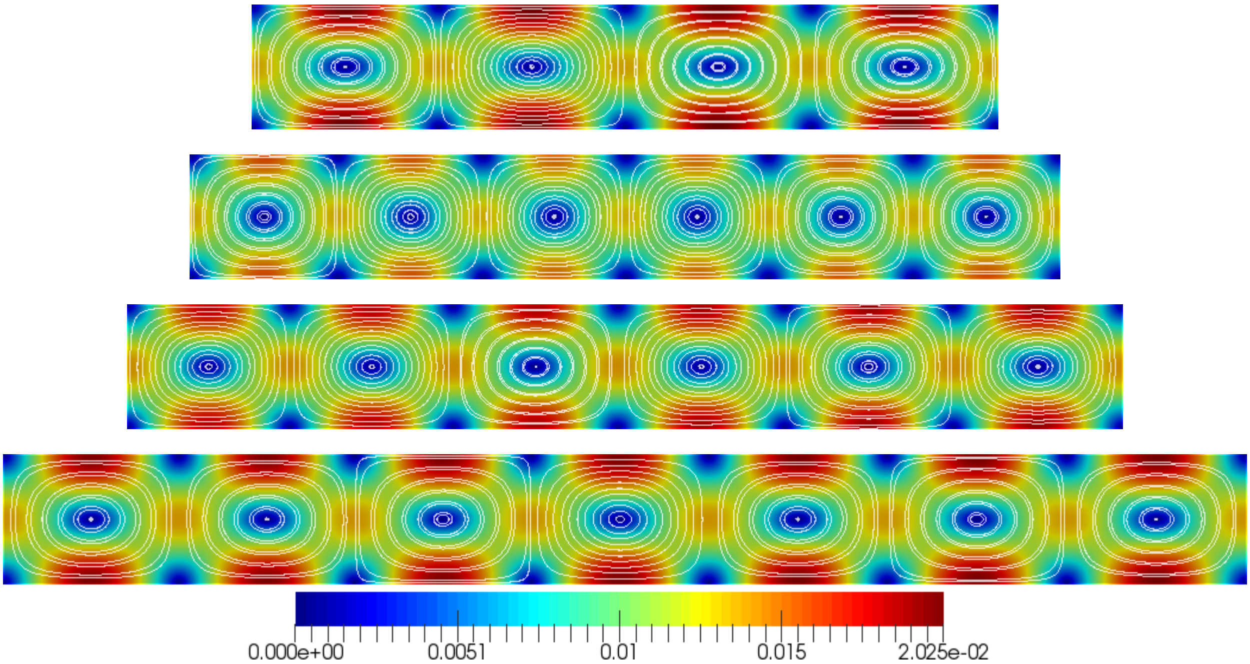

Figure 3: Snapshots of the velocity magnitude along with streamlines for the problem of Rayleigh-Bénard convection using different aspect ratios. From top to bottom $\frac{L}{H} = 6$, 7, 8 and 10.

5.3. Problem of flow over a heated airfoil

In this example we consider a two-dimensional flow over an airfoil-like body kept at a hot temperature θ_H and placed in a rectangular domain filled with a Newtonian fluid. The fluid enters from the left with a uniform velocity $\boldsymbol{u} = (U_\infty, 0)^\top$ and at a cold temperature θ_C as it flows past the airfoil. The airfoil is inclined with an attack angle ω and over which no-slip boundary conditions are imposed. The upper and lower walls are maintained at the cold temperature θ_C and are subject to no-penetration boundary conditions for the velocity while the outlet wall is insulated with no-flux boundary conditions for the velocity, see Figure 5 for an illustration of the domain and the associated boundary conditions used for this flow problem. The fluid is assumed to have a temperature-dependent viscosity and thermal conductivity according to the following laws

$$\nu(\theta) = \gamma_0 \exp\left(\frac{\theta_C}{\theta}\right), \qquad \lambda(\theta) = \kappa\left(1 + 0.3\frac{\theta - \theta_C}{\theta_H - \theta_C}\right).$$

Here, we solve the system (4) subject to the Boussinesq approximation for which the source terms are given by

$$\alpha\, \boldsymbol{f}(\theta) = \beta \boldsymbol{g}\left(\theta - \theta_C\right), \qquad g = 0,$$

where $\boldsymbol{g} = (0, 9.8\ m/s^2)^T$ is the gravitational force and β is the coefficient of thermal expansion. Note that for this class of mixed convection problems, the flow is characterized by the two non-dimensional Reynolds number Re and the Prandtl number Pr defined as

$$Re = \frac{\rho U_\infty L}{\gamma_0}, \qquad Pr = \frac{\kappa}{\gamma_0},$$

where the density ρ and the chord length L are set to unit in this example. In addition, as in most unsteady flow simulations, we also define the drag coefficient C_d and the lift coefficient C_l by

$$C_d = \frac{F_1}{\frac{1}{2}\rho U_\infty L}, \qquad C_l = \frac{F_2}{\frac{1}{2}\rho U_\infty L},$$

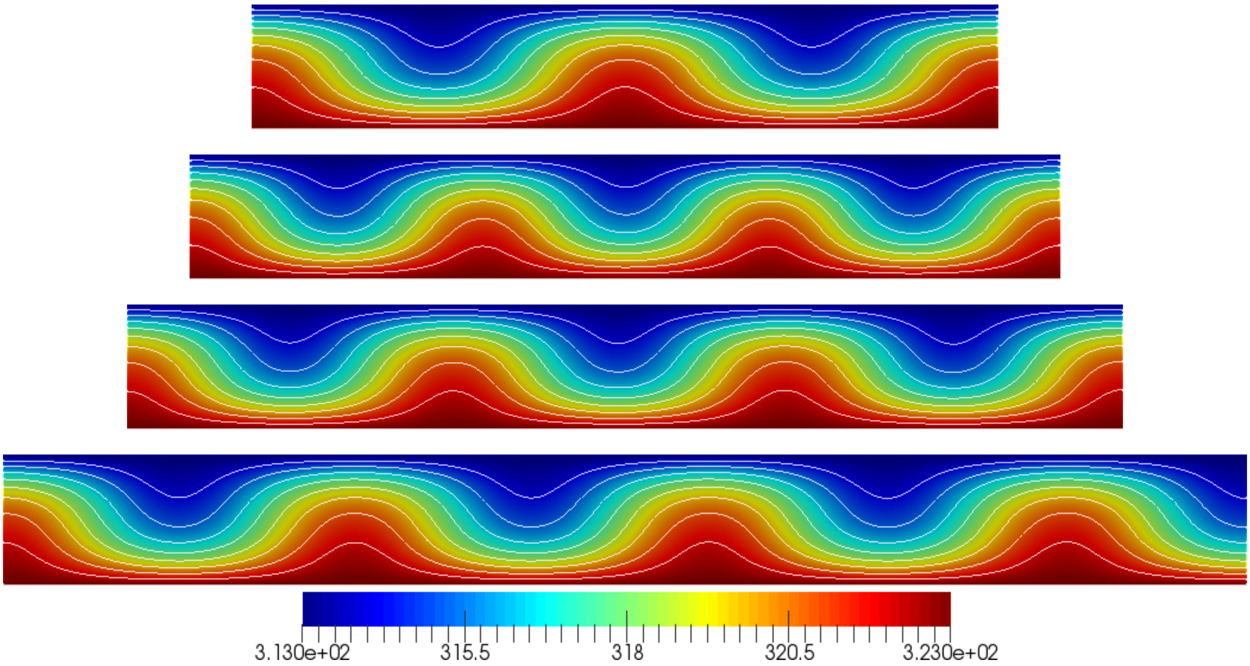

Figure 4: Snapshots of the temperature along with isothermal lines for the problem of Rayleigh-Bénard convection using different aspect ratios. From top to bottom $\dfrac{L}{H} = 6$, 7, 8 and 10.

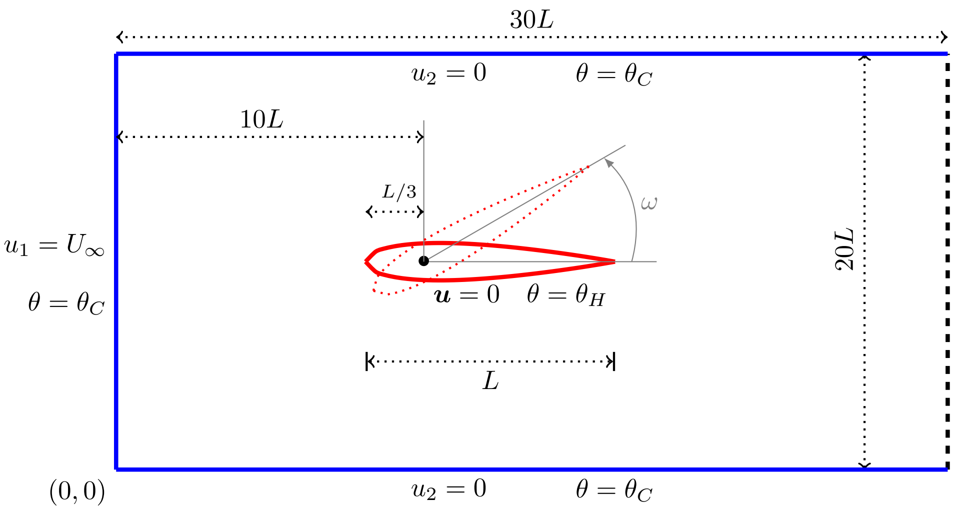

Figure 5: Domain configuration along with the boundary conditions used in our simulations for the problem of flow over a heated airfoil.

where $\mathbf{F} = (F_1, F_2)^\top$ is the force acting on the airfoil and it is computed using

$$\mathbf{F} = \oint_{\partial \mathcal{A}} (-p\boldsymbol{I} + \nu(\theta)\nabla \boldsymbol{u}) \cdot \boldsymbol{n} \, ds,$$

where $\partial \mathcal{A}$ is the airfoil boundary, $\boldsymbol{I}$ the unit 2×2-matrix and $\boldsymbol{n}$ the unit outward normal vector on $\partial \mathcal{A}$. In our computations for this flow problem, $L = 1\ m$, $\beta = 3 \times 10^{-3}\ /K$, $U_\infty = 1\ m/s$, $\theta_C = 300\ K$, $\theta_H = 320\ K$.

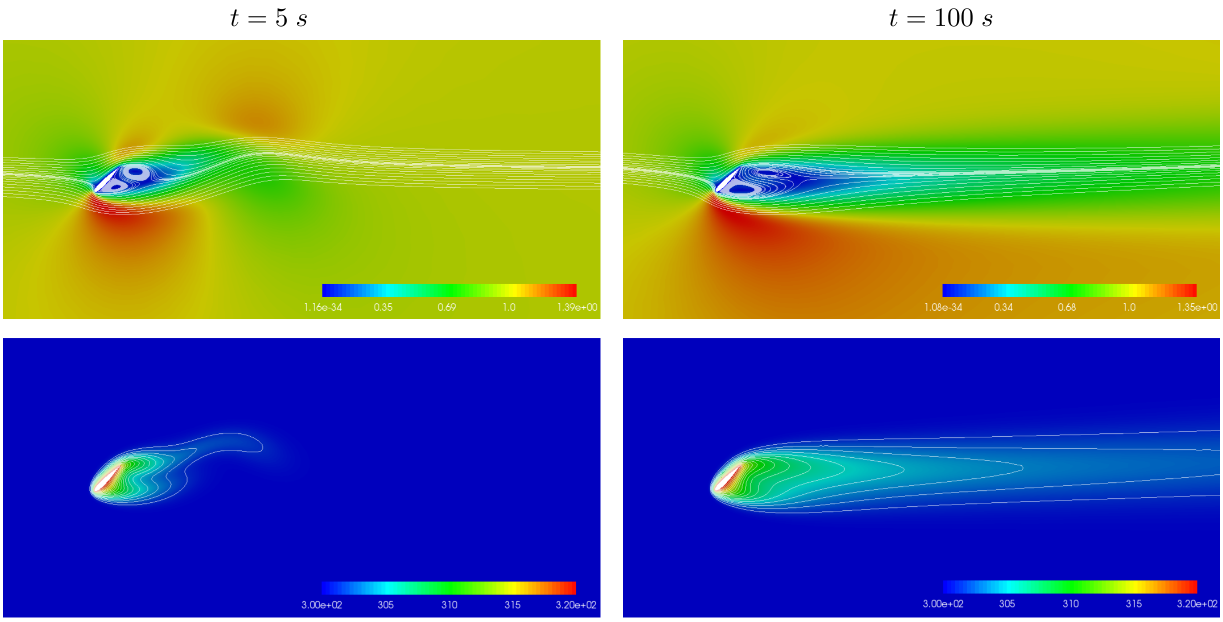

Figure 6: Snapshots of the velocity magnitude along with streamlines (first row) and temperature distributions along with isotherms (second row) for the problem of flow over a heated airfoil using $\omega = 45°$ at two different instants $t = 5$ s (first column) and $t = 100$ s (second column).

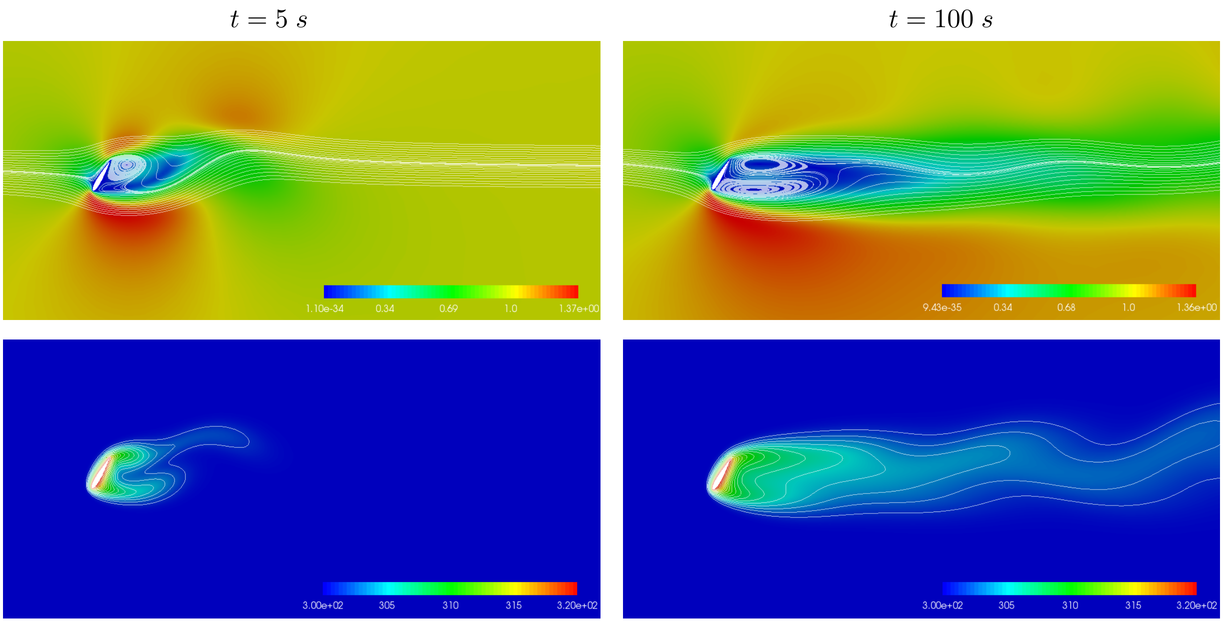

Figure 7: Same as Figure 6 but using $\omega = 60°$.

An unstructured triangular mesh of 22974 mixed elements with 11487 pressure nodes and 45664 velocity and temperature nodes is employed in our simulations, whereas the timestep Δt is fixed to 0.05 s and the obtained numerical results are presented at two different instants namely, $t = 5$ s and 100 s for the Prandtl number $Pr = 0.71$ and the Reynolds number $Re = 100$ using five different values of the inclination angle

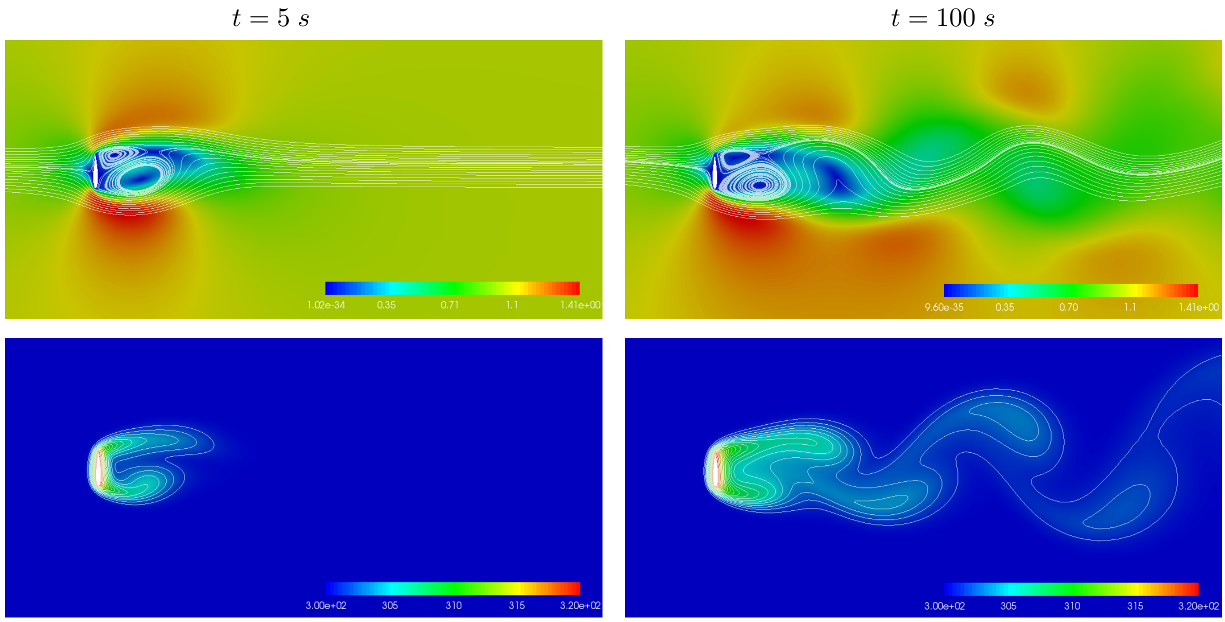

Figure 8: Same as Figure 6 but using $\omega = 90°$.

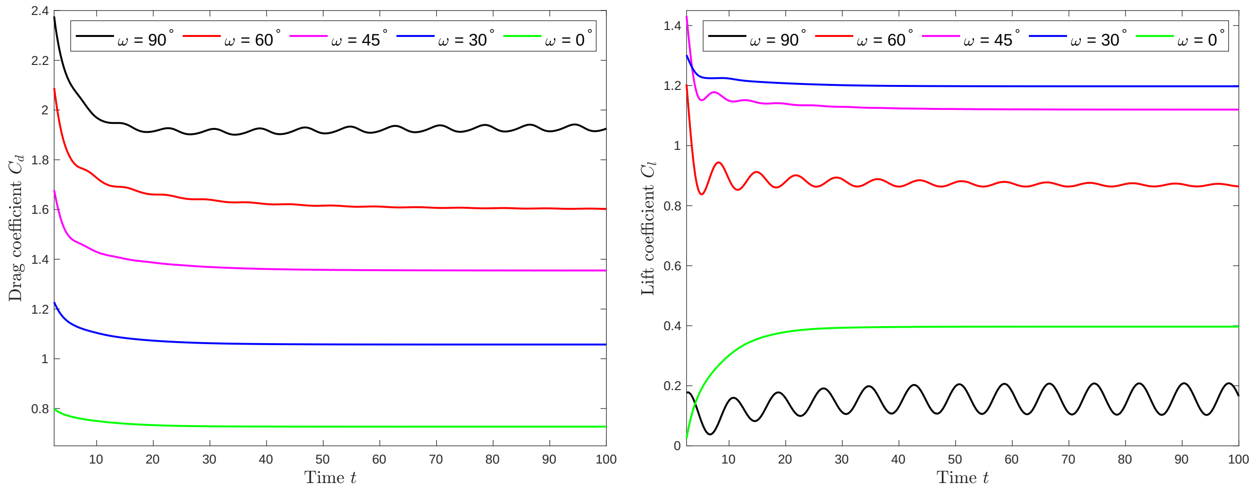

Figure 9: Time evolution of the drag coefficient (left) and the lift coefficient (right) for the problem of flow over a heated airfoil using different inclination angles.

$\omega = 0°$, $30°$, $45°$, $60°$ and $90°$.

Figure 6 depicts the temperature distributions along with isotherms and the streamlines along with the velocity magnitudes obtained at the selected instants $t = 5\ s$ and $t = 100\ s$ using the inclination angle $\omega = 45°$. Those results obtained using the inclination angles $\omega = 60°$ and $\omega = 90°$ are presented in Figure 7 and Figure 8, respectively. For the considered mixed convection at $Re = 100$ and up to the inclination angle $\omega = 45°$, the flow is still reaching a steady regime after the transient effects disappear. For $\omega = 60°$, the flow already develops a nonstationary state with longer two recirculation zones and moderate oscillations in the wake behind the airfoil. As the airfoil is further inclined towards the vertical position at $\omega = 90°$, the downstream region becomes more agitated with larger recirculation zones and more frequent oscillations

Table 1: Averaged Nusselt number for the problem of flow over a heated airfoil using different inclination angles.

	$\omega = 0°$	$\omega = 30°$	$\omega = 45°$	$\omega = 60°$	$\omega = 90°$
Nu	205.422	181.634	177.823	176.295	178.384

in the downstream region where the vortex shedding is clearly recognizable. These unsteady effects can clearly be seen in Figure 9 where the time evolution of the drag coefficient C_d and the lift coefficient C_l are depicted for the selected values of the inclination angle. We can observe a transition to the unsteady behavior in this figure under the influence of the inclination angle ω as the drag and lift coefficients maintain oscillatory features starting from $\omega = 60°$. It is also noticeable that the airfoil experiences important drag when it is more inclined which is expected since in this case more surface of the body is exposed to the main flow. These results also confirm that the proposed time viscosity-splitting method is very attractive since the computed flow solutions remain stable and accurate for the thermal convection flows.

From the obtained temperature distributions we observe that the isotherms are more distorted behind the airfoil which indicates that at the considered Reynolds number, the advection is reasonably strong and it is the dominant mode of heat transfer over the conduction and natural convection generated by the buoyancy force such that the heat released from the source is mainly transported downstream by the upcoming flow. This process is also influenced by the inclination angle of the airfoil since it controls the flow development at the fixed Re and Pr numbers. This dominance of convective heat transfer is also checked by calculating the averaged Nusselt number Nu over the airfoil surface defined as a ratio of the heat transfer by convection to the heat transfer by conduction as

$$Nu = \oint_{\partial \mathcal{A}} \frac{\partial \theta}{\partial \boldsymbol{n}} ds,$$

where $\partial \mathcal{A}$ is the airfoil surface and $\boldsymbol{n}$ its associated unit outward normal vector. Table 1 summarizes the obtained values of the averaged Nusselt number Nu at time $t = 100$ s using the considered inclination angles. It is clear from the obtained results that the averaged Nusselt number takes high values (> 100) for all considered inclination angles which indicates greater convective heat transport ongoing in the main flow region. Overall we can conclude that the main features of this test case including transient and the interplay between heat transport and flow properties have been successfully captured by the proposed time viscosity-splitting method.

6. Conclusions

In this work a viscosity-splitting method is proposed and analyzed for a class of generalized natural convection problems in which the viscosity and thermal conductivity are temperature-dependent along with a more general source term. We have conducted a detailed error analysis and managed to prove first-order error estimates for the velocity and temperature solutions in the L^2 and H^1 norms, and 1/2-order error for the pressure solution in the L^2 norm. Unlike most of the fractional-step methods appearing in the literature, the temperature in our time integration scheme is transported by a non-divergence-free velocity field. This property renders the error analysis of the proposed viscosity-splitting method more subtle as some additional terms appear in its formulation, due the new convection term in the temperature, which may deteriorate the order of convergence. Therefore, an involved treatment was elaborated in order to maintain the full first-order of the viscosity-splitting method. The theoretical error estimates for the velocity and the temperature as well as the performance of the method were validated using three numerical examples of incompressible flows with temperature-dependent viscosity and thermal conductivity. In future work, we are interested in extending the obtained results to more complex thermal flows involving non-Newtonian fluids. Establishing error estimates for the fully discrete problems using the mixed finite element method will also be considered for future work.

Appendix A. Formulation of the mixed finite element method

For the space discretization of the domain $\overline{\Omega} = \Omega \cup \partial\Omega$, we generate a quasi-uniform partition $\Omega_h \subset \overline{\Omega}$ of elements $\mathcal{T}_k$ (triangles or quadrilaterals in two space dimensions) such that $\overline{\Omega} = \cup_{k=1}^{N_e} \mathcal{T}_k$, where N_e is the number of elements of Ω_h, h a space discretization parameter and $\mathcal{T}_j$ the finite elements. For the conforming finite element spaces for the velocity/temperature and pressure, we use the mixed Taylor-Hood $\mathbb{P}_2$-$\mathbb{P}_1$ finite elements *i.e.*, polynomials of second degree for the velocity and temperature and polynomials of first degree for the pressure. It is well known that for such elements the discrete velocity and pressure solutions satisfy the inf-sup condition, see for instance [67]. The associated finite element spaces are defined as

$$\begin{aligned} V_h &= \left\{ u_h \in C^0(\overline{\Omega}) : \quad u_h\big|_{\mathcal{T}_j} \in P_2(\mathcal{T}_j), \quad \forall\, \mathcal{T}_j \in \Omega_h \right\}, \\ Q_h &= \left\{ p_h \in C^0(\overline{\Omega}) : \quad p_h\big|_{\mathcal{T}_j} \in P_1(\mathcal{T}_j), \quad \forall\, \mathcal{T}_j \in \Omega_h \right\}, \end{aligned}$$

where $P_2(\mathcal{T}_j)$ and $P_1(\mathcal{T}_j)$ are polynomial spaces defined in the element $\mathcal{T}_j$. Here, since the velocity field is a vector of two dimensions, the associated finite element space is defined as $\boldsymbol{V}_h = V_h \times V_h$. Thus, we formulate the finite element solutions to $\boldsymbol{u}^n(\boldsymbol{x}) \in \boldsymbol{V}_h$, $\theta^n(\boldsymbol{x}) \in V_h$ and $p^n(\boldsymbol{x}) \in Q_h$ as

$$\boldsymbol{u}_h^n(\boldsymbol{x}) = \sum_{j=1}^{N_u} \boldsymbol{U}_j^n \varphi_j(\boldsymbol{x}), \qquad \theta_h^n(\boldsymbol{x}) = \sum_{j=1}^{N_u} \Theta_j^n \varphi_j(\boldsymbol{x}) \qquad p_h^n(\boldsymbol{x}) = \sum_{k=1}^{N_p} P_k^n \psi_k(\boldsymbol{x}), \tag{A.1}$$

where N_u and N_p are respectively, the numbers of velocity/temperature and pressure mesh points in Ω_h. The solutions $\boldsymbol{U}_j^n = \left(U_j^n, V_j^n\right)^\top$, Θ_i^n and P_k^n are the corresponding nodal values of $\boldsymbol{u}_h^n(\boldsymbol{x})$, $\theta_h^n(\boldsymbol{x})$ and $p_h^n(\boldsymbol{x})$, respectively. These values are defined as $\boldsymbol{U}_j^n = \boldsymbol{u}_h^n(\boldsymbol{x}_j)$, $\Theta_j^n = \theta_h^n(\boldsymbol{x}_j)$ and $P_k^n = p_h^n(\boldsymbol{y}_k)$ where $\{\boldsymbol{x}_j\}_{j=1}^{N_u}$ and $\{\boldsymbol{y}_k\}_{k=1}^{N_p}$ are respectively, the sets of velocity/temperature and pressure mesh points in Ω_h, with $N_p < N_u$ and $\{\boldsymbol{y}_1, \ldots, \boldsymbol{y}_{N_p}\} \subset \{\boldsymbol{x}_1, \ldots, \boldsymbol{x}_{N_u}\}$. In (A.1), $\{\varphi_j\}_{j=1}^{N_u}$ and $\{\psi_k\}_{k=1}^{N_p}$ are respectively, the sets of global nodal basis functions of the velocity/temperature and the pressure characterized by the property $\varphi_i(\boldsymbol{x}_j) = \delta_{ij}$ and $\psi_i(\boldsymbol{y}_k) = \delta_{ik}$ with δ denotes the Kronecker symbol. Hence, the fully discrete formulation of the steps (18)-(21) reads:

Step 1: For all $\boldsymbol{v}_h \in \boldsymbol{V}_h$, compute $\bar{\boldsymbol{u}}_h^{n+1} \in \boldsymbol{V}_h$ solution of

$$\begin{aligned} \int_{\Omega_h} \frac{\bar{\boldsymbol{u}}_h^{n+1} - \boldsymbol{u}_h^n}{\Delta t} \cdot \boldsymbol{v}_h \, d\boldsymbol{x} + \int_{\Omega_h} \left(\boldsymbol{u}_h^n \cdot \nabla\right) \bar{\boldsymbol{u}}_h^{n+1} \cdot \boldsymbol{v}_h \, d\boldsymbol{x} + \int_{\Omega_h} \nu\left(\theta_h^n + \mathcal{R}_\theta^{n+1}\right) \nabla \bar{\boldsymbol{u}}_h^{n+1} : \nabla \boldsymbol{v}_h \, d\boldsymbol{x} = \\ \alpha \int_{\Omega_h} \boldsymbol{f}\left(\theta_h^n + \mathcal{R}_\theta^{n+1}\right) \cdot \boldsymbol{v}_h \, d\boldsymbol{x}. \end{aligned} \tag{A.2}$$

Step 2: For all $\varphi_h \in V_h$, compute $\bar{\theta}_h^{n+1} \in V_h$ solution of

$$\begin{aligned} &\int_{\Omega_h} \frac{\bar{\theta}_h^{n+1} - \theta_h^n}{\Delta t} \varphi_h \, d\boldsymbol{x} + \int_{\Omega_h} \bar{\boldsymbol{u}}_h^{n+1} \cdot \nabla \bar{\theta}_h^{n+1} \varphi_h \, d\boldsymbol{x} + \int_{\Omega_h} \frac{1}{2} \bar{\theta}_h^{n+1} \nabla \cdot \bar{\boldsymbol{u}}_h^{n+1} \varphi_h \, d\boldsymbol{x} + \\ &\int_{\Omega_h} \lambda(\theta_h^n + \mathcal{R}_\theta^{n+1}) \nabla \bar{\theta}_h^{n+1} \cdot \nabla \varphi_h \, d\boldsymbol{x} = -\int_{\Omega_h} \lambda(\theta_h^n + \mathcal{R}_\theta^{n+1}) \nabla \mathcal{R}_\theta^{n+1} \cdot \nabla \varphi_h \, d\boldsymbol{x} - \int_{\Omega_h} \bar{\boldsymbol{u}}_h^{n+1} \cdot \nabla \mathcal{R}_\theta^{n+1} \varphi_h \, d\boldsymbol{x} \\ &\qquad - \int_{\Omega_h} \frac{1}{2} \mathcal{R}_\theta^{n+1} \nabla \cdot \bar{\boldsymbol{u}}_h^{n+1} \varphi_h \, d\boldsymbol{x} + \int_{\Omega_h} g^{n+1} \varphi_h \, d\boldsymbol{x} + \langle \theta_N^{n+1}, \varphi_h \rangle - \int_{\Omega_h} \partial_t \mathcal{R}_\theta^{n+1} \varphi_h \, d\boldsymbol{x}. \end{aligned} \tag{A.3}$$

Step 3: For all $(\boldsymbol{v}_h, q_h) \in \boldsymbol{V}_h \times Q_h$, compute $\left(\boldsymbol{u}_h^{n+1}, p_h^{n+1}\right) \in \boldsymbol{V}_h \times Q_h$ solution of the following Stokes problem

$$\int_{\Omega_h} \frac{\boldsymbol{u}_h^{n+1} - \bar{\boldsymbol{u}}_h^{n+1}}{\Delta t} \cdot \boldsymbol{v}_h \, d\boldsymbol{x} + \int_{\Omega_h} \nu(\bar{\theta}_h^{n+1} + \mathcal{R}_\theta^{n+1}) \nabla \boldsymbol{u}_h^{n+1} : \nabla \boldsymbol{v}_h \, d\boldsymbol{x} - \int_{\Omega_h} p_h^{n+1} \nabla \cdot \boldsymbol{v}_h \, d\boldsymbol{x} = \int_{\Omega_h} \nu(\theta_h^n + \mathcal{R}_\theta^{n+1}) \nabla \bar{\boldsymbol{u}}_h^{n+1} : \nabla \boldsymbol{v}_h \, d\boldsymbol{x}, \quad \text{(A.4)}$$

$$- \int_{\Omega_h} q_h \, \nabla \cdot \boldsymbol{u}_h^{n+1} \, d\boldsymbol{x} = 0.$$

Step 4: For all $\varphi_h \in V_h$, compute $\theta_h^{n+1} \in V_h$ solution of

$$\int_{\Omega_h} \frac{\theta_h^{n+1} - \bar{\theta}_h^{n+1}}{\Delta t} \varphi_h \, d\boldsymbol{x} + \int_{\Omega_h} \lambda(\bar{\theta}_h^{n+1} + \mathcal{R}_\theta^{n+1}) \, \nabla \theta_h^{n+1} \cdot \nabla \varphi_h \, d\boldsymbol{x} = \int_{\Omega_h} \lambda(\theta_h^n + \mathcal{R}_\theta^{n+1}) \, \nabla \bar{\theta}_h^{n+1} \cdot \nabla \varphi_h \, d\boldsymbol{x}. \quad \text{(A.5)}$$

Injecting the approximations (A.1) in the above discrete steps, results in linear systems of the following forms

$$\left(\frac{1}{\Delta t} \mathbf{M}_u + \mathbf{N}_u + \mathbf{K}_u(\theta^n) \right) \widetilde{\boldsymbol{U}}^{n+1} = \widetilde{\mathbf{F}}_u(\boldsymbol{u}^n, \theta^n), \quad \text{(A.6)}$$

$$\left(\frac{1}{\Delta t} \mathbf{M}_\theta + \mathbf{N}_\theta + \mathbf{K}_\theta(\theta^n) \right) \widetilde{\Theta}^{n+1} = \widetilde{\mathbf{F}}_\theta(\bar{\boldsymbol{u}}^{n+1}, \theta^n), \quad \text{(A.7)}$$

$$\begin{pmatrix} \frac{1}{\Delta t} \mathbf{M}_u + \mathbf{K}_u(\bar{\theta}^{n+1}) & \mathbf{B}^T \\ \mathbf{B} & \mathbf{0} \end{pmatrix} \begin{pmatrix} \boldsymbol{U}^{n+1} \\ P^{n+1} \end{pmatrix} = \begin{pmatrix} \mathbf{F}_u(\bar{\boldsymbol{u}}^{n+1}, \theta^n) \\ \mathbf{0} \end{pmatrix}, \quad \text{(A.8)}$$

and

$$\left(\frac{1}{\Delta t} \mathbf{M}_\theta + \mathbf{K}_\theta(\bar{\theta}^{n+1}) \right) \Theta^{n+1} = \mathbf{F}_\theta(\boldsymbol{u}^n, \theta^n, \bar{\theta}^{n+1}), \quad \text{(A.9)}$$

where $\boldsymbol{U}^{n+1} = \left(U^{n+1}, V^{n+1}\right)^\top$ and $\widetilde{\boldsymbol{U}}^{n+1} = \left(\widetilde{U}^{n+1}, \widetilde{V}^{n+1}\right)^\top$ with each component is a vector with unknown entries $\boldsymbol{U}_j^{n+1} = \left(U_j^{n+1}, V_j^{n+1}\right)^\top$ and $\widetilde{\boldsymbol{U}}_j^{n+1} = \left(\widetilde{U}_j^{n+1}, \widetilde{V}_j^{n+1}\right)^\top$ $(j = 1, \ldots, N_u)$, respectively. Here, Θ^{n+1}, $\widetilde{\Theta}^{n+1}$ and P^{n+1} are respectively, vectors with unknown entries Θ_i^{n+1}, $\widetilde{\Theta}_i^{n+1}$ and P_k^{n+1} $(i = 1, \ldots, N_u$ and $k = 1, \ldots, N_p)$ as defined in (A.1), $\mathbf{M}_u$, $\mathbf{N}_u$, $\mathbf{K}_u$, $\mathbf{M}_\theta$, $\mathbf{N}_\theta$, $\mathbf{K}_\theta$ and $\mathbf{B}$ are matrices whose element entries are given by

$$\begin{aligned}
(\boldsymbol{M}_u)_{ij} &= \int_{\Omega_h} \boldsymbol{\varphi}_j \cdot \boldsymbol{\varphi}_i \, d\boldsymbol{x}, \\
(\boldsymbol{N}_u)_{ij} &= \int_{\Omega_h} (\boldsymbol{u}^n \cdot \nabla \boldsymbol{\varphi}_j) \cdot \boldsymbol{\varphi}_i \, d\boldsymbol{x}, \\
(\boldsymbol{K}_u(\theta))_{ij} &= \int_{\Omega_h} \nu \left(\theta + \mathcal{R}_\theta^{n+1}\right) \nabla \boldsymbol{\varphi}_j \colon \nabla \boldsymbol{\varphi}_i \, d\boldsymbol{x}, \\
(\boldsymbol{M}_\theta)_{ij} &= \int_{\Omega_h} \varphi_j \varphi_i \, d\boldsymbol{x}, \\
(\boldsymbol{N}_\theta)_{ij} &= \int_{\Omega_h} (\bar{\boldsymbol{u}}^{n+1} \cdot \nabla \varphi_j) \varphi_i \, d\boldsymbol{x}, \\
(\boldsymbol{K}_\theta(\theta))_{ij} &= \int_{\Omega_h} \lambda \left(\theta + \mathcal{R}_\theta^{n+1}\right) \nabla \varphi_j \cdot \nabla \varphi_i \, d\boldsymbol{x}, \\
B_{ij} &= -\int_{\Omega_h} \psi_i \nabla \cdot \boldsymbol{\varphi}_j d\boldsymbol{x}.
\end{aligned}$$

and $\widetilde{\boldsymbol{F}}_u$, $\widetilde{\boldsymbol{F}}_\theta$, $\boldsymbol{F}_u$ and $\boldsymbol{F}_\theta$ are the corresponding right-hand side vectors. It should be stressed that the lifting $\mathcal{R}_\theta$ in the above equations is obtained by solving the following well-posed problem

$$-\Delta\mathcal{R}_\theta = 0, \qquad \mathcal{R}_\theta = \theta_D \quad \text{on } \Gamma_D, \qquad \frac{\partial\mathcal{R}_\theta}{\partial\boldsymbol{n}} = 0 \quad \text{on } \Gamma_N.$$

Data availability

The data that support the findings of this study are available from the corresponding author upon reasonable request.

Conflict of interest

The authors have no competing interests to declare that are relevant to the content of this paper.

Acknowledgment

The authors would like to thank an anonymous referee for giving very helpful comments and suggestions that have greatly improved this paper.

References

[1] O. Prakash, A. Kumar, Solar greenhouse drying: A review, Renewable and Sustainable Energy Reviews 29 (2014) 905–910.
[2] C. Yan, H. Li, Y. Tang, X. Ding, X. Yuan, Y. Liang, S. Zhang, A novel ultra-thin vapor chamber with composite wick for portable electronics cooling, Applied Thermal Engineering 226 (2023) 120340.
[3] E. El-Bialy, S. Shalaby, Recent developments and cost analysis of different configurations of the solar air heaters, Solar Energy (2023) 112091.
[4] A. Bejan, Convection heat transfer, John wiley & sons, 2013.
[5] D. Shang, Free convection film flows and heat transfer, Springer, 2006.
[6] D. D. Joseph, On the stability of the Boussinesq equations, Arch. Ration. Mech. Anal. 29 (1965) 32–57.
[7] P. Rabinowitz, Existence and nonuniqueness of rectangular solutions of the Bénard problem, Archive for Rational Mechanics and Analysis 29 (1968) 32–57.
[8] D. Sattinger, Group Theoretic Methods in Bifurcation, Vol. 762, Springer, Berlin, 1978.
[9] C. Bernardi, B. Métivet, B. Pernaud-Thomas, Couplage des équations de Navier-Stokes et de la chaleur: le modèle et son approximation par éléments finis, RAIRO Modélisation Mathématique et Analyse Numérique 29 (7) (1995) 871–921.
[10] M. Gaultier, J. Lezaun, Equations de Navier-Stokes couplées à des équations de la chaleur: Résolution par une méthode de point fixe en dimension infinie, Ann. Sci. Math. 13 (1989) 1–17.
[11] S. A. Lorca, J. L. Boldrini, Stationary solutions for generalized Boussinesq models, Journal of Differential equations 124 (2) (1996) 389–406.
[12] M. Gunzburger, Y. Saka, X. Wang, Well-posedness of the infinite Prandtl number model for convection with temperature-dependent viscosity, Anal. Appl 7 (2009) 297–308.
[13] M. Kronbichler, T. Heister, W. Bangerth, High accuracy mantle convection simulation through modern numerical methods: High accuracy mantle convection simulation, Geophysical Journal International 191 (1) (2012) 12–29.
[14] T. Heister, J. Dannberg, R. Gassmöller, W. Bangerth, High accuracy mantle convection simulation through modern numerical methods–ii: realistic models and problems, Geophysical Journal International 210 (2) (2017) 833–851.
[15] A. Chorin, Numerical solution of the Navier–Stokes equations, Math. Comp. 22 (1968) 745–762.
[16] R. Temam, Sur l'approximation de la solution des équations de Navier-Stokes par la méthode des pas fractionnaires (I), Archive for Rational Mechanics and Analysis 32 (2) (1969) 135–153.
[17] L. J. P. Timmermans, P. D. Minev, F. N. V. D. Vosse, An Approximate Projection Scheme for Incompressible Flow Using Spectral Elements, International Journal for Numerical Methods in Fluids 22 (7) (1996) 673–688.
[18] J. Guermond, J. Shen, On the error estimates for the rotational pressure-correction projection methods, Mathematics of Computation 73 (248) (2004) 1719–1737.
[19] G. Karniadakis, M. Israeli, S. Orszag, High-order splitting methods for the incompressible Navier–Stokes equations, Journal of Computational Physics 97 (2) (1991) 414–443.
[20] S. A. Orszag, M. Israeli, M. O. Deville, Boundary conditions for incompressible flows, Journal of Scientific Computing 1 (1) (1986) 75–111.
[21] J. Shen, On error estimates of the projection methods for the Navier-Stokes equations: Second-order schemes, Mathematics of Computation 65 (215) (1996) 1039–1066.
[22] J. Bell, P. Colella, H. Glaz, A second-order projection method for the incompressible Navier-Stokes equations, J. of Comp. Physics 85 (2) (1989) 257–283.

[23] J.-L. Guermond, L. Quartapelle, On stability and convergence of projection methods based on pressure Poisson equation, International Journal for Numerical Methods in Fluids 26 (9) (1998) 1039–1053.

[24] J. L. Guermond, P. Minev, J. Shen, Error analysis of pressure-correction schemes for the time-dependent Stokes equations with open boundary conditions, SIAM Journal on Numerical Analysis 43 (1) (2006) 239–258.

[25] H. Choi, H. Choi, J. Yoo, A fractional four-step finite element formulation of the unsteady incompressible Navier-Stokes equations using supg and linear equal-order element methods, Computer Methods in Applied Mechanics and Engineering 143 (3-4) (1997) 333–348.

[26] H. Sammouda, A. Belghith, C. Surry, Finite element simulation of transient natural convection of low-Prandtl-number fluids in heated cavity, International Journal of Numerical Methods for Heat & Fluid Flow 9 (5) (1999) 612–624.

[27] D. Lo, D. Young, Y. Lin, Finite-element analysis of 3D viscous flow and mixed-convection problems by the projection method, Numerical Heat Transfer, Part A: Applications 48 (4) (2005) 339–358.

[28] P. Nithiarasu, A unified fractional step method for compressible and incompressible flows, heat transfer and incompressible solid mechanics 18 (2008) 111–130.

[29] W. Wang, J. Wu, X. Feng, A novel pressure-correction projection finite element method for incompressible natural convection problem with variable density, Numerical Heat Transfer, Part A: Applications 74 (2) (2018) 1001–1017.

[30] S. Armfield, A. Schultz, Unsteady natural convection in tall side-heated cavities, International journal for numerical methods in fluids 40 (8) (2002) 1009–1018.

[31] K. A. Dittko, M. Kirkpatrick, S. Armfield, Natural convection in a sidewall heated cube using an immersed boundary method, ANZIAM Journal 52 (2010) C535–C548.

[32] S.-J. Liang, Y.-J. Jan, C.-A. Huang, A quasi-implicit time-advancing scheme for 3D Rayleigh-Bénard convection, Numerical Heat Transfer, Part B: Fundamentals 63 (5) (2013) 371–394.

[33] H. Welhezi, N. Ben-Cheikh, B. Ben-Beya, Numerical analysis of natural convection between a heated cube and its spherical enclosure, International Journal of Thermal Sciences 150 (2020) 105828.

[34] Y. Qian, T. Zhang, On error estimates of the projection method for the time-dependent natural convection problem: first order scheme, Computers & Mathematics with Applications 72 (5) (2016) 1444–1465.

[35] Y. Qian, T. Zhang, The second order projection method in time for the time-dependent natural convection problem, Applications of Mathematics 61 (3) (2016) 299–315.

[36] J. Wu, X. Feng, F. Liu, Pressure-correction projection FEM for time-dependent natural convection problem, Communications in Computational Physics 21 (4) (2017) 1090–1117.

[37] J. Deteix, A. Jendoubi, D. Yakoubi, A coupled prediction scheme for solving the Navier-Stokes and convection-diffusion equations, SIAM Journal on Numerical Analysis 52 (5) (2014) 2415–2439.

[38] Y.-B. Yang, B.-C. Huang, Y.-L. Jiang, Error estimates of an operator-splitting finite element method for the time-dependent natural convection problem, Numerical Methods for Partial Differential Equations 39 (3) (2023) 2202–2226.

[39] Y. Hou, W. Yan, J. Hou, A fractional-step DG-FE method for the time-dependent generalized Boussinesq equations, Communications in Nonlinear Science and Numerical Simulation 116 (2023) 106884.

[40] J. Blasco, R. Codina, A. Huerta, A fractional-step method for the incompressible Navier-Stokes equations related to a predictor-multicorrector algorithm, Internat. J. Numer. Methods Fluids 28 (10) (1998) 1391–1419.

[41] Y. Lung-an, Viscosity-splitting scheme for the Navier-Stokes equations, Numerical Methods for Partial Differential Equations 7 (4) (1991) 317–338.

[42] R. Glowinski, T.-W. Pan, J. Periaux, A fictitious domain method for external incompressible viscous flow modeled by Navier-Stokes equations, Computer Methods in Applied Mechanics and Engineering 112 (1-4) (1994) 133–148.

[43] J. Blasco, R. Codina, Error estimates for an operator-splitting method for incompressible flows, Appl. Numer. Math. 51 (1) (2004) 1–17.

[44] F. Guillén-González, M. Redondo-Neble, New error estimates for a viscosity-splitting scheme in time for the three-dimensional Navier-Stokes equations, IMA J. Numer. Anal. 31 (2) (2011) 556–579.

[45] D. Yakoubi, Enhancing the viscosity-splitting method to solve the time-dependent Navier-Stokes equations, Communications in Nonlinear Science and Numerical Simulation 123 (2023) 107264.

[46] M. El-Amrani, A. Obbadi, M. Seaid, D. Yakoubi, Error estimates for a viscosity-splitting scheme in time applied to non-Newtonian fluid flows, Computer Methods in Applied Mechanics and Engineering 419 (2024) 116639.

[47] R. Temam, Navier-Stokes Equations: Theory and Numerical Analysis, Vol. 343, American Mathematical Soc., 2001.

[48] A. M. Quarteroni, A. Valli, Numerical Approximation of Partial Differential Equations, 1st Edition, Springer Publishing Company, Incorporated, 2008.

[49] R. A. Adams, Sobolev Spaces, Academic Press New York, 1975.

[50] F. Boyer, P. Fabrie, Mathematical Tools for the Study of the Incompressible Navier-Stokes Equations and Related Models, Vol. 183 of Applied Mathematical Sciences, Springer, New York, 2013.

[51] J.-L. Lions, E. Magenes, Problèmes Aux Limites Non Homogènes et Applications, Vol. 1, Dunod, 1968.

[52] J.-M. Bernard, Density results in Sobolev spaces whose elements vanish on a part of the boundary, Chinese Annals of Mathematics. Series B 32 (6) (2011) 823–846.

[53] P. Constantin, C. foias, Navier-Stokes equations, Chicago Lectures in Math. Series, Univ. of Chicago Press (1988).

[54] J. G. Heywood, R. Rannacher, Finite-Element Approximation of the Nonstationary Navier–Stokes Problem. Part IV: Error Analysis for Second-Order Time Discretization, SIAM Journal on Numerical Analysis 27 (2) (1990) 353–384.

[55] Y. He, Two-level method based on finite element and Crank-Nicolson extrapolation for the time-dependent Navier-Stokes equations, SIAM Journal on Numerical Analysis 41 (4) (2003) 1263–1285.

[56] J. G. Heywood, R. Rannacher, Finite element approximation of the nonstationary Navier-Stokes problem. I. regularity of solutions and second-order error estimates for spatial discretization, SIAM Journal on Numerical Analysis 19 (2) (1982)

275–311.
[57] J. Shen, On error estimates of projection methods for Navier-Stokes equations: First-order schemes, SIAM Journal on Numerical Analysis 29 (1) (1992) 57–77.
[58] J. Shen, Remarks on the pressure error estimates for the projection methods, Numerische Mathematik 67 (4) (1994) 513–520.
[59] S. Agmon, A. Douglis, L. Nirenberg, Estimates near the boundary for solutions of elliptic partial differential equations satisfying general boundary conditions. I, Communications on pure and applied mathematics 12 (4) (1959) 623–727.
[60] S. Agmon, A. Douglis, L. Nirenberg, Estimates near the boundary for solutions of elliptic partial differential equations satisfying general boundary conditions II, Communications on pure and applied mathematics 17 (1) (1964) 35–92.
[61] W. Layton, Introduction to the numerical analysis of incompressible viscous flows, SIAM, 2008.
[62] L. Rebholz, A. Viguerie, M. Xiao, Efficient nonlinear iteration schemes based on algebraic splitting for the incompressible Navier-Stokes equations, Mathematics of Computation 88 (318) (2019) 1533–1557.
[63] J. Deteix, G. Ndetchoua Kouamo, D. Yakoubi, Well-posedness of a semi-discrete Navier-Stokes/Allen-Cahn model, Journal of Mathematical Analysis and Applications 496 (2) (2021) 124816.
[64] V. Girault, P.-A. Raviart, Finite Element Methods for the Navier-Stokes Equations, Vol. 5, Springer-Verlag, Berlin, 1986.
[65] C. Soong, P. Tzeng, D. Chiang, T. Sheu, Numerical study on mode-transition of natural convection in differentially heated inclined enclosures, International Journal of Heat and Mass Transfer 39 (14) (1996) 2869–2882.
[66] L. Khezzar, D. Siginer, I. Vinogradov, Natural convection in inclined two dimensional rectangular cavities, Heat and Mass Transfer 48 (2012) 227–239.
[67] D. Boffi, F. Brezzi, M. Fortin, Mixed Finite Element Methods and Applications, Vol. 44, Springer Berlin Heidelberg, Berlin, Heidelberg, 2013.